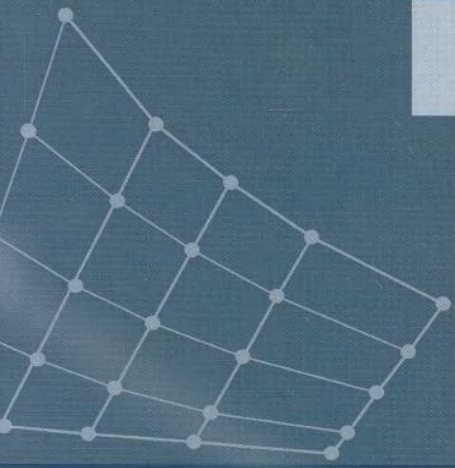

SPRINGER LABORATORY

W.-M. Kulicke · C. Clasen

Viscosimetry of Polymers and Polyelectrolytes

Springer

Springer
Berlin
Heidelberg
New York
Hong Kong
London
Milano
Paris
Tokyo

Springer Laboratory

Werner-Michael Kulicke · Christian Clasen

Viscosimetry of Polymers and Polyelectrolytes

With 71 Figures and 20 Tables

Springer

Professor Dr. Werner-Michael Kulicke
e-mail: kulicke@chemie.uni-hamburg.de

Dr. Christian Clasen
e-mail: clasen@chemie.uni-hamburg.de

Universität Hamburg
Fachbereich 13,
Institut für Technische und
Makromolekulare Chemie
Bundesstraße 45
20146 Hamburg
Germany

ISBN 3-540-40760-X Springer-Verlag Berlin Heidelberg New York

Library of Congress Cataloging-in-Publication Data
Kulicke, Werner-Michael.
Viscosimetry of polymers and polyelectrolytes / Werner-Michael Kulicke, Christian Clasen.
p. cm. – (Springer laboratory)
Includes bibliographical references and index.
ISBN 3-540-40760-X (acid-free paper)
1. Polymers--Viscosity--Measurement--Laboratory manuals. 2. Polyelectrolytes--Viscosity--Measurement--Laboratory manuals. I. Clasen, Christian. II. Title. III. Series

QD381.9.R48K85 2004
547'.7'0287–dc22

2003065470

Springer-Verlag is a part of Springer Science+Business Media
springeronline.com

Printed in Germany

Coverdesign: Erich Kirchner, Heidelberg
Typesetting: Fotosatz-Service Köhler GmbH, Würzburg

Printed on acid-free paper 2/3020/ xv – 5 4 3 2 1 0

Laboratory Manual Series in Polymer Science

Editors

Prof. Howard G. Barth
DuPont Company
P.O. box 80228
Wilmington, DE 19880-0228
USA
e-mail: Howard.G.Barth@usa.dupont.com

Priv.-Doz. Dr. Harald Pasch
Deutsches Kunststoff-Institut
Abt. Analytik
Schloßgartenstr. 6
64289 Darmstadt
Germany
e-mail: hpasch@dki.tu-darmstadt.de

Editorial Board

PD Dr. Ingo Alig
Deutsches Kunststoff-Institut
Abt. Physik
Schlossgartenstr. 6
64289 Darmstadt
Germany
email: ialig@dki.tu-darmstadt.de

Prof. Josef Janca
Université de La Rochelle
Pole Sciences et Technologie
Avenue Michel Crépeau
17042 La rochelle Cedex 01
France
email: jjanca@univ.lr.fr

Prof. W.-M. Kulicke
Inst. f. Technische u. Makromol. Chemie
Universität Hamburg
Bundesstr. 45
20146 Hamburg
Germany
email: kulicke@chemie.uni-hamburg.de

Prof. H. W. Siesler
Physikalische Chemie
Universität Essen
Schützenbahn 70
45117 Essen
Germany
email: hw.siesler@uni-essen.de

Springer Laboratory Manuals in Polymer Science

Pasch, Trathnigg: HPLC of Polymers
ISBN: 3-540-61689-9 (hardcover)
ISBN: 3-540-65551-4 (softcover)

Mori, S.; Barth, H.G.: Size Exclusion Chromatography
ISBN: 3-540-65635-9

Pasch, H.; Schrepp, W.: MALDI-TOF Mass Spectrometry of Synthetic Polymers
ISBN: 3-540-44259-6

Kulicke, Clasen: Viscosimetry of Polymers and Polyelectrolytes
ISBN: 3-540-40760-X

Hatada, Kitayama: NMR Spectroscopy of Polymers
ISBN: 3-540-40220-9

Preface

Viscosimetry is to this day an easy accessible, but at the same time significant analytical method for the characterization of polymers in solution. It is therefore widely used in the technical chemistry and chemical engineering like pharmaceutical, medical, polymer processing and food industries as well as in research institutes and universities. Viscosimetry allows for a fast and low-priced determination of relevant parameters such as solution structure, volume fraction, coil dimensions, molar mass, viscosity or thermodynamical properties of a polymer in solution.

The importance of viscosimetry as an independent area in the field of polymer analytics becomes clear through the Nobel prices awarded for two works in this area. The name of the 1953 honored Prof. Hermann Staudinger for his proof of the existence of polymers is still used in viscosimetry in the intrinsic viscosity (German: "Staudingerindex") (see "Intrinsic viscosimetry" in Chap. 4). In 1974, Prof. Paul J. Flory was honored with the Nobel price for his groundbreaking works on the conformation of polymers in solution and his name is conserved for posterity in the Flory constant (see "The Fox-Flory theory" in Chap. 8).

During the last few years, the importance of viscosimetry as a means of determination of the influence of molecular structure parameters such as molar mass, concentration, solvent, temperature, shear rate, chemical structure, and degree of branching or tacticity on the property viscosity of a polymer solution has been established on numerous national and international conferences and congresses on polymer analytics. On the other hand, it has become clear that at the moment, no textbook or instruction manual is available that presents this extensive topic in a concise way. To impart information about viscosimetry and the determination of its structure-property relationships are therefore the main goals of this book.

In addition to this, a general knowledge of the broad behavioral spectrum of polymer solutions is of outmost importance for the proper handling of viscosimetric equipment and the interpretation of data. Therefore, this laboratory handbook is intended as a guideline for the practical everyday application of viscosimetry as well as a comprehensive companion for the interpretation of viscosimetric data from simple to complex polymer solutions.

This book originated from the practical experiences during the supervision of the practical laboratory courses in polymer analytics at the Institut für Technische Chemie, Technical University of Braunschweig with Prof. J. Klein, to whom we would like to express our thanks at this point. The continuation of this work at the Institut für Technische und Makromolekulare Chemie, University of Hamburg and

especially the contact of the authors and the colleagues at the Institute with the industry have made it possible for the many practical examples and problems to find their way into this book. At this point we would like to thank Prof. H. U. Moritz and Prof. W. Kaminsky, the latter for the support in clarifying the question of the coil dimensions of tactic polymers in solution. We would also like to thank the colleagues in other laboratories for their help, in particular Prof. J. Klein, Prof. E. Killmann and Dr. Horn for the "Polyelectrolytes" symposia series. It is not possible to list all the contacts and discussions with colleagues around the world at international and national conferences on polymer analytics, especially the meetings of the American Society of Rheology (SOR), the European Society of Rheology (ESR) and the national meetings of the European societies. Furthermore, we would like to thank the members of the workgroup for their contribution to this book, especially Dr. M. Matthies and Dipl.-Chem. M. Knarr for their help with the manuscript and Dr. C. Seidel and Dipl.-Chem. J. P. Plog for the revision of the English version of this book. Last but not least we would like to thank Dr. H.-M. Laun, Prof. D. Lechner and Prof. H. Münstedt for helpful comments and their extended review of the manuscript.

We hope that this book serves as a tutorial as well as a comprehensive companion that covers the broad area of viscosimetry of polymers in solution.

Hamburg, November 2003

W.-M. Kulicke
C. Clasen

List of Symbols and Abbreviations

a	Exponent of the $[\eta]$-M-relationship
A	Area, Eyring coefficient
A	Heterogeneity class of $[\eta]$-M-relationship
A_{FS}	Fuoss term
A_2	2. Virial coefficient
A_3	3. Virial coefficient
b	Bond length
B	Heterogeneity class of $[\eta]$-M-relationship
B_1, B_2, B_3	Constants of the virial equation
c	Concentration
C	Heterogeneity class of $[\eta]$-M-relationship
C_∞	Characteristic ratio
CD	Circular dichroism
c^*	Critical concentration of polymer coil overlap
c_L	Drag coefficient
$c^*_{[\eta]}$	Critical concentration of viscosimetry
c^*_{LS}	Critical concentration of light scattering
$c \cdot [\eta]$	Overlap parameter
CMC	Carboxymethyl cellulose
d	Diameter of a polymer coil
D	Heterogeneity class of $[\eta]$-M-relationship
D	Capillary diameter
DIN	German industrial standards
DMSO	Dimethylsulfoxide
DNA	Deoxyribonucleic acid
E	Flow activation energy (Eyring equation)
EG	Ethylene glycol
Eq.	Equation
f	Function
F	Force, sphere factor of the visco-balance
Fig.	Figure
g	Gravity constant
h	Height, cylinder height
h', h''	Geometry factors of concentric cylinder fixtures (ISO 3219)
$\bar{h}$	Average height of the liquid column in a capillary viscosimeter

Δh	Correction factor of cylinder height
HDPE	High-density poly(ethylene)
HES	Hydroxyethyl starch
HESEC	Hydroxyethylsulfoethyl cellulose
ISO	International Organization for Standardization
IUPAC	International Union of Pure and Applied Chemistry
K	Constant, constant of the capillary viscosimeter, constant of the Höppler viscosimeter, Fikentscher constant
K_b	Known capillary constant
K_{FS}	Fuoss constant
$K_{[\eta]}$	Constant of the Kuhn-Mark-Houwink-Sakurada equation ($[\eta]$-M-equation)
K_H	Huggins constant
K_K	Kramer constant
K_M	Martin constant
K_n	Constant of the $[\eta]$-M-equation determined with number average molar masses
K_{SB}	Schulz-Blaschke constant
K_w	Constant of the $[\eta]$-M-equation determined with mass average molar masses
KMHS	Kuhn-Mark-Houwink-Sakurada equation
$K/M_u^{0.5}$	Dimension factor of steric hindrance
l	Length, capillary length
L_p	Persistence length
LDPE	Low-density poly(ethylene)
m	Correction factor of the Hagenbach correction
m_{coil}	Mass of a single polymer coil
m_i	Mass of fraction i
$m_{polymer}$	Mass of the polymer
M	Molar mass
M_n	Number average molar mass
M_u	Molar mass of a monomer unit
M_w	Mass average molar mass
M_z	Centrifuge average molar mass
M_η	Viscosity average molar mass
M_1, M_2	Start and end marks at capillary and falling sphere viscosimeters, molar mass of different solvent components
n	Number, rotational frequency
N	Number of bonds in a polymer chain
N_A	Avogadro number
NaN_3	Sodium azide
NaOH	Sodium hydroxide
p	Pressure
Δp	Pressure difference
pH	Reciprocal hydrogen ion concentration

P	Degree of polymerization
PAAc	Poly(acrylic acid)
PAAcNa	Sodium poly(acrylate)
PAAm	Poly(acrylamide)
PAAm/AAcNa	Sodium poly(acrylamide-*co*-acrylate)
PAAm/M	Poly(acrylamide-*co*-methacryloxyethyl-*N,N,N*-trimethyl-ammoniumchloride)
PB	Poly(butadiene)
PE	Poly(ethylene)
PP	Poly(propylene)
PGA	Poly(L-glutamic acid)
PGE	Poly(glutamic acid benzyl ester)
PHIC	Poly(hexylisocyanate)
PIB	Poly(isobutene)
PipAAm	Poly(*n*-isopropyl-acrylamide)
PS	Poly(styrene)
PSSNa	Sodium poly(styrene sulfonate)
PTMAC	Poly(acrylamide-*co*-(*N,N,N*-trimethyl-*N*-[2-methacryloethyl]-ammonium chloride)
PVA	Poly(vinyl alcohol)
PVC	Poly(vinyl chloride)
q	Polydispersity correction factor
q_n	Polydispersity correction factor for number average molar masses
q_w	Polydispersity correction factor for mass average molar masses
Q	Polydispersity
r	Radius of a sphere
$\langle r^2 \rangle^{1/2}$	Average end-to-end distance
r_o	End-to-end distance of a polymer coil with unperturbed dimensions
r_{oo}	End-to-end distance of a freely jointed chain
R	Radius, gas constant
R_a	Inner radius of the outer cylinder
R_G	Radius of gyration
$R_{G,\theta}$	Radius of gyration at theta-condition
$R_{H,\theta}$	Hydrodynamic radius at theta-conditions
R_i	Outer radius of the inner cylinder
R_s	Radius of the shaft
R_{sph}	Equivalent radius of a hard sphere
R_1, R_2, R_3, R_4	Radii of the double gap fixture
Re	Reynolds number
s	Slope
SEC	Size exclusion chromatography
t	Time
t_b	Flow time in a capillary viscosimeter with a known capillary constant

$t_{solution}$	Characteristic measurement time of a polymer solution
$t_{solvent}$	Characteristic measurement time of the solvent
t_{min}	Minimum flow time
T	Temperature, torque
TCB	Trichlorobenzene
U	Heterogeneity
u	Velocity
Δu	Velocity difference
V	Volume
V_{coil}	Equivalent volume of a single polymer coil in solution
$V_{polymer}$	Volume of polymer in solution (equivalent fraction)
$V_{solvent}$	Volume of free solvent
VI	Viscosity index
w(M)	Fraction of molar mass
x	Distance
x_i	Molar fraction
x, y, z	Direction in space
w_i	Mass fraction
y_1, y_2	Fraction (w_1, x_i, or ϕ_i)
α	Cone angle
α_{RG}	Expansion factor for the radius of gyration
$\alpha^3_{[\eta]}$	Expansion factor for the intrinsic viscosity
δ_{cc}	Radius ratio R_a/R_i
ε	Correction factor of the Flory constant for non-theta-conditions
ϕ, ϕ_i	Volume fraction
Φ	Flory constant
Φ_θ	Flory constant at theta-condition
$\dot{\gamma}$	Shear rate
$\dot{\gamma}_{crit}$	Critical shear rate of the onset of non-Newtonian flow behavior
$\dot{\gamma}_{max}$	Maximum shear rate
ϑ	Hagenbach correction
η	Dynamic viscosity
$[\eta]$	Intrinsic viscosity, limiting viscosity number
$[\eta]_\theta$	Intrinsic viscosity at theta conditions
η_0	Zero shear viscosity, viscosity of a solution before the onset of aging effects
η_1, η_2	Viscosity of different solvent components
η_i	Relative viscosity increment
η_{inh}	Inherent viscosity
η_{ln}	Logarithmic viscosity number
η_p	Polymer viscosity
η_s	Solvent viscosity
η_t	Time dependent viscosity
η_{sp}	Specific viscosity
η_r	Relative viscosity

ν	Kinematic viscosity, Flory exponent (exponent of the R_G-M-relationship)
θ	Theta-condition, torsion angle
ρ	Density
ρ_1, ρ_2	Density of different solvent components
ρ_{equ}	Equivalent density (density of the polymer coil in the solution conformation without the solvent)
$\rho_{solution}$	Solution density
$\rho_{solvent}$	Solvent density
σ	Hindrance parameter
σ_{21}	Shear stress
σ_a	Shear stress at the outer cylinder wall
σ_i	Shear stress at the inner cylinder wall
τ	Bond angle, relaxation time
ω	Angular frequency
ξ	Radius conversion factor
ζ	Correction factor for short range rotational interactions

Table of Contents

1 Introduction and Objective

Viscosimetry is one of the basic analytical methods for examining the structure and the properties of polymer fluids. Many different polymers from varying production processes are utilized in solution in diverse applications. Furthermore, it is possible, by varying the molar mass of one and the same polymer system, to tailor specifically the properties of the polymer to the area of use. Polymers are chain- or thread-shaped molecules that take on a coil-like structure in dilute solutions. Even though the molecule continuously changes its form under the influence of statistic thermodynamic movement, it fills out a constant spherical space in solution over a time average. In principle, a molecule can also take the shape of compact aggregated spherical particles (glycogen, globular proteins), or in the case of ionic polymers take on a linear rod-like structure, since through the same charges on the chain repelling forces are taking effect (Fig. 1.1).

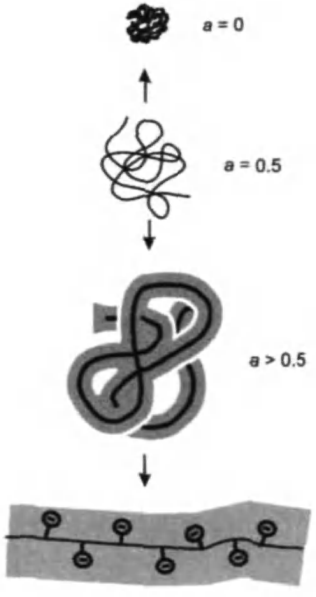

Fig. 1.1. Schematic representation of the different stages of the solution conformation of dissolved polymers: compact (a=0), pseudo-ideal unperturbed dimensions (theta conditions, a=0.5), good solvent (a<0.5), rigid rod ($a \leq 2$)

Theoretical approaches to determine solution structures of neutral polymers act on the assumption of the pseudo ideal state. Here the solvation forces from the solvent and the aggregation forces of the chain segments are in an equilibrium where the coil appears to be unaffected by forces. This pseudo ideal state is called the theta state. Theta conditions exist when the exponent a of the $[\eta]$-M-relationship has the value a=0.5 and at the same time the value of the second virial coefficient is A_2=0 (see the chapter "The $[\eta]$-M-relationship" in this monograph). Accordingly, a pseudo ideal solvent is called theta solvent and the corresponding temperature is called theta temperature. As Flory showed in his Nobel price lecture [1], the theta state can be described mathematically exactly from the chemical structure of the chain.

Real polymer solutions mostly do not occur in the theta state. Both, the undisturbed dimensions of the polymer coils and other states of solution can be experimentally determined with the help of viscosimetry.

Polymers in solution are used in a broad range of molar masses in a multitude of applications. Ultra high molecular polyelectrolytes (polycations) are used as flocculation agents for wastewater treatment. Here, the electrostatic interactions of the polymer and the solid particles in the solution are used [2, 3]. The use of either polycations with a high molar mass or a combined use of polycations and polyanions depends on the separation problem [4]. Other polymers with high molar masses are being used for the drag reduction in aqueous solutions [5], e.g. poly(ethylene oxide) (PEO) to increase the range of fire extinguishing systems and oil-soluble vinyl copolymers or poly(isobutene) (PIB) in oil pipelines [6]. Other application areas include the use of sodium poly(acrylamide-*co*-acrylate) (PAAm/AAcNa) in enhanced oil recovery (polymer flooding) [7]. Even bodily biopolymers with a high molar mass, such as the hyaluronic acid in the synovial fluid of the knee joint provide, for example, the right lubrication [8, 9]. Polymers with a very low molar mass, such as poly(acrylic acids) are used as encrustation inhibitors. Other low molar mass polymers such as poly(methylmethacrylate) or styrene-isoprene- or styrene-butadiene copolymers with molar masses of 1×10^4–2×10^4 g/mol are utilized to improve the viscosity index (VI) of motor oils [10]. Biopolymers from renewable sources find many areas of use in solution. An example is hydroxyethyl starch (HES) with a range of the molar mass of $M=7\times10^4$–3×10^5 g/mol for the use in medical applications as blood plasma expander [11, 12]. In this case, the colloid osmotic pressure of the polymer is used to propagate the flow of tissue water into the veins. Additional areas of application for polymers with a broad molar mass range are given in Fig. 1.1.

For all the polymer solutions described above, a characterization of the molar mass and the flow properties had to be made in order to tailor the properties to the area of use. Practically the determination of the molar mass and the solution structure is done using viscosimetry. The solution structure, or to be more precise, the solution conformation of a polymer is the constant volume requirement of the coiled thread-like molecule over the time average. The description of the dimensions of the coil is made in practice by using the intrinsic viscosity $[\eta]$ that represents a measure for the density of the thread-like molecule in solution. Within a

theta solvent, the polymer thread can be viewed as infinitely thin for all practical reasons (Fig. 1.1).

In a so-called "good" solvent the solvating envelope around the polymer chain increases, the thread appears to become thicker, and the volume requirement increases (see Fig. 1.1). The volume requirement also increases with an increasing molar mass and the accompanying elongation of the polymer chain. The effect of this increased volume requirement on the flow behavior of the solution can be measured directly using viscosimetry. Especially for the very broad range of molar masses in which polymers in solution find applications (Fig. 1.2), the measurement of the viscosity is a method of characterization, which can be used over the whole range.

The viscosity of a polymer solution is not only dependent on the molar mass, but also on the concentration, the solvent, the type and composition of the polymer solution fraction, the temperature and the pressure. The measurement of the viscosity, therefore, is not only for the practical and simple determination of a single product trait. Besides a simple single-point measurement and the quality control, viscosimetry allows for a much deeper insight into the flow properties of a polymer solution. The increase of the internal friction of a solution (the "viscosity") can be

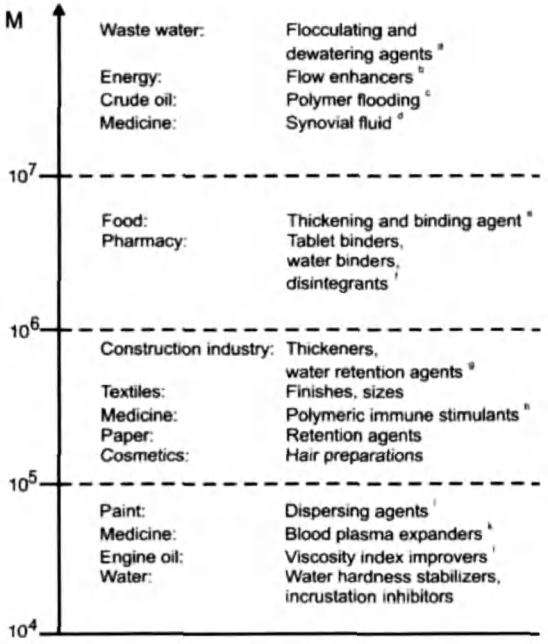

Fig. 1.2. Application areas of polymers in solution, depending on the wide range of molar masses. For further reading on the listed subjects. a:[2–4], b:[5, 6], c:[7, 78, 79], d:[8, 9], e:[80, 81], f:[82], g:[83], h:[84], i:[85, 86], k:[11, 12], l:[10]

Table 1.1. Problem solving via viscosimetric parameters and structure-property relationships

Task	Measurement categories
Viscosity level	η, η_r, η_{sp}, η_{red} (single point measurements)
Polyelectrolyte character	η_{sp}, η_{red}, salt concentration
Molar mass	$[\eta]$,$[\eta]$-M-relationship
Conformation	$[\eta]$, a, α^3
Change in conformation, (solvent influence), aging	η, $\eta_r[\eta]$, solvent, time, temperature
Structure-impact	$[\eta]$ for special applications

described using well-defined laws of physics that themselves offer further information about the structure of the polymer in solution and its interaction with the solvent. Besides determining the pure viscosity using viscosimetry, it is possible to get information about the molar mass of the polymer, its interaction with solvent molecules (especially the size of the surrounding solvent envelope and therefore the density of the polymer in solution), the rigidity of the chain, the volume requirement and the dimensions of the polymer coil (radius of gyration), the critical concentration c*, the intermolecular interactions of the polymer coils, and special structure parameters of a system from comparative measurements. Furthermore, direct information about the solution structure can be obtained using an $[\eta]$-M-relationship (Kuhn-Mark-Houwink-Sakurada-relationship).

For practical reasons, it is especially relevant to be able to determine directly the molar mass M of a polymer from the $[\eta]$-M-relationship using only simple viscosimetry. However, often it is enough to be able to perform a single-point measurement with viscosimetry in order to verify the product properties for the daily incoming and outgoing goods control. Relevant application areas are listed in Table 1.1.

Since the knowledge about molar mass determination using viscosimetry and determination of the coil dimensions is of fundamental importance for technical problem solving, these are the main topics of this book. It will give detailed case studies and theoretical background about the different independent variables, like concentration, molar mass, quality of the solvent, chemical nature of the polymer, polyelectrolyte character, composition of copolymers, influence of the substitution pattern for renewable raw materials and the degree of branching.

Before the practical aspects of viscosimetry and the theoretical interpretation of the experiments can be discussed, it is necessary to go into detail about the basic concepts of viscosimetry.

2 Basic Concepts

2.1 Viscosity

The viscosity η is defined as the ratio of the shear stress σ_{21} and the shear rate $\dot{\gamma}$:

$$\eta = \frac{\sigma_{21}}{\dot{\gamma}} \tag{2.1}$$

The shear stress σ_{21}, as can be seen in Fig. 2.1, is the force F [N] that is exerted on the surface element A [m^2] parallel to the direction of the flow:

$$\sigma_{21} = \frac{F}{A} \tag{2.2}$$

The shear stress has the unit [Pa], which is the same as for a pressure. In former times, the unit [dyn/cm^2] was often used:

$$1\ \text{Pa} = 1\ \text{N/m}^2 = 10\ \text{dyn/cm}^2 = 1\ \text{kg/(m/s}^2) \tag{2.3}$$

The shear rate $\dot{\gamma}$ describes how fast the fluid layers move in respect to one another in a laminar flow profile. It is described as the ratio of the velocity difference Δv [m/s] of two fluid layers and the distance Δh between them. The unit of the shear rate is a reciprocal time and is given as [s^{-1}]:

$$\dot{\gamma} = \frac{\Delta v}{\Delta h} \tag{2.4}$$

The dynamic viscosity η (see Eq. 2.1) has the unit [Pa s]. An old unit is [P] ("Poise"):

$$1\ \text{Pa s} = 0.1\ \text{P} = 1\ \text{N s/m}^2 = 1\ \text{kg/(s m)} \tag{2.5}$$

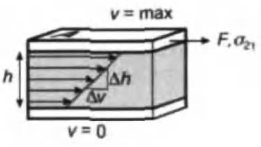

Fig. 2.1. Schematic representation of a flow field between two parallel plates. The force F acts on the area A, resulting in the shear stress. The shear rate is determined by the velocity difference Δv between two fluid layers separated by the distance Δh

Table 2.1. Dynamic viscosities for different fluids at 20 °C (Data from [19, 113])

Substance	Dynamic viscosity η (mPa s)
Gas/air	0.01–0.02/0.018
Pentane	0.23
Acetone	0.32
Benzine	0.54–0.65
Water	1.00
Ethanol	1.2
Quicksilver	1.55
Blood plasma 20 °C/37 °C	1.7/1.2
Wine/fruit juice	2–5
Milk/cream	5–10
Glycol	20
Sulfuric acid	25
Sugar syrup (60%)	57
Olive oil	~100
Motor oil	50–1000
Gear oil	300–800
Ricinus oil	1000
Glycerin	1480
Honey	$\sim 10^4$
Silicon rubber	10^4–10^5
Bitumen, tar, pitch	10^6–10^{12}
Glas melt (500 °C)	$\sim 10^{15}$

Often, the units [mPa s] or [cP] are used for a liquid with low viscosity, since water has a viscosity of about 1 mPa s:

$$1 \text{ mPa s} = 1 \text{ cP} \tag{2.6}$$

The broad range of dynamic viscosities of different liquids is shown in Table 2.1.

The equations shown above are strictly speaking only valid if the flow profile is a pure laminar flow. Above a critical shear rate, the flow becomes increasingly turbulent and deviates from laminar flow. This kind of shear flow is not reached in the viscosimeter types described below though.

A different form of viscosity, one that is used widely in viscosimetry, is the kinematic viscosity ν, which is defined as the ratio of the dynamic viscosity η and the density ρ of the solution [kg/m^3]:

$$\nu = \frac{\eta}{\rho} \tag{2.7}$$

The kinematic viscosity has the unit [mm^2/s], older units are Stokes [St] or centiStokes [cSt]:

$$1\ \mathrm{mm^2/s} = 1\mathrm{cST} = 0.01\ \mathrm{St} \tag{2.8}$$

The use of the kinematic viscosity especially in the viscosimetry is widespread, because many of the types of viscosimeters described in a later chapter determine a kinematic viscosity directly, that can be transformed into the dynamic viscosity, if the density of the solution is known. However, since the deduction of the following units of viscosimetry is done using the dynamic viscosity, the term "viscosity" will mean the dynamic viscosity.

The ratio of the viscosity η of a solution to that of the pure solvent η_s is the relative viscosity and is called η_r (instead of η_{rel}) according to IUPAC (International Union of Pure and Applied Chemistry):

$$\eta_r = \frac{\eta}{\eta_s} \tag{2.9}$$

If the viscosity is conceived as the sum of the solvent viscosity η_s and a viscosity from the dissolved polymer η_p,

$$\eta = \eta_p + \eta_s \tag{2.10}$$

then the ratio of the dissolved polymer viscosity η_p to the solvent viscosity η_s can be called the specific viscosity η_{sp} of the polymer in that solvent:

$$\eta_{sp} = \frac{\eta_p}{\eta_s} = \frac{\eta - \eta_s}{\eta_s} = \eta_r - 1 \tag{2.11}$$

According to IUPAC, the specific viscosity is a relative viscosity increment η_i, but this is not common practice in the literature. An overview of the viscosities η_s of common solvents can be found in Table 2.2. With that list, the relative or specific viscosity can be calculated from the dynamic viscosity of a polymer solution.

It is important to notice that the listed solvent viscosities are only valid for the given temperature. Viscosities for many substances at different temperatures or with different solvent systems are listed, e.g. in the "Handbook of Physics and Chemistry" [13] or in [14]. The often-used dependence of the viscosity of water on the temperature is listed in Table 2.3. The viscosity of mixtures of solvents needs a special treatment, and the increase in viscosity through intermolecular interactions between solvent molecules in multicomponent solvents will be discussed in the later chapter "The viscosity of mixtures of solvents".

Table 2.2. Dynamic viscosities of solvents at a pressure of 1 bar and for different temperatures [25]. Values in parentheses for higher saturation pressures

Solvent	Dynamic viscosity η (mPa s)			
	0 °C	20 °C	50 °C	100 °C
n-Pentane	0.281	0.230	(0.177)	(0.119)
Cyclopentane	0.557	0.438	0.324	–
n-Hexane	0.397	0.310	0.241	–
Cyclohexane	–	0.97	0.610	–
Heptane	0.519	0.410	0.303	(0.198)
Octane	0.703	0.538	0.386	0.245
Nonane	0.97	0.711	0.489	0.299
Decane	1.29	0.91	0.602	0.360
Undecane	1.71	1.17	0.75	0.435
Dodecane	2.28	1.52	0.92	0.51
Tetradecane	–	2.18	1.25	0.68
Dichloromethane	0.536	0.434	–	–
Trichloromethane	0.70	0.562	0.42	–
Tetrachloromethane	1.35	0.974	0.654	(0.387)
Benzene	0.91	0.650	0.437	(0.261)
Toluene	0.77	0.588	0.420	0.272
o-Xylene	1.10	0.803	0.556	0.346
Acetone	0.390	0.316	0.244	–
2-Butanone	0.539	0.423	0.311	–
2-Pentanone	0.644	0.501	0.366	0.238
Methanol	0.81	0.588	0.393	–
Ethanol	1.78	1.20	0.698	(0.326)
Isopropanol	4.56	2.37	1.03	–
Glycol	55	19.9	6.6	1.99
Glycerol	12100	1480	180	14.8
Cyclohexanol	–	68	12.1	–
Cyclohexanone	–	2.18	1.29	–
Formic acid	–	1.78	1.03	0.542
Acetic acid	–	1.22	0.791	0.458
Nitric acid	2.28	0.88	0.61	–
Sulfuric acid	48	25	8.8	–

Table 2.3. Viscosity of water from 0 °C to 100 °C. Data from [13, 25]

Temperature (°C)	Dynamic viscosity η (mPa s)	Kinematic viscosity ν (mm²/s)
0	1.792	1.792
5	1.520	1.520
10	1.3069	1.3073
15	1.1383	1.1393
20	1.0020	1.0038
25	0.8903	0.8929
30	0.7975	0.8010
35	0.7193	0.7236
40	0.6531	0.6582
50	0.5470	
60	0.4665	
70	0.4040	
80	0.3544	
90	0.3145	
100	0.2818	

2.2 Molar Mass

The most important value for characterizing a polymer is its molar mass. Because of the very small mass m_{coil} of a polymer coil, it is standard practice to use the mass of 6.023×10^{23} particles. This amount is called a mol and is denoted with the Avogadro constant N_A. The mass of one mol molecules has the symbol M and the unit [g mol^{-1}]:

$$M = m_{coil} \cdot N_A \tag{2.12}$$

For polymers, the degree of polymerization P is often used instead of the molar mass M. The degree of polymerization describes how many monomer units make up a polymer molecule. The molar mass M can be calculated from the degree of polymerization, if the molar mass of a monomer unit in the chain M_u is known:

$$M = M_u \cdot P \tag{2.13}$$

The molar mass of a monomer unit M_u can be calculated through simple addition of the (known) molar masses of the atoms that make up the monomer unit. It is important to notice that for example for polymers from polycondensation reactions the molar mass of a monomer unit M_u in the polymer chain is not equal to the molar mass of a monomer unit before the polymerization!

In most cases, not all polymer molecules have the same molar mass or degree of polymerization in a polymer sample. To describe exactly the polymer sample, it would be necessary to determine the fraction $w(M)$ of each molar mass M in the

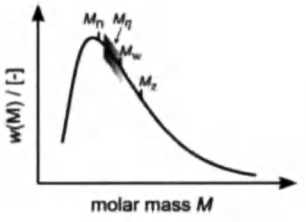

Fig. 2.2. Schematic molar mass distribution with number average molar mass M_n, mass average molar mass M_w, centrifuge average molar mass M_z and viscosity-average molar mass M_η

sample as shown in Fig. 2.2. This exact determination of the molar mass distribution is a considerably more elaborate effort, so that almost solely the mean values of the molar mass of a polymer are given.

For the mean values, the following different cases are listed below:

The number average molar mass M_n is the mean value of the molar mass that can be calculated from the ratio of the sum of the mass of all molecules and the number of all molecules:

$$M_n = \frac{\Sigma\, n_i \cdot M_i}{\Sigma\, n_i} = \Sigma\, x_i \cdot M_i \tag{2.14}$$

The mass average M_w of the molar mass can be determined, if the fractions of the mass

$$m_i = n_i \cdot M_i \tag{2.15}$$

of the single molecules are averaged over the total mass:

$$M_w = \frac{\Sigma\, m_i \cdot M_i}{\Sigma\, m_i} = \Sigma\, w_i \cdot M_i \tag{2.16}$$

Since the higher molar masses in a sample are weighted higher for the mass average molar mass, it has generally a higher value than the number average molar mass (see Fig. 2.2).

A less used mean value is the centrifugal average molar mass M_z. It shows even higher values than the mass average molar mass:

$$M_z = \frac{\Sigma\, m_i \cdot M_i^2}{\Sigma\, m_i \cdot M_i} \tag{2.17}$$

With viscosimetry, a viscosity average molar mass is determined. As can be seen in Fig. 2.2, it lies between M_n and M_w. Its definition and determination is described in detail in a later chapter "The viscosity average of the molar mass".

The determination of a mean value of a molar mass does not give any information about the form and breadth of the distribution of the molar mass. To get some

information about the molar mass distribution, the ratio of M_w and M_n can be calculated:

$$Q = \frac{M_w}{M_n} \tag{2.18}$$

The ratio Q is called the polydispersity of a polymer sample, sometimes given as the inhomogeneity U of a sample:

$$U = Q - 1 \tag{2.19}$$

A polydispersity of Q=1 indicates a sample with no distribution and a single molar mass. The bigger Q gets, the broader the distribution becomes.

3 Execution of Viscosity Measurements

3.1 Introduction

The practical execution of viscosity measurements requires the use of good laboratory practice even if the experiments are relatively easy to do. Besides the basic safety regulations for the use of chemicals and liquids, a tidy sample preparation and a precise execution of the experiment is the prerequisite for the determination of the exact viscosimetry parameters of a polymer solution.

The choice of the viscosimeter depends on the kind of polymer, solvent and the kind of assignment. The next section "Types of viscosimeters" is therefore dedicated to the detailed description of established viscosimeter types and measurement techniques, the measurement ranges and limits and also the effort that is associated with each. From high-precision standard measurement systems according to DIN or ISO standards to very simple systems like the flow cup or the Brookfield viscosimeter, the following section describes in detail the exact steps to take for the determination of a viscosity like sample preparation, cleaning of the viscosimeter, execution of the experiment and the subsequent analysis of the experimental data. An extra section is devoted to the viscosimetry of surface-active substances, which can lead to foam formation in a sample. Another important point is the so-called aging of polymers that can lead to changing viscous properties within a sample after only a couple of days of storage. Below, the phenomenon of aging and its effects on the execution of the experiment is discussed in detail.

3.2 Types of Viscosimeters

There are roughly three classes of viscosimeters available: the capillary viscosimeter, the rotational viscosimeter, and the falling-ball viscosimeter. Both the capillary and the rotational viscosimeters are built in different versions that allow for the exact determination of the viscosity in well-defined flow fields. Especially rotational viscosimeters allow the exact adjustment of a constant flow profile, thus are available in high precision and expensive versions as rotational rheometers. Capillary viscosimeters are the best compromise between the exact determination of viscosity and a well-priced measurement device, and are therefore the most commonly found type of viscosimeters. Both rotational and capillary viscosimeters are available in simple and inexpensive versions as Brookfield viscosimeters and flow

cups. These instruments do not have a defined flow profile and cannot be used to determine an exact viscosity, but are widely used in quality control and management. Falling-ball viscosimeters are also relatively simple measurement devices with an undefined flow profile, but allow for a determination of the viscosity after a calibration with standard fluids.

3.2.1 Capillary Viscosimeter

Capillary viscosimeters belong to the type of effluent viscosimeters. They are the most commonly used viscosimeters for the determination of the intrinsic viscosity.

Different capillary viscosimeters are shown in Fig. 3.1. The flow of the examined liquid sample is achieved through gravity. The sample flows under its own weight through a known capillary length l with a defined radius R. The running times of a known sample volume between two measurement points (M_1 and M_2) are measured. With the help of these running times, the kinematic viscosity can be calculated. In contrast to other types of viscosimeters, the temperature in capillary viscosimeters can be well regulated, because the entire closed capillary can be immersed in a water bath. For the Ostwald viscosimeter shown in Fig. 3.1a it is important that an exact amount of the sample is filled into the device, since the hy-

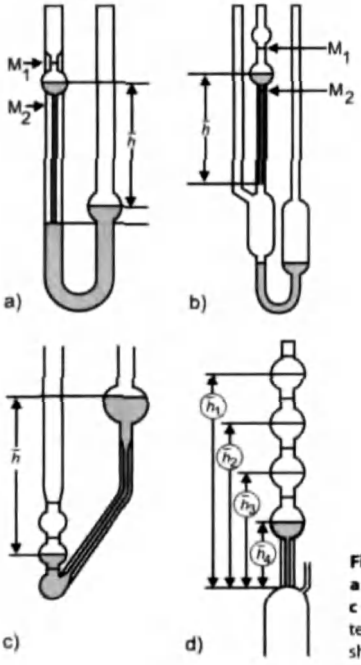

Fig. 3.1 a–d. Different types of capillary viscosimeters: **a** Ostwald viscosimeter; **b** Ubbelohde viscosimeter; **c** Cannon-Fenske viscosimeter; **d** multi-level viscosimeter for different average heights $\bar{h}$ and different average shear rates in one experiment

drostatic pressure depends on the filling level. When different filling levels are used, different running times are measured for the same sample.

Ubbelohde viscosimeters build according to ISO 3105 or DIN 51562, as shown in Fig. 3.1b have the advantage that the hanging level of the capillary accounts for the same mean height $\bar{h}$ of the outgoing liquid and therefore for the hydrostatic pressure.

The Cannon-Fenske viscosimeter build according to DIN 51336 (Fig. 3.1c) can be used to measure non-transparent liquids that leave a film on the glass in the area of the measurement points and therefore do not allow for exact time taking. A specialty is the multi-level Ubbelohde viscosimeter shown in Fig. 3.1d, which can be used to investigate the dependence of the viscosity on the shear rate. Because of the various heights of the fluid levels, different pressures and therefore different shear rates affect the liquid. Thus it can be determined if the measured viscosities are independent of the shear stress or the shear rate.

Besides these viscosimeters, several other special-purpose designs have been developed (Micro Ubbelohde viscosimeter DIN 51562; Cannon-Ubbelohde semi micro viscosimeter ISO 3105; BS/IP/U-tube viscosimeter DIN 51372; BS/IP/SL viscosimeter ISO 3105; Vogel-Ossag DIN 51561). Those are tailored to specific needs and are not further discussed at this point.

The Hagen-Poiseuille Law describes the capillary flow for Newtonian fluids:

$$\frac{V}{t} = \frac{\pi \cdot R^4 \cdot \Delta p}{8 \cdot \eta \cdot l} \tag{3.1}$$

with

$$\Delta p = \rho \cdot g \cdot \bar{h} \tag{3.2}$$

The volume V that flows through the capillary per time unit t is determined by constant geometry factors, like the radius R and the length l of the capillary, the mean filling height $\bar{h}$, and the variable quantities of the liquid, the viscosity η, and the density ρ. By applying external pressure, it is possible to vary the pressure term in the Hagen-Poiseuille Law. With these capillary viscosimeters build according to DIN 53014, it is possible to set up different shear viscosities. With the so-called high-pressure capillary viscosimeters, shear rates of up to $10^6\ s^{-1}$ can be reached. The velocity profile in the capillary is shown in Fig. 3.2.

At the capillary wall, the shear stress σ_{21} and the shear rate $\dot{\gamma}$ are at a maximum, whereas the flow velocity is zero. The flow velocity has its maximum in the middle, where the shear stress and the shear rate are zero. The quantities are functions of the radius R, therefore only the maximum values at the wall of the capillary are given, since they are necessary for the exact determination of the intrinsic viscosity:

$$\sigma_{21,\max} = \frac{\Delta p \cdot R}{2 \cdot l} \tag{3.3}$$

$$\dot{\gamma}_{\max} = \frac{4 \cdot V}{\pi \cdot R^3 \cdot t} \tag{3.4}$$

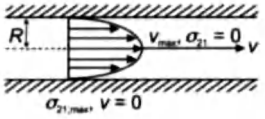

Fig. 3.2. Velocity profile in a capillary viscosimeter. The fluid velocity v has a parabolic profile with a maximum in the middle of the capillary; the shear rate $\dot{\gamma}$ and the shear stress τ have a maximum at the capillary wall and are zero in the middle of the capillary

Even under normal ambient pressure relatively high shear rates occur at the wall of capillary viscosimeters (especially for small capillary diameters and low viscosity liquids), that can lead to a falsification of the results for so-called non-Newtonian liquids (see later in this monograph). In Tables 3.1 and 3.2 the maximum occurring shear rates for the admissible minimal running times t_{min} of the capillary are given for the standard Ubbelohde capillary viscosimeter (ISO 3105) and the Micro Ubbelohde capillary viscosimeter (DIN 51562).

For polymer solutions that are in the non-Newtonian flow region for the shear rate range of the capillary, the shear rate calculated with Eq. (3.4) has to be corrected. The true shear rate at the capillary wall can be determined using the Weissenberg-Rabinowitsch equation [15]:

$$\gamma_{max,corr} = \frac{1}{4}\,\dot{\gamma}_{max}\left[3 + \frac{d\ln\left(\frac{V}{t}\right)}{d\ln\sigma_{21,max}}\right] \tag{3.5}$$

Table 3.1. Parameters for Ubbelohde Capillary Viscosimeters (ISO 3103 and DIN 51562) with Ref. numbers 501.., 530.., 532.., capillary number (No.), capillary diameter (D), capillary constant (K), minimum measurable flow time (t_{min}), maximum shear rate at minimum flow time ($\dot{\gamma}_{max}$) and kinematic viscosity range (ν)

Ref. No.	No.	D/(mm)	K	t_{min}/(s)	$\dot{\gamma}$/(s^{-1})	ν/(mm^2/s)
...00	0	0.36	0.001	300	4290	0.2–1.2
...03	0c	0.46	0.003	160	3790	0.5–3
...01	0a	0.53	0.005	120	3306	0.8–5
...10	I	0.63	0.01	90	2613	1.2–10
...13	Ic	0.84	0.03	50	1983	3–30
...11	Ia	0.95	0.05	40	1711	5–50
...20	II	1.13	0.1	40	1008	10–100
...23	IIc	1.50	0.3	40	430	30–300
...21	IIa	1.69	0.5	40	300	50–500
...30	III	2.01	1	40	179	100–1000
...33	IIIc	2.65	3	40	78	300–3000
...31	IIIa	3.00	5	40	54	500–5000
...40	IV	3.60	10	40	31	1000–10,000
...43	IVc	4.70	30	40	14	3000–30,000
...41	IVa	5.34	50	40	9	5000–50,000
...50	V	6.40	100	40	5	10,000–100,000

Table 3.2. Parameters for Micro-Ubbelohde Capillary Viscosimeters (DIN 51562) with Ref. numbers 536.., 537.., 538.., capillary number (No.), capillary diameter (D), capillary constant (K), minimum measurable flow time (t_{min}), maximum shear rate at minimum flow time ($\dot{\gamma}_{max}$) and kinematic viscosity range (ν)

Ref. No.	No.	D/(mm)	K	t_{min}/(s)	$\dot{\gamma}$/(s^{-1})	ν/(mm^2/s)
...10	I	0.40	0.01	30	4085	0.4–6
...13	Ic	0.53	0.03	30	1756	1.2–18
...20	II	0.70	0.1	30	762	4–60
...23	IIc	0.95	0.3	30	304	12–180
...30	III	1.26	1	30	130	40–800

However, in viscosimetry using a capillary viscosimeter normally the viscosity is not calculated from the maximum shear rate and the shear stress but rather from the Hagen-Poiseuille-Law (Eq. 3.1).

Since the laminar capillary flow takes time to develop, an inlet length can be defined, wherein the layers close to the wall are decelerated and the layers close to the axis are accelerated. From this stems a correction term from Hagenbach for the Hagen-Poiseuille-Law, that is especially relevant for short measuring times. Another correction has to be made for the increased friction in the inlet length that leads to an increased pressure drop. This error can be corrected according to Couette through an apparent extension of the capillary. These two terms are combined into the Hagenbach-Couette correction term, which is added to the equation for the viscosity:

$$\eta = \frac{\pi \cdot R^4 \cdot \Delta p \cdot t}{8 \cdot V \cdot l} - \frac{m \cdot \rho \cdot V}{8 \cdot \pi \cdot l \cdot t} \tag{3.6}$$

The correction factor m can be determined by comparing measurements of capillaries with the same diameter but different lengths. Generally, the Hagenbach-Couette correction term comes in a table together with commercially available capillaries.

3.2.1.1 Flow Cups

The flow cup is a relative-capillary viscosimeter. The outlet nozzle is a very short capillary, and the propulsive force is the hydrostatic pressure of the liquid, which during the tests flows under its own weight from the central outlet nozzle on the bottom of the cup. The flow cup has a defined geometry with a given volume for the sample liquid. For the measurement, the nozzle is closed, the cup is filled with the sample liquid and then the time is measured that the liquid takes to completely drain out of the cup. From that efflux time, the kinematic viscosity ν is calculated. Up to this day many different flow cups are used around the world (see Fig. 3.3).

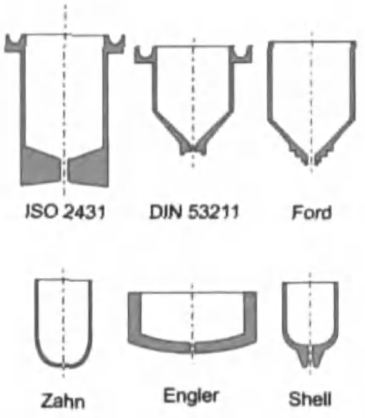

Fig. 3.3. Several designs for flow cups [19]

For efficient viscosimetric measurements, only ISO cups (ISO 2431) should be used. The length of the capillary is 20 mm. The shear rates lie—for efflux times t=30–100 s—between $\dot{\gamma}$=60 and 1500 s^{-1}. They depend on the capillary radius R, which can be varied through interchangeable outlet nozzles. The calculation of the mean shear rate is made using the Hagen-Poiseuille-Law:

$$\dot{\gamma} = \left(4 \cdot \frac{V}{t \cdot \pi \cdot R^3}\right) \tag{3.7}$$

The shear rate changes in a certain range with the decreasing liquid volume during the experiment. Note that only in case of a Newtonian flow process a calculation makes sense.

For all flow cups there are equations—mostly empirical and therefore complicated—for the calculation of the kinematic viscosity ν from the efflux time t. For ISO Cups the following equations are given:

3-mm nozzle: $\nu = 0{,}443 \times t - (200/t)$;

4-mm nozzle: $\nu = 1{,}37 \times t - (200/t)$;

5-mm nozzle: $\nu = 3{,}28 \times t - (200/t)$;

6-mm nozzle: $\nu = 6{,}90 \times t - (200/t)$;

In former times many different cups have been used: AFNOR (previously: Coups NFT, France), BS cup (British Standards), DIN (since 1941; DIN 53 211, replaced in 1996 with DIN-EN-ISO 2431), Engler (since 1884; for mineral oils, DIN 51560), Ford (ASTM D1200), Shell (ASTM D4212), Zahn (ASTM D4212) and for mineral oil, liquid bitumen or tar: Redwood (IP 70/57) and Saybolt Universal/Saybolt Furol (ASTM D88, D244, D2161, E102). The different cup types differ in the capillary

diameter and the different angles within the cup itself. Because of the different cups different units are used: Degree Engler (°*E*), Redwood-1-Seconds (*RIS*), Saybolt/Universal-Seconds (*SUS*) or Saybolt/Furl-Seconds (*SFS*) [16].

The test with the flow cup is a one-point measurement and only gives a viscosity value that is determined under the given measurement conditions. In the short capillary, no stationary laminar flow profile can be build up, since the inlet and acceleration part is often greater than the viscous part. Because of the undefined flow form in the short capillary, further parameters cannot be determined. Even though flow cups are still a widely used method for the determination of a characteristic efflux time for example for coating compounds.

3.2.2 Rotational Viscosimeter

According to DIN 53018, simple rotational viscosimeter have a coaxial cylinder system with a cup (inner radius R_a) and a cylinder with an outer radius R_i and a length h, that is lowered into the cup. For the Couette system, the outer cup is moved and the measurement of the torque T takes place at the inner cylinder. For the Searle system on the other hand, the inner cylinder is moved.

For the Couette type, the radius dependent speed of rotation ω is zero for the case of $r=R_i$ and at the maximum of the outer cup for the case of $r=R_a$. The shear stress σ_{21} is nearly constant for a narrow gap:

$$\sigma_{21} = \frac{T}{2\pi \cdot R_i \cdot R_a \cdot h} \tag{3.8}$$

This is in contrast to the capillary viscosimeter, where the shear stress always increases over the radius from zero to the maximum. The constant shear rate and therefore the viscosity can be calculated:

$$\dot{\gamma} = \frac{2 \cdot R_i \cdot R_a}{R_a^2 - R_i^2} \cdot \omega \tag{3.9}$$

$$\eta = \frac{(R_a^2 - R_i^2)}{4\pi \cdot h \cdot R_a^2 \cdot R_i^2} \cdot \frac{T}{\omega} \tag{3.10}$$

Since the front surfaces of the cylinder also have an influence on the torque, it is necessary to have a correction of the end effects. The end effects are perceptible in an apparent increase of the cylinder length h. The correction term Δh is determined by measuring with different depths of immersion, and then plotting the measured torques T against the depth of immersion. From the equation

$$T = \frac{4\pi \cdot \omega \cdot R_i^2 \cdot R_a^2 \cdot \eta}{R_a^2 - R_i^2} \cdot (h + \Delta h) \tag{3.11}$$

Δh is the negative y-axis intersection. This is independent of the viscosity η, i.e., all straight lines for all different viscosities intersect at the point T=0 and h=$-\Delta h$. This is only true for Newtonian fluids or in the case of a Non-Newtonian fluid if the region of the zero shear viscosity is not left in any measurement. Since the shear rate is not constant over the gap, another correction for non-Newtonian fluids, similar to the Weissenberg-Rabinowitsch correction (Eq. 3.5), is necessary:

$$\dot{\gamma} = \dot{\gamma}_{\text{measured}} \frac{1 - \left(\frac{R_i}{R_a}\right)^{2s}}{s \cdot \left[1 - \left(\frac{R_i}{R_a}\right)\right]^2} \tag{3.12}$$

s is the slope of the double logarithmic scale of $\dot{\gamma}$ over σ_{21}:

$$s = \frac{d \log \dot{\gamma}}{d \log \sigma_{21}} \tag{3.13}$$

The correction term has to be calculated for each shear stress value and used to correct the shear rate. If s is very small, it is negligible.

Because of centrifugal forces in the Searle System, crosscurrents can arise, that are called Taylor vortices. Couette Systems on the other hand have the disadvantage that temperature control of the rotating outer cylinder is achieved only with complicated equipment. Most rotational viscosimeters are therefore built in the Searle Type.

The option of shear rate control in rotational viscosimeters makes it possible to detect shear rate dependent flow phenomena. Variants with high-precision motors and torque sensors are called rheometers and are used in research projects above and beyond the viscosimetry (see also [15, 17, 18]). In these instruments, other measurement systems besides the cylinder geometries are used, that are described in the following chapters.

3.2.2.1 Coaxial Cylinder

For the rotational cylinder, viscosimeter shown in Fig. 3.4 the geometry parameters are given in ISO 3219. In order to narrow down the slit width to achieve a linear distribution of the stresses and shear rate, the maximum admissible radius ratio δ_{cc} is given in the ISO norm:

$$\delta_{cc} = R_a / R_i \leq 1,2 \tag{3.14}$$

For standard systems δ_{cc}=1.0847 should be the norm. In addition, h/R_i=3, h'/R_i=1, h''/R_i=0,3 (with the radius R_S of the measurement body) and α=120°+1°. The size of h, h', h'' and R_S are all relative to R_i.

The mean shear stress σ_{21}=$(\sigma_i+\sigma_a)/2$, with σ_i at the measurement body surface and σ_a at the measurement cup surface, is in the ISO measurement system:

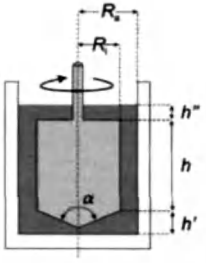

Fig. 3.4. Concentric cylinders according to ISO 3219

$$\sigma_{21} = \frac{(1 + \delta_{cc}^2)}{2 \cdot \delta_{cc}^2} \cdot \frac{M}{2\pi \cdot h \cdot R_i^2 \cdot c_L} \tag{3.15}$$

The resistance coefficient c_L=1.10 describes the front surface correction. A greater measurement body radius increases the measurement sensitivity.

For all ISO cylinder measurement systems applies [19]:

$$\sigma_{21} = \frac{0.0446 \cdot M}{R_i^3} \tag{3.16}$$

The average shear rate in a cylinder system $\dot{\gamma}=(\dot{\gamma}_1+\dot{\gamma}_a)/2$, with $\dot{\gamma}_1$ at the measurement body surface and $\dot{\gamma}_a$ at the measurement cup surface, is for ISO measurement systems:

$$\dot{\gamma} = \frac{(1 + \delta_{cc}^2)}{(\delta_{cc}^2 - 1)} \cdot \omega \tag{3.17}$$

For all ISO cylinder measurement systems applies: $\dot{\gamma} = 1.291 \times n$ (n is the rotational frequency). The shear rate in an ISO cylinder is not constant at every position in the measurement slit. Between the two measurement surfaces, the total difference of the shear rates even in a narrow ISO system is about 16%.

The viscosity in an ISO cylinder system is given as

$$\eta = \frac{0.0446 \cdot M}{R_i^3 \cdot 1{,}291 \cdot n} \tag{3.18}$$

3.2.2.2 Cone and Plate Systems

Cone and plate systems (Fig. 3.5) allow the build up of a defined constant shear field with only a very small amount of polymer liquid. Because they require high precision motor drives and sensors and because of the high error when wrong distance alignments are used, cone and plate systems are mostly found in expensive rheometers that are capable of more sophisticated kinds of stress fields than the pure shear flow. Nevertheless, they can be used for pure viscosity measurements.

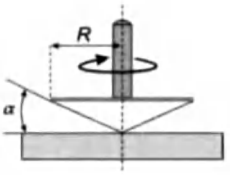

Fig. 3.5. Cone and plate fixture. The tip of the cone is flattened (~50 µm) to avoid additional friction

The cone and plate system according to DIN 53018 and ISO 3219 [27] has a measurement body with a cone like surface and a flat plate. The geometrical measures of the cone are defined by the cone radius R and the cone angle α. The ISO norm recommends α=1° and excludes cone angles of α>4°. In order to avoid any errors due to direct contact of the cone with the plate, the tip of the cone is taken off for several micrometers. Particles of a size that can cause them to be stuck in the slit between the cone and the plate have to be removed before the measurement. If this is not possible, the parallel disc system has to be used instead.

The (constant) shear stress in a cone and plate system depends on the cone radius R and is given as

$$\sigma_{21} = \frac{3 \cdot M}{2\pi \cdot R^3} \tag{3.19}$$

A greater cone radius increases the measurement sensitivity for smaller torques or shear stresses. The shear rate is independent of the position in the measuring slit:

$$\dot{\gamma} = \frac{\omega}{\tan \alpha} \tag{3.20}$$

The simplified equation presumes that at small angles α tanα is equal to α. As mentioned above, α=1° is preferred. The viscosity is given as

$$\eta = \frac{3 \cdot M \cdot \alpha}{2\pi \cdot R^3 \cdot \omega} \tag{3.21}$$

3.2.2.3 Parallel Discs

Parallel disc systems have the advantage that even solutions with larger particles or highly viscous or elastic liquids can be measured, since the liquid is, unlike the cone and plate system, not squeezed in a narrow slit. Like the cone and plate system, it is mostly used in expensive rheometer systems, but can also be used for viscosimetry measurements. A disadvantage in comparison with the cone and plate system is that no constant shear rate is build up over the radius of the plate. Especially with high molecular samples, there is a chance of determining the wrong viscosity values (see also later in this monograph Chapter 5.4 "Shear rate").

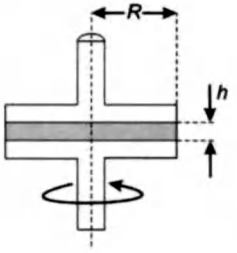

Fig. 3.6. Parallel disc fixture

The geometry of the measuring plate is determined through the plate radius R (Fig. 3.6) and the distance h. According to DIN 53018, the plate distance h should be very small compared to the radius R. In a parallel disc system, the shear stress is also only dependent on the radius:

$$\sigma_{21} = \frac{2 \cdot M}{\pi \cdot R^3} \tag{3.22}$$

The shear rate is given as:

$$\dot{\gamma} = \frac{\omega \cdot R}{h} \tag{3.23}$$

Other than in a cone and plate system, it is not constant over the radius! The mean viscosity is calculated from:

$$\eta = \frac{2 \cdot M \cdot h}{\pi \cdot R^4 \cdot \omega} \tag{3.24}$$

3.2.2.4 Mooney/Ewart System

The Mooney/Ewart system (Fig. 3.7) is a combined cylinder/cone and plate geometry, wherein the same shear rate or shear stress can be set up over the whole measuring slit (cylinder and cone and plate).

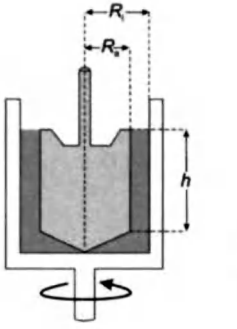

Fig. 3.7. Mooney-Ewart fixture. Combination of a cone and plate and a concentric cylinder fixture

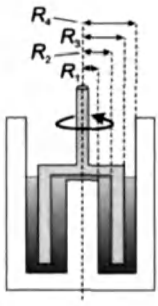

Fig. 3.8. Double gap fixture for low viscous fluids

Since the surface for the power transmission is big compared to that of the plain cone/plate system, the Mooney/Ewart system is suitable for low viscous liquids. The advantage in comparison to normal cylinder geometries is the avoidance of edge effects at the lower cylinder wall for the smaller sample volume. The Mooney/Ewart system requires a high precision setting of the vertical distance, and is therefore as the cone and plate system mostly used in rheometer systems.

3.2.2.5 Double Gap Systems

For very low viscous liquids, the double gap geometry (DIN 54453) is used (Fig. 3.8). The shear area is doubled in comparison to the plain cylinder geometry, since both gaps are filled with the liquid. The inner cylinder should also be temperature controlled to avoid a temperature gradient in the liquid. According to DIN 54453, a radius ratio of 1.15 should not be exceeded:

$$\frac{R_4}{R_3} = \frac{R_2}{R_1} \leq 1.15 \tag{3.25}$$

3.2.2.6 Zimm-Crothers Viscosimeter

The Zimm-Crothers viscosimeter is a special rotational viscosimeter that works with extremely low shear rates [20]. For this reason, the Zimm-Crothers viscosimeter is particularly suitable for solutions of polymers with very high molar masses. The range of molar masses that can be detected reaches from 10^5 to approx. 10^8 g mol^{-1}. A rotating magnetic field induces a torque in a magnetisable rotor that floats in the sample solutions carried by the surface tension. Using a ferromagnetic material for the rotor and avoiding turbulent flow fields, the induced torque depends only on the geometry parameters of the rotor and its remanence characteristics but not on the rotational speed of the magnetic field.

The shear stress acting on the sample is

$$\sigma_{21} = \eta \cdot \frac{8 \cdot \pi \cdot \omega \cdot r_1^2 \cdot r_2^2}{(r_1 + r_2)^2 \cdot (r_2 - r_1)^2} \ln \frac{r_2}{r_1} \tag{3.26}$$

where ω is the rotational speed of the rotor, which is determined by a marker on the rotor that crosses a light barrier with each rotation. The photo sensor is placed outside of the rotor for older types of Zimm-Crothers viscosimeters in contrast to Fig. 3.9. Zimm-Crothers viscosimeters can measure at shear stresses down to $\sigma_{21}=10^{-4}$ Pa and shear rates of 0.2 s^{-1} [21]. With these values, the intrinsic viscosities for all dilute polymer solutions can be determined in the zero shear viscosity range. If only the relative viscosity is of interest, the determination of the rotational time of the rotor is sufficient:

$$\eta_r = \frac{t_{solution}}{t_{solvent}} \tag{3.27}$$

One disadvantage of this method is that it is not possible to measure surface-active solutions, since the self-centering of the rotor depends on the surface tension of the sample. Another disadvantage is that different types of rotors for different solution densities have to be used.

3.2.2.7 Brookfield Viscosimeter

Brookfield viscosimeters also belong to the group of rotational viscosimeters. In contrast to the devices described earlier, this viscosimeter does not generate a defined shear field. The Brookfield viscosimeter consists mainly of a disc or a pin that is rotating with a defined velocity in the sample fluid. The torque that is required to achieve this rotational speed directly yields a viscosity through comparison with a calibration fluid. The range of measurable viscosities can be adjusted by variation of the disc geometry.

Because of the lack of a defined shear field, there is no correlation between rotational speed and shear rate possible. Hence, a determination of the influence of the shear rate on the viscosity is not possible.

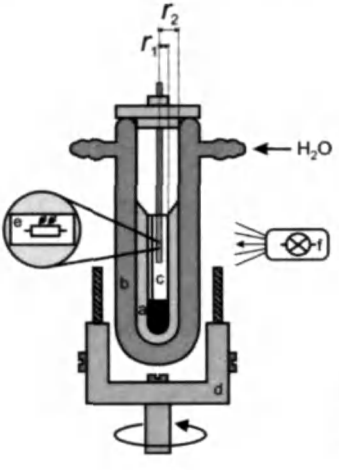

Fig. 3.9 a–f. Zimm-Crothers viscosimeter for low shear rates and strongly shear thinning fluids: **a** test fluid; **b** stator with temperature control liquid; **c** rotor; **d** rotating magnet; **e** photo diode; **f** light source

Nevertheless, Brookfield viscosimeters are the widely used devices for quality management; they are a fast and cheap alternative for conducting one-point measurements. In addition to this, many companies use special stirring systems that are custom tailored for a specific application. However, for the determination of the intrinsic viscosity or an exact viscosity devices like the Brookfield viscosimeter are not appropriate.

3.2.3 Falling Sphere Viscosimeters

3.2.3.1 The Free Falling Sphere

A falling sphere viscosimeter (Fig. 3.10) consists of a tube with the radius R, which is filled with the sample solution. In this tube, a sphere with the radius r is falling through the sample fluid. After a short period of acceleration, the velocity reaches a constant value, which results from the equilibrium between frictional resistance and gravity. The time t is measured that the sphere needs to cover the distance l between two marks M_1 and M_2.

The calculation of the viscosity is based on Stokes' Law, which is effective for infinitely expanded fluids:

$$\eta = \frac{2 \cdot g \cdot r^2 \cdot \Delta\rho \cdot t}{9 \cdot l} \tag{3.28}$$

Infinitely expanded means for practical use that $R \gg 10r$. $\Delta\rho$ is the difference between the density of the sphere and the fluid. Thus the viscosity η is a function of the falling time t. For a ratio of radii of $r/R \approx 0.1$, the equation has to be corrected according to Schurz [22]:

$$\eta_{corr} = \eta \cdot \left(1 - 2.1 \cdot \frac{r}{R}\right) \tag{3.29}$$

It is important that the sphere velocity does not increase too much, so that inertia effects can be neglected. The Reynolds number Re

$$Re = \frac{r \cdot \rho \cdot v}{\eta} \tag{3.30}$$

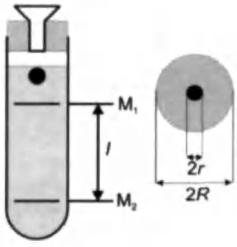

Fig. 3.10. Falling sphere viscosimeter

has to be smaller than 0.3. In this equation, v is the velocity of flow. For Re between 0.3 and 1 a correction term has to be added according to Oseen [22]:

$$\eta_{corr} = \frac{\eta}{1 + 0{,}188 \cdot Re} \tag{3.31}$$

The advantage of this type of viscosimeter is an easy temperature control. The disadvantages of this method are the growing influence of wall effects with the declining ratio of r/R, short measuring times in low viscous fluids and irregular velocities in inhomogeneous and high viscous fluids.

3.2.3.2 The Höppler Viscosimeter

A special form of the falling sphere viscosimeter is the Höppler viscosimeter (Fig. 3.11), which works with a sphere with a diameter very close to the diameter of the sloped tube.

The determination of the viscosity with this device is done according to DIN 53015. The relative flow around the sphere is similar to the flow through a gap. In the Höppler viscosimeter, the slope of the falling tube is 10° and its diameter is 16 mm. In this case, a sphere with a diameter of approx. 15 mm is used to achieve a sliding state. Evaluation of the state of flow is very difficult and in some cases impossible. For this reason, a calibration of the device with a calibration fluid is very important. With these calibration measurements, a constant K can be obtained:

$$\eta = K \cdot \Delta\rho \cdot t \tag{3.32}$$

The influence of the Reynolds number Re is negligible, because in contrast to a free falling sphere, the flow profile is dominated by the wall effects. The diameter of the sphere should not be too small. If the gap between the tube and the sphere gets smaller than 0.1 mm, the effects of roughness of the tube and sphere gain too much influence on the results. An evaluation of the shear rate is not possible, so that an application of this type of viscosimeter for fluids with a strong non-Newtonian flow behavior is not advisable. An attempt to empirically determine the shear rate in a micro falling sphere viscosimeter is described in [23].

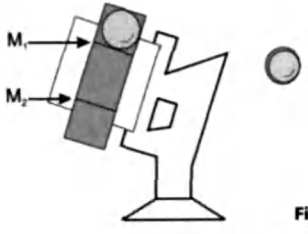

Fig. 3.11. Höppler viscosimeter

3.2.3.3 The Viscobalance

The principle of the viscobalance as a "pulling sphere viscosimeter" is related to the falling sphere viscosimeter. However, in this case the sphere is attached to the viscobalance and pulled through the sample fluid in a calibrated tube. The traction is usually measured by different weights that are applied on the other side of the arm of the balance. A determination of the viscosity η via the time t needed for the movement of the sphere along a defined distance has to be done via the following equation:

$$\eta = F \cdot G \cdot t \tag{3.33}$$

with F the so-called sphere factor for a given sphere and G the applied force.

If F is unknown, the sphere factor has to be determined as described for the Höppler viscosimeter via calibration measurements. An exact evaluation of the state of flow is not possible. When a doubling of the traction does not lead to half the measuring time, it is very likely that the sample shows a non-Newtonian flow behavior, since the product of force and time should be constant for a Newtonian fluid. Advantages of the viscobalance are the great measuring range and the possibility to examine nontransparent and high viscous fluids of unknown density.

3.3 Experimental Proceedings for a Viscosimetric Measurement

The most commonly used type of viscosimeter for the determination of the intrinsic viscosity or for single point measurements is the capillary viscosimeter. As the reproducibility with this type of viscosimeter depends on the clean execution of the measurement, a detailed description of the proceedings for a viscosimetric measurement is given below.

3.3.1 Sample Preparation

For viscosimetric measurements to have a good reproducibility, a clean preparation of the sample is very important (Fig. 3.12). The preparation must be identical for every polymer solution that has to be measured, so that a reliable comparison of the measurements is assured.

For an exact initial mass of the polymer, the net amount of polymer in the sample has to be determined. For hygroscopic polymers (like the water-soluble polymer PAAm), the dry content of the polymer has to be known. The dry content of the polymer can be determined via thermogravimetric methods or lyophilization. In addition to this, the salt content of the polymer (for commercial ionic polymers up to 30%) or the content of other foreign matter has to be determined, for example via reprecipitation or washing of the sample. When this is done, it is advisable to define a standard unit for the concentration. Since the unit for the intrinsic vis-

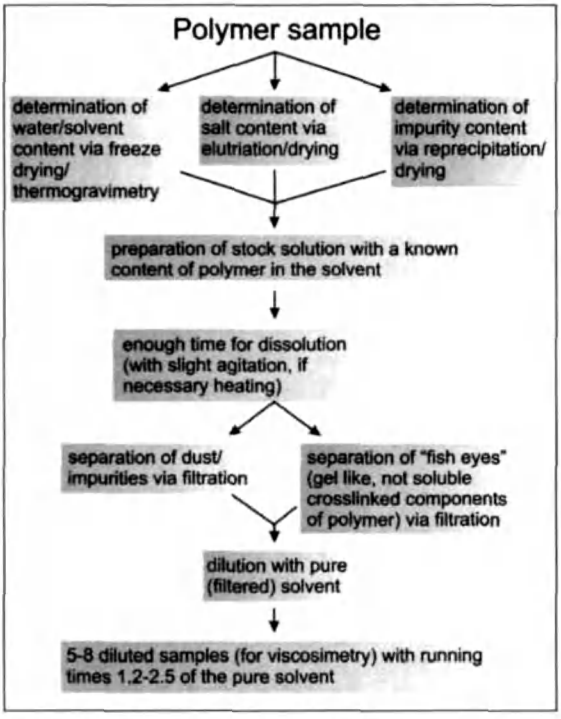

Fig. 3.12. Flowchart of the sample preparation for viscosimetric measurements

cosity itself is stated as [ml g^{-1}] (or [cm^3 g^{-1}]), it is advisable to define the initial concentration standard as [g ml^{-1}] or [g cm^{-1}]. It should also be kept in mind that for solvents other than water the solvent density cannot be assumed ~1 g ml^{-1}. In these cases, the unit [g ml^{-1}] should not be referred to as a mass concentration.

For polyelectrolytes a dilute salt solution is recommended as a solvent (for example a 0.1 mol/l $NaNO_3$ solution) in order to eliminate polyelectrolyte effects. In addition to this, a disinfectant should be added (for example 200 ppm NaN_3) against bacterial contamination of aqueous polymer solutions.

When the stock solution is prepared (the stock solution should not exceed the running time of the solvent by a maximum factor of 2.5, this is to be determined empirically), a suitable dilution series can be made. For best results, there should be at least seven (better ten) different concentrations measured for a single polymer, to minimize the error of the following linear regression. Even the solution with the lowest concentration should give results that can be evaluated. As a guideline the relative viscosity should not fall below η_r=1.2 for the lowest concentrated solution. To achieve a good homogeneity in the solution, the dissolution process should last for at least a few hours (the use of a shaker table is recommended). An-

other way to shorten the time for dissolving the polymer is to work at a higher temperature, but it has to be made sure that the higher temperature does induce any degradation or chemical reaction on the polymer.

Right before the viscosimetric measurement the sample should be filtered to avoid a pollution of the viscosimeter with dirt particles. Solutions with a low viscosity should be filtered with a glass filter of a porosity of 2–4 (equals a pore diameter of approx. 10–100 µm); higher viscous solutions should be filtrated with filters of mesh size ~0,3 mm (see DIN 4188).

In addition to impurities like dust particles, so-called "fisheyes", that are typical especially for commercial products, have to be separated from the solution. These "fisheyes" are due to non-homogenously dissolved, partially crosslinked polymers that appear at synthesis conditions for high molar masses where an additional initiation of the reaction becomes necessary [24]. In addition to this, so-called "hot spots", which can appear in a polymerization reactor, also lead to polymers that show insoluble fractions. The simplest reason for these "fisheyes" though is that the solution itself is not yet homogenously dissolved. In this case, a longer dissolution time is advised.

These general difficulties arising during sample preparation are shown in Fig. 3.13 for a concrete example. The polymer carboxymethyl cellulose (CMC), dissolved in 0.1 mol/l $NaNO_3$, shows the previously described "fisheyes", that are insoluble even after a long period of time. Separation of these gel particles via filtration or centrifugation leads, in dependence of the separation conditions, to very different results. This is shown in Fig. 3.13 for a plot of the reduced viscosity vs the concentration in order to determine the intrinsic viscosity. The gel particles show very different sizes; very small ones can pass the pores of a filter and lead to a strong increase in viscosity, while big particles are able to absorb temporarily the higher molecular section of a polymer and thus hold them back in the filter residue.

The pore size itself does not provide enough information on how the viscous properties of a solution vary with filtration. For example the results of the viscosimetric measurements after filtration with a nylon net filter with 11 µm pore size lie above these for filtration with a glass filter with a pore size of 100–160 µm. In addition to this, absorption on the filter material or a degradation of the polymer in elongational flow fields in the filter pores influence the actual molar mass that passes through the filter. There is no universal rule for the right way of filtration depending on what polymer system is used; this has to be determined via comparing measurements.

If the solutions have to be stored over longer periods of time, it has to be kept in mind that some polymers are likely to show aging effects (see section "Aging and criteria of stability" below).

3.3.1.1 Cleaning of a Viscosimeter

For the execution of exact viscosimetric measurements with good reproducibility, a clean viscosimeter is of crucial importance. Even the smallest dust particles on a microscopic scale lead to a deviation of the running times of several percent. The dust particles that adhere to the wall of the capillary lead to a longer running time,

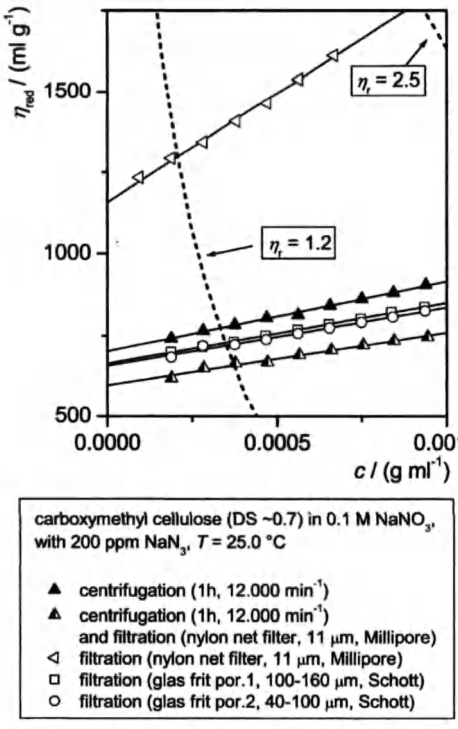

Fig. 3.13. Reduced viscosity as a function of the concentration for a carboxymethyl cellulose (DS~0.7) with a high content of gel particles. The solution was filtered with different types of filters and pore sizes. In addition to the filtration in some solutions the gel particles were separated by centrifugation

which is hard to identify as such. This error becomes even more important with a decreasing diameter of the capillary.

Similar to dust particles, oil films and grease lead to longer running times and therefore to measuring errors.

When solutions with different surface tensions are to be analyzed with the same capillary, it has to be neatly cleaned in advance, because even the smallest drops of solution that adhere at the wall of the capillary again lead to measuring errors. In order not to contaminate the viscosimeter with the cleaning detergent, it is advisable to filtrate the cleaning detergent itself. The use of filters made of paper is not advisable because of microscopic fibers that could peel off the filter.

As a cleaning agent an aqueous solution of 15% hydrochloric acid and 15% hydrogen peroxide is suitable. If it is the first cleaning of a viscosimeter after a longer storage time or transportation this solution is to be left in the capillary for at least 12 h. It is important that not only the capillary part but also every other part of the glass viscosimeter is filled with the cleaning agent.

Afterwards the viscosimeter is to be washed with deionized water and then with a water soluble and volatile organic solvent like acetone. To accomplish the cleaning process, the viscosimeter has to be dried with dust free air via compressed air (it has to be assured that no oil is released from the compressed air connector).

WARNING: The viscosimeter must not be dried in a cabinet drier because that could lead to a permanent alteration of the capillary diameter!

Between the single measurements, the viscosimeter is to be flushed with dust free solvent, and one has to assure that the capillary itself is rinsed properly with an appropriate device like a water jet pump. This step should be repeated at least three times. If such a device is not available, the cleaning agent should be left in the capillary for at least 10 min.

3.3.2 Execution of the Experiment and Test Evaluation

A dilution series of at least six solutions is prepared of the stock solution of the polymer in a solvent of choice (see above) so that the range of relative viscosities varies from 1.2–2.5 and that the minimum running time of the capillary is not surpassed. As the relative viscosities and the running times are not determined before the test itself, the dilution series has to be modified afterwards if necessary, when the relative viscosities can be estimated in dependence of the concentration. If it should be necessary, a different type of capillary has to be chosen to fit the observed running times to the requirements of the capillary. In Tables 3.1 and 3.2 the minimal running times and the range of kinematic viscosities are listed for the standard types of capillaries according to ISO 3105 and DIN 51562. The corresponding dynamic viscosities have to be evaluated with knowledge of the density ρ of the solution via Eq. (2.7). The viscosimeter has to be cleaned according to the discussion in the previous section before it is filled with the sample solution. Afterwards the sample is filled into the filling tube of the viscosimeter (right tube in Fig. 3.1b). The right fluid quantity is usually marked by two marks on the viscosimeter. After the filling of the viscosimeter, it has to stay in the temperature control bath for a sufficient period of time, so that the temperature is adjusted. Generally, 10 min is a long enough period to ensure a constant temperature. To achieve the best accuracy of measurement with a capillary viscosimeter the temperature should not vary more than ±0.1 K.

After closing the pressurization opening (left tube in Fig. 3.1b), the sample solution is to be carefully sucked in the middle tube via a water jet pump or an adequate device, until the meniscus clearly exceeds the upper mark M_1. Opening all three openings starts the experiment. This causes the liquid column to separate at the lower end of the capillary and to form a suspended level at the dome of the reservoir. The measurement is executed by measuring the time it takes for the meniscus of the solution to drop from the mark M_1 to M_2.

First of all the pure solvent has to be measured several times until the running times are constant. The capillary then is to be filled and flushed with the sample solution of the lowest concentration for at least two times. With the third filling, the measurement can start by recording the running times. For an evaluation of the ex-

act running time, the sample solution should be measured at least three times, but not more than five times, because of possible evaporation of the solvent. The other sample solutions are measured the same way afterwards in the order of increasing concentrations.

The use of an automatic filling device and the determination of the running time via light barriers at the marks M_1 and M_2 facilitates the measurement and minimizes personal errors.

The running times have to be corrected afterwards. For short running times this is to be done according to Hagenbach (see "Capillary viscosimeter" above). In practice, this is usually not done according to Eq. (3.6) though, but correction times ϑ are listed by the manufacturer for the particular capillary and have to be subtracted from the measured running times t:

$$t_{corr} = t - \vartheta \tag{3.34}$$

The running times that are tabulated together with the correction times also give information on the range of running times for which a sensible evaluation is possible.

It still has to be considered that even with the Hagenbach correction, the minimal running time for the particular capillary must not be under run (see Tables 3.1 and 3.2). For capillaries with big inner diameter (bigger than No. Ic in Tables 3.1and 3.2) a Hagenbach correction is not possible, because the correction would only apply for running times below the minimum running time. According to Eq. (3.6) the viscosity can be determined via the (corrected) running times. With only the running time and the density of the solution being variables, the constant values are merged to the so-called capillary constant K:

$$\eta = K \cdot \rho \cdot t \tag{3.35}$$

The capillary constant K is a specific factor for a particular capillary and is determined and provided by the manufacturer. Should this constant not be known, it has to be determined. This is to be done with a calibration oil of known viscosity η and density ρ via the running times and Eq. (3.35) or comparison of the running times t of a given solution in the unknown capillary with the running times t_b of the same sample in a capillary with a known capillary constant K_b:

$$K = \frac{K_b \cdot t_b}{t} \tag{3.36}$$

For both methods, maintaining of a constant temperature is of great importance. A good review of calibration fluids for viscosimeters is given in [25].

A redetermination of the capillary constant is also necessary when solutions were used that are corrosive for glass or the viscosimeter was repaired by a glassblower. In these cases, great alterations of the capillary constant may result and a recalibration is necessary. The required procedures for a recalibration are usually also described in the viscosimeter manual.

For the evaluation of the kinematic viscosity ν via Eq. (2.7) only the determination of the running time is necessary. Knowledge of the density of the solution is not necessary:

$$\nu = \frac{\eta}{\rho} = K \cdot t \tag{3.37}$$

In addition, for the evaluation of the relative viscosity η_r (Eq. 2.9), only the determination of the running times of the pure solvent and the sample solution is necessary. The assumption is that the density of the dilute polymer solution $\rho_{solution}$ equals the density of the pure solvent $\rho_{solvent}$, because of the very small polymer concentration η_r:

$$\eta_r = \frac{\eta}{\eta_s} = \frac{K \cdot \rho_{solution} \cdot t_{solution}}{K \cdot \rho_{solvent} \cdot t_{solution}} = \frac{t_{solution}}{t_{solvent}} \tag{3.38}$$

For the determination of the intrinsic viscosity $[\eta]$ of the particular polymer-solvent system, the specific viscosity η_{sp} can be evaluated from the relative viscosity η_r via Eq. (2.11). With the specific viscosity and known concentrations of the solutions, the evaluation can be directly started according to Eq. (4.9) in "Determination of the intrinsic viscosity by viscosimetric measurements" in the next chapter. With the determined intrinsic viscosity $[\eta]$, the critical concentration of the viscosimetry can be evaluated according Eq. (7.7).

3.4 Viscosimetric Measurements of Surface-Active Samples

Viscosimetric measurements of surface-active samples in capillary viscosimeters are often hindered by vesication. In addition to a variation of the running times by bubbles of air in the reservoir and the no longer existing laminar flow profile in the capillary, an exact determination of the running times is not possible, because the foam formation on the fluid meniscus interface is particularly strong. Especially fully automated viscosimeter systems with light barriers at the marks M_1 and M_2 provide no exact data in this case.

In order to remove any bubbles from the capillary, the method described in Fig. 3.14 should be applied.

First of all the capillary is filled as normal with closed ventilation tube as shown in Fig. 3.14a. Afterwards the filling tube is to be closed (Fig. 3.14b), then the ventilation tube is to be opened and slight pressure has to be applied on the capillary tube manually (with a pipette filler for example). The bubbles have to be driven into the ventilation tube carefully so that the capillary is free of bubbles. It is important to assure that the meniscus in the capillary tube reaches the opening of the ventilation tube, but does not fall below the opening so that the bubbles can ascent into the ventilation tube completely. Afterwards the ventilation tube has to be closed and the capillary has to be refilled with bubble free solution from the reservoir

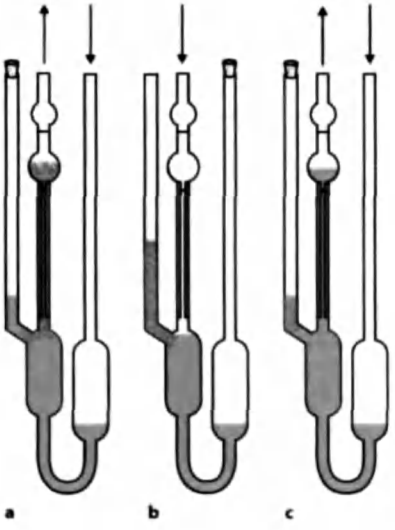

Fig. 3.14 a–c. Surfactant solutions in a capillary viscosimeter. To avoid bubbles in the capillary during the measurement: **a** fill the capillary as usual; **b** close the right tube and apply slight pressure to the middle tube. Push all solution with bubbles in the left tube; **c** close the left tube and refill the capillary. Repeat steps b and c if necessary

(Fig. 3.14c). The steps b) and c) have to be repeated if necessary until the meniscus in the capillary tube is absolutely free of bubbles. As a part of the sample solution remains in the ventilation tube with this method, more sample solution than the manufacturer of the viscosimeter recommends should be used.

3.5 Aging and Criteria of Stability

Time dependent effects on the material functions, that show a time dependent alteration of the viscosity, are widely known from medical, cosmetic, and pharmaceutical industries. For nearly all of these applications, substances usually consist of three or more ingredients, so that these aging effects are usually due to variations in the crystallinity or phase separation effects.

Water-soluble polymers on the other hand are simpler systems that have been used in a wide variety of technical applications in the past. To improve their effectiveness and to find new possible applications the structure in solution on a molecular basis was researched in detail. It was shown that different water-soluble polymers show various effects of instability that reduce their effectiveness for the particular application. This phenomenon called aging is known from literature and was discussed by different authors. An example for such an aging process is shown in Fig. 3.15.

This figure shows that the viscosity of PVA in DMSO is independent of the storage time in contrast to the aqueous solution, which shows an increase of the viscosity over time [26, 27]. In addition to this, the changes in the solution characteristics were determined via elastic and inelastic light scattering [28]. All authors

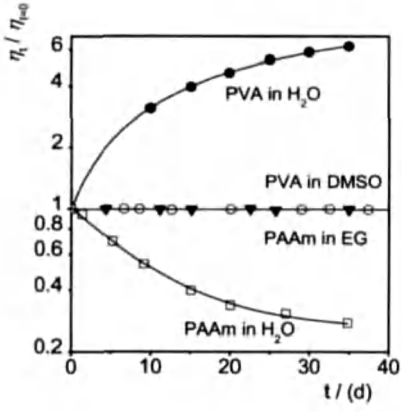

Fig. 3.15. Aging effects in polymer solutions. Quotient of the time dependent viscosity of a polymer solution, η_t, and the viscosity of a freshly prepared solution, η_0, as a function of the time t. The viscosity can increase with time as shown for poly(vinyl alcohol) (PVA), or decrease as shown for poly(acrylamide) (PAAm) in aqueous solution. Changing the solvent to dimethylsulfoxide (DMSO) or ethylene glycol (EG) can prevent the aging. Data from [30]

agree that association and reformation of the polymer molecules via hydrogen bonds or the formation of microgels in the form of small crystalline regions induce this aging phenomenon.

Besides an increase of the viscosity with storage time, polymers like poly(acrylamide)s or poly(acrylamide-*co*-acrylates) in aqueous solution show a decreasing viscosity and intrinsic viscosity with increasing storage time. Degradation of the polymer coil could be excluded as a reason for this aging behavior, so that a change in the conformation of the isolated coil is most likely to induce this decrease of the material functions with increasing storage time [29]. Analysis regarding the molar mass of the different PAAm samples showed that aging does not take effect below a molar mass of $M_w > 1 \times 10^6$ g mol^{-1}. In this range size exclusion chromatography (SEC) could show that the hydrodynamic radius decreased with increasing storage time. Light scattering on the other hand showed that the molar mass of the samples did not change with the storage time but that the radius of gyration decreased. For a detailed characterization of the influence of aging effects on the material functions see [29, 30]. Stabilization of PAAm over time was not possible via variation of the pH-value (1 to 12) or via addition of hydroquinone or sodium sulfate. In contrast to that, an addition of 2 vol.% 2-propanol to the aqueous solution or storage below 239 K stabilized the solution.

Comparison of the pure PAAm with the ionic poly(acrylamide-*co*-acrylates) (PAAm/AAcNa) showed that the viscosity of the ionic species decreased even stronger with time. The examined PAAm/AAcNa showed a decrease of more than 90% of its viscous behavior after storage in aqueous solution. Like for the pure PAAm, light scattering did not show a decrease in the molar mass for the PAAm/AAcNa [31–33].

The phenomenon of decreasing viscosity was also found in solutions of poly (L-glutamic acid) (PGA) [34]. Aqueous solutions of PGA showed a comparable aging effect like PAAm or PAAm/AAcNa at a constant pH-value of 5.7. Measure-

ments of the circular dichroism (CD) of these samples showed that at a temperature of 25 °C the angle of rotation decreased, because of a decreasing content of α-helices.

Another example for decreasing material functions in dependence of time is sodium poly(styrene sulfonate) (PSSNa). For a homologous series of this polymer, a decrease in viscosity was found above a molar mass of 1.8×10^6 g mol^{-1} [35]. The determination of the intrinsic viscosity described in Chap. 5, Fig. 4 was therefore only performed for molar masses $\leq 1.8\times10^6$ g mol^{-1}, because higher molar masses show a time dependent intrinsic viscosity. With the addition of high salt concentrations (0.5 mol/l Na_2SO_4) or low storage temperatures (−34 °C) those aging effects were eliminated.

Additional aging effects could be found for graft copolymers (starch-acrylamide copolymers [36], synthetic amylose [36], poly(acrylamide-*co*-methacryloxyethyl-*N,N,N,*-trimethylammoniumchloride) PAAm/M [30] and poly(acrylamide-*co*-sodium-2-sulfoethylmethacrylate) [37].

3.6 Storage Stability and Quality Management

The average molar mass is of crucial importance for polymers. The average molar mass characterizes the chain length of a polymer molecule, which is of great importance to the processing and overall performance of the polymer as described below.

The different types of stresses that act on the macromolecule can lead to changes in the main chain (usually degradation) so that they cannot be used anymore for their intended application. The determination of the average chain length or the average degree of polymerization is very important for the construction of production facilities, specification of optimal processing parameters and the determination of the physical and chemical characteristics of the product. Therefore, a characterization of the chain length is of crucial importance [38]. The quality management that has to be done in order to detect changes in the molar mass usually consists of viscosimetric measurements via capillary viscosimeters. The determined viscosity of the sample provides information on the resulting product profile and processability as shown in the following examples.

An application for viscosimetry is for oil and additives measurements in the petroleum chemistry. Here the viscosity is an important characteristic for the flow and lubricating properties of a specific oil. Via blending of different petroleum raffinates, basic oils with different viscosities can be obtained. The characteristic profile can then be further optimized by addition of chemical additives (for example viscosity index enhancers or oxidation or corrosion inhibitors). The potential of a lubricating film is dependent of its thickness, which is itself dependent of its viscosity. In addition to this, the viscosity of oil shows a strong dependence from the temperature. At low temperatures (in winter, cold start of the engine), the viscosity of an oil has to be high enough, so that the oil can still reach the wearing points. At high temperatures (in summer, very high strains), a good build-up of the lubri-

cating film has to be ensured, so that even at very low viscosities no breaking of the film occurs.

Furthermore the durability of an engine oil is limited because of aging effects that occur automatically with long duration times, but also with entering of grime and other foreign matter [39, 40]. For a production plant, regular measurements of the viscosity assure good product quality. In contrast to that, in a development facility the influence of the temperature on the viscosity of new oil-additive compounds is characterized. A commonly used characteristic for the viscosity-temperature behavior (VT-behavior) of oil is the viscosity index VI. The VI-value of oil is determined via the viscosities at 40 °C and 100 °C. A minor dependence of the viscosity on the temperature leads to a high VI-value, oils for engines and transmissions usually have high VI-values [41].

Another example for quality management via viscosimetry is the food industry. The raw materials, semi-finished products and end products used in the food industry have very different rheological properties. The temperature, content of water, strain, storage time and the conditions of transport are just a few parameters that have influence on the mainly non-Newtonian flow behavior of food masses. Knowledge of the viscosity is of crucial importance for the food industry and machine building, but in different regards [41].

Via the determined viscosities, useful information can be obtained about molecular structure and chemical constitution. For example, the knowledge of the viscosity is of crucial importance for the beer brewing process. A beer with a viscosity above 1,7 mPa s is hard to filtrate, which leads to a declining capacity. On the other hand, a higher viscosity has a positive effect on the wholeheartedness and the stability of the foam of the beer. For this reason the main aim of viscosimetric measurements here is the optimization of filtration methods and the quality control of malt, flavor and beer [42].

3.7 Single Point Measurements

The intrinsic viscosity usually is the characteristic value that is used to specify the storage stability and the quality of a product (see Chap. 4). Based on the storage stability a change of the intrinsic viscosity $[\eta]$ in dependence of the time gives information on the stability (aging, degradation). Based on a constant product quality (for example different batches), the intrinsic viscosity has to stay the same.

However, the determination of the intrinsic viscosity needs the preparation, filtration and determination of the running times of a series of concentrations for every measurement. The storage stability and the quality of the product can be controlled much easier via single point measurements however. Besides time and money saving, single point measurements do not need a range of concentrations for the determination of the intrinsic viscosity, but only the running time of a single concentration.

For this reason the concentration should be selected in the range of possible relative viscosities, that means the running time should be between 1–2.5 times the

running time of the pure solvent (see "Sample preparation" in this chapter). As it is always the same sample solution that is measured, it has to be prepared and homogenized only once. Filtration is the only step that is to be taken before measuring the running times.

When checking the storage stability of aqueous systems, one has to keep in mind that the solvent and the sample container are sterile to avoid degradation by microorganisms. For this reason an agent for sterilization should be added to the solvent, for example sodium azide NaN_3 (approx. 200 ppm).

Single point measurements are commonly used to determine the intrinsic viscosity via the so-called Fikentscher K-value. This method is, as shown in "Determination of the intrinsic viscosity by viscosimetric measurements" in Chap. 4, only applicable under very special conditions and should not be used anymore. Generally, single point measurements only serve for the determination of a viscosity value.

4 The Intrinsic Viscosity

4.1 The Dilute Solution

The number of parameters that have influence on the flow behavior of a polymer solution is, as will be shown in the upcoming chapters, enormous and makes it difficult to interpret the viscosimetric measurements. For this reason, viscosimetric measurements are carried out with dilute sample solutions to minimize the interactions of the single polymer molecules. In this case, only the interactions between the polymer and the solvent are determined. The dilute state of solution is shown in Fig. 4.1.

The polymer molecules are isolated from each other in solution. They take on the statistically most likely conformation and form a coil. The dimension of this coil in dilute solution is what affects the viscous properties of a polymer solution. Despite of the regional isolation between the coils, as shown in Fig. 4.1, there are interactions that take effect during the flow process. These interactions are only prevented when the state of the so-called *ideal dilute solution* is reached. In this case, the polymer concentration c→0 and the single polymer molecule only interacts with the solvent. The following description for the determination of the intrinsic viscosity is based on this idealized state of solution.

4.2 The Ideal Viscosity Correlation by Einstein

The viscosity enhancing properties of a polymer coil can be described via a Taylor-series:

$$\eta_{sp} = B_1 \cdot \phi + B_2 \cdot \phi^2 + B_3 \cdot \phi^3 + \ldots \tag{4.1}$$

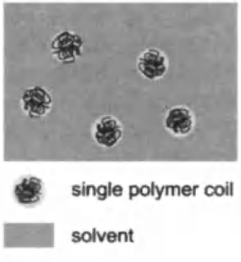

Fig. 4.1. Schematic view of a dilute polymer solution. The concentration is below the critical concentration c^* at which the solution volume is totally filled with polymer coils. Although the polymer coils are separated from each other, intermolecular interactions can still occur in a flow field

Here the fraction of the polymer in solution is given by the volume fraction ϕ:

$$\phi = \frac{V_{\text{polymer}}}{V_{\text{solution}}} \tag{4.2}$$

Fortunately, all higher powers in Eq. (4.1) can be disregarded for an ideal state of dilution! According to Einstein, the polymer coils are assumed to be perfectly inelastic and behave like hard spheres. Therefore, the following simple (and experimentally confirmed) relationship is obtained:

$$\eta_{\text{sp}} = 2.5 \cdot \phi \tag{4.3}$$

The volume of the polymer coils V_{polymer} can be described via the ratio of the mass m_{polymer} of the polymer to its density ρ_{equ}. This density ρ_{equ} does not correspond with the density in the dry state, but with the density of the polymer in solution, where solvent molecules surround the polymer chain:

$$\phi = \frac{V_{\text{polymer}}}{V_{\text{solution}}} = \frac{\left(\frac{m_{\text{polymer}}}{\rho_{\text{equ}}}\right)}{V_{\text{solution}}} = \frac{c}{\rho_{\text{equ}}} \tag{4.4}$$

With this, the specific viscosity is

$$\eta_{\text{sp}} = 2.5 \cdot \frac{c}{\rho_{\text{equ}}} \tag{4.5}$$

The specific viscosity, introduced in Chap. 2 still depends on the concentration according to Eq. (4.5). In order to obtain the true viscosity enhancing properties of a polymer, the reduced viscosity η_{red} is introduced:

$$\eta_{\text{red}} = \frac{\eta_{\text{sp}}}{c} = \frac{2.5}{\rho_{\text{equ}}} \tag{4.6}$$

This reduced viscosity only depends on a polymer specific property, its density in solution.

The unit of the reduced viscosity is defined via the used concentration unit, which is usually [g ml^{-1}] for viscosimetric measurements. With this, the unit for the reduced viscosity is [ml g^{-1}].

However, the reduced viscosity is also not totally independent of the concentration. Even though viscosimetric measurements are performed in the range of dilute solutions (below the critical concentration c*, where the single polymer coils start to interpenetrate), small polymer interactions (that are decreasing with a decreasing concentration) have to be considered. The true viscosity enhancing properties of a polymer is therefore the reduced viscosity extrapolated to c→0:

$$[\eta] = \lim_{\substack{c \to 0 \\ \dot{\gamma} \to 0}} \eta_{\text{red}} \tag{4.7}$$

According to the IUPAC nomenclature, the intrinsic viscosity should be named limiting viscosity number but this denomination is not widely used yet. As shown in Eq. (4.7), another condition for the determination of the intrinsic viscosity is that the shear rate has to be $\dot{\gamma} \rightarrow 0$. The influence of the shear rate on the determination of the intrinsic viscosity is discussed in Chap. 5.

The intrinsic viscosity $[\eta]$ has the same unit, [ml g^{-1}], as the reduced viscosity η_{red}. For a better understanding, the intrinsic viscosity can be considered as a measure for the volume demand of the single polymer coil in ideally diluted solution. The intrinsic viscosity is proportional to the reciprocal density of the polymer coil in solution according to Eqs. (4.6) and (4.7).

The intrinsic viscosity $[\eta]$ represents the most relevant variable to describe the viscous behavior of a polymer solution and most viscosimetric measurements have the aim of its determination. Therefore, in the upcoming chapters the focus will be on a detailed description of the determination of the intrinsic viscosity, the influence parameters on the intrinsic viscosity and the establishment of structure-property-relationships with the intrinsic viscosity.

4.3 Determination of the Intrinsic Viscosity by Viscosimetric Measurements

The intrinsic viscosity can be determined experimentally with the first two terms in Eq. (4.1). In a real polymer solvent system the state of an ideally dilute solution is never reached, even very dilute solutions have a finite amount of polymer. The second term in Eq. (4.1) captures these interactions between the single polymer coils in a not ideally dilute solution. When Eqs. (4.3)–(4.7) are inserted in Eq. (4.1), a linear dependency of the reduced viscosity η_{red} from the concentration c is obtained:

$$\eta_{red} = \frac{\eta_{sp}}{c} = [\eta] + B_2 \cdot [\eta]^2 \cdot c \tag{4.8}$$

For the execution of the experiment, the specific viscosities for a dilution series of the polymer have to be determined as described in Chap. 3. The intrinsic viscosity $[\eta]$ is determined from the y-axis intercept of a plot of η_{sp}/c (or η_{red}) vs the concentration c and an extrapolation of the linear fit of the data to $c \rightarrow 0$, as can be seen in Figs. 4.2 and 4.3.

The relative viscosities η_r of a dilution series (and therefore the relation of the running times of the solution and the pure solvent in a capillary viscosimeter according to Eq. (3.38)) should lie between 1.2 and 2.5, to assure an exact analysis. These limits of the relative viscosity are shown in Fig. 4.3. The data points below the critical value of the relative viscosity of 1.2 show deviations from the linear fit and should not be included in the extrapolation to the y-axis for the determination of the intrinsic viscosity.

The same polymer in the same solvent can show a wide range of intrinsic viscosities, depending on its molar mass. Poly(styrene) standards in two different solvents as shown in Fig. 4.4 cover three decades of intrinsic viscosities.

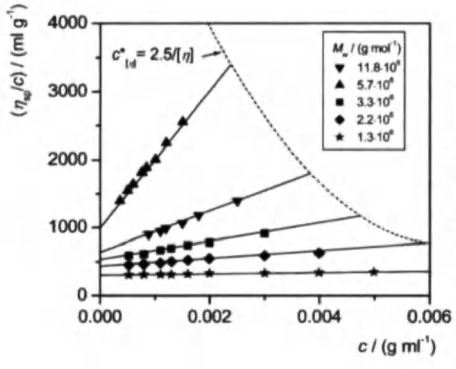

Fig. 4.2. Reduced viscosity η_{red} as a function of the concentration c for different molar masses of the polycation poly(acrylamide-*co*-(*N,N,N*-trimethyl-*N*-[2-methacryloethyl]-ammoniumchloride) (PTMAC) in 0.1 mol/l $NaNO_3$ solution. Data from [87]. All data points are measured at concentrations below the critical concentration $c^*_{[\eta]}$. The copolymer consists of 8 mol% TMAC and 92 mol% AAm

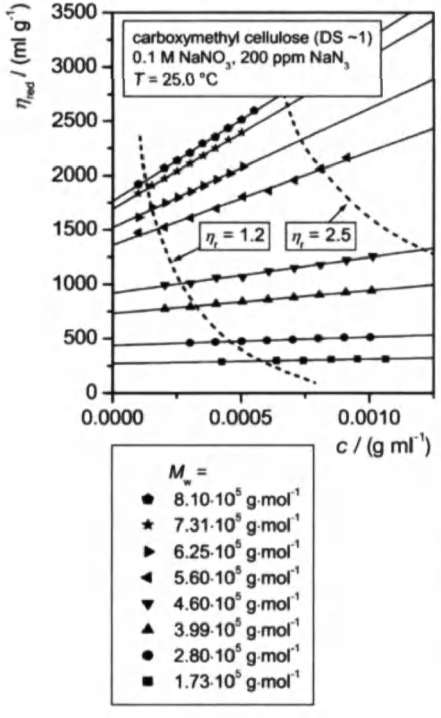

Fig. 4.3. Viscosity η_{red} as a function of the concentration c for carboxymethyl cellulose (CMC) of different molar masses in 0.1 mol/l $NaNO_3$ solution with 200 ppm NaN_3 at T=25 °C. The degree of substitution with carboxymethyl groups is constant at DS≈1. In addition the relative viscosity range of η_r=1.2–2.5 is shown in which the data points for a good viscosimetric measurement should lie

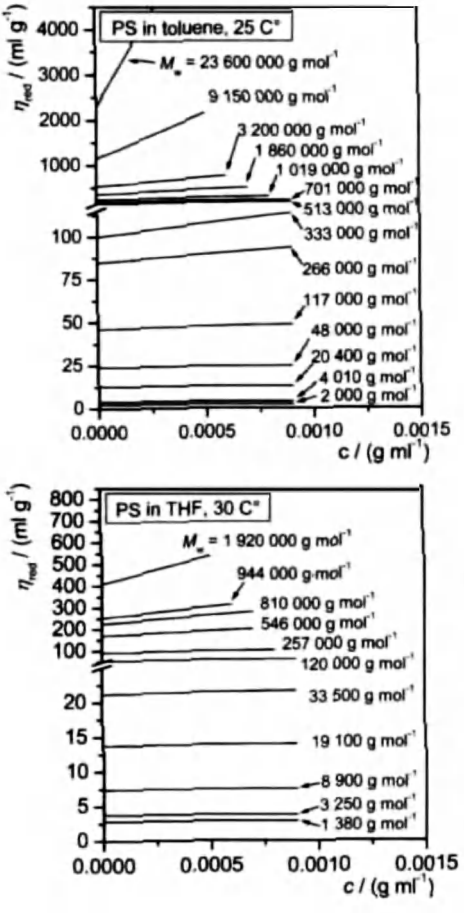

Fig. 4.4. Reduced viscosity η_{red} as a function of the concentration c for poly(styrene) samples of a broad range of molar masses in toluene at T=25 °C and in tetrahydrofuran (THF) at T=30 °C. The intrinsic viscosities range from $[\eta]$=5–2300 ml g^{-1} for the toluene solution and from $[\eta]$=2.3–408 ml g^{-1} for the THF solution. Data for PS in THF as a courtesy from PSS Polymer Standards Service, Mainz, Germany, PS in toluene from [88]

Equation (4.8) is in accordance with the empirical Huggins equation. The factor B_2 is equivalent to the product of the intrinsic viscosity squared and the Huggins constant K_H:

$$\eta_{red} = \frac{\eta_{sp}}{c} = [\eta] + K_H \cdot [\eta]^2 \cdot c \tag{4.9}$$

The Huggins coefficient K_H is constant for a given polymer-solvent system. However, the slope of the curves in Fig. 4.4 also depends on the intrinsic viscosity squared according to Eq. (4.9). Whereas for polymer samples with low molar masses and low intrinsic viscosities the curves in Fig. 4.4 almost seem to be inde-

pendent of the concentration, steep slopes are observed for polymer samples with high intrinsic viscosities and high molar masses.

Terms of higher order in Eq. (4.1) cannot be neglected for rising polymer concentrations due to the increasing intermolecular interactions (see "Concentration on molar mass" in Chap. 5). The linear region determined by the first two terms in Eq. (4.1) is only observed at low concentrations. In addition to this, measurement errors at low concentrations are more likely due to the small rise of the viscosity with the concentration.

These problems also occur in highly coiled and compact systems where the intermolecular interactions between polymer coils are reduced because of the small coil diameter (see for example acetyl starch in Fig. 4.5).

For highly coiled polymers, a high concentration is required to reach the desired range of the relative viscosity of η_r=1.2–2.5. Again, in these concentration ranges a deviation from the linear behavior can be observed. The intermolecular interactions between the polymer coils lead to an additional increase of the viscosity and therefore to higher reduced viscosities than predicted by the Huggins equation, as it can be seen in Fig. 4.5.

Therefore, the following empirical equations were developed to extend the linear range and to minimize the error in the extrapolation for the determination of the intrinsic viscosity. According to the Schulz-Blaschke equation, the reduced viscosity η_{red} can be plotted as a function of the specific viscosity η_{sp}:

$$\eta_{red} = [\eta] + K_{SB} \cdot [\eta] \cdot \eta_{sp} \tag{4.10}$$

The Kraemer equation utilizes the inherent viscosity η_{inh}:

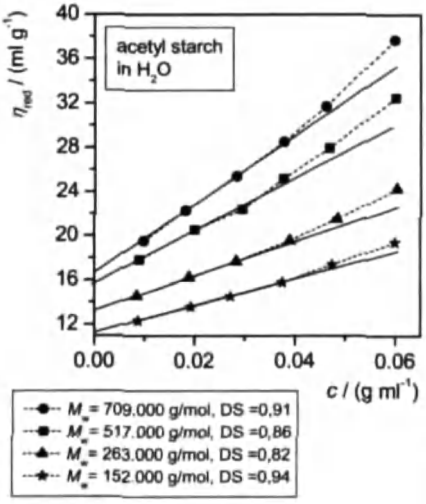

Fig. 4.5. Reduced viscosity η_{red} as a function of the concentration c for acetyl starch of different molar masses in aqueous solution at T=25 °C. The degree of substitution (DS) with acetyl groups is nearly constant at DS=0.9. Due to the compact structure of the polymer coil the concentrations of the dilution series are relatively high to reach the required relative viscosity range of η_r=1.2–2.5

$$\eta_{inh} = \frac{\ln(\eta_r)}{c} \tag{4.11}$$

This results in the following equation:

$$\eta_{inh} = [\eta] + K_K \cdot [\eta]^2 \cdot c \tag{4.12}$$

The Martin equation (also known as the Bungenberg-de Jong equation) utilizes the common logarithm of the reduced viscosity:

$$\lg \eta_{red} = \lg [\eta] + K_M \cdot [\eta] \cdot c \tag{4.13}$$

The Solomon-Ciuta equation allows for the calculation of the intrinsic viscosity from a single concentration:

$$[\eta] = \frac{\sqrt{2(\eta_{sp} - \ln \eta_r)}}{c} \tag{4.14}$$

The Kraemer equation as well as the Solomon-Ciuta equation are strictly speaking only valid for a Huggins constant K_H=1/3 [21]. Thus in case of doubt a linear fit should be obtained initially from the Huggins equation.

A comparison of a plot of the reduced viscosity as a function of the concentration according to the Huggins and as a function of the specific viscosity according to the Schulz-Blaschke equation is shown in Fig. 4.6. In this case, both plots lead to the same intersection with the y-axis, but the Schulz-Blaschke plot allows for a linear extrapolation of the data.

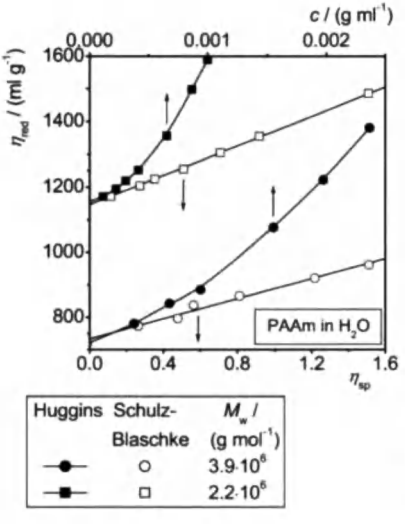

Fig. 4.6. Reduced viscosity η_{red} plotted as a function of the concentration c according to the Huggins equation and as a function of the specific viscosity according to the Schulz-Blaschke equation. Two poly(acrylamide) samples with different molar masses are shown, data from [89]. In the shown examples, the longer linear region of the Schulz-Blaschke plot allows for better extrapolation to $c \rightarrow 0$ for the determination of the intrinsic viscosity

There is no general recommendation for the usage of the above equations. The applicability of one of the equations has to be tested for each polymer solution.

There are special equations for the analysis of polyelectrolytes. They are discussed in detail in Chap. 5.

Until recently the Fikentscher K was used as a characteristic value for widely-used polymers like poly(vinyl chloride) (PVC) or poly(styrene) (PS) in solution [43]:

$$\lg(\eta_r) = \left[\frac{75 \cdot 10^{-6} K^2}{1 + 1.5 \cdot 10^{-3} \cdot K \cdot c} + 10^{-3} \cdot K\right] \cdot c \tag{4.15}$$

The parameter K was assumed to be independent of the concentration but dependent of the molar mass. The determination of K was carried out with a single viscosity measurement. In reality the Fikentscher K depends on the concentration and shows only small changes with the molar mass for high molar mass polymers [44]. It should be used only in a small and known concentration and molar mass range, for which the K value was determined. In all other cases, the intrinsic viscosity should be used as a characteristic value for polymer solvent systems.

5 Parameters Affecting the Intrinsic Viscosity

5.1 Concentration and Molar Mass

The concentration is not a true parameter affecting the intrinsic viscosity since the intrinsic viscosity is defined in ideal dilution (c→0) according to Eq. (4.7). Nevertheless, the influence of the concentration on the reduced viscosity η_{red} is of great importance for the determination of the intrinsic viscosity.

At low concentrations, the specific viscosity η_{sp} of a polymer solution increases linearly with the concentration c. The Huggins Eq. (4.9) was developed to eliminate this concentration dependence. Dividing the specific viscosity η_{sp} by the concentration c gives the reduced viscosity η_{red}, which should be independent of the concentration. The observed linear relation between the reduced viscosity η_{red} is caused by intermolecular interactions. The Huggins constant K_H is a measure for these intermolecular interactions (see Chap. 5). The linear relationship between the reduced viscosity η_{red} and the concentration c is only valid at low concentrations. As soon as the concentration is so high that interactions between several polymer coils become important, η_{red} increases superproportional with the concentration. This behavior can clearly be seen in Fig. 5.1.

In particular, at high molar masses the linear region is attained only at very low concentrations. The additional interactions already start at concentrations below the critical concentration c^* (see Chap. 7) where the solution volume is totally filled

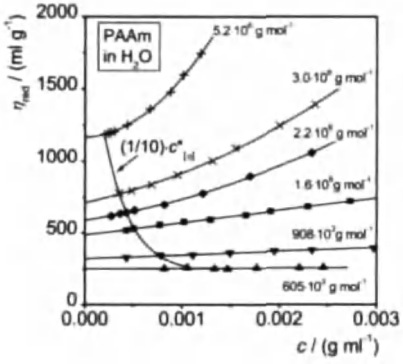

Fig. 5.1. Reduced viscosity η_{red} as a function of the concentration c for poly(acrylamide) (PAAm) of different molar masses in aqueous solution. The mass average molar masses M_w are given for each data set. The value of 1/10 of the critical concentration c^*_{inl} of the viscosimetry (at which already 10% of the solution volume is filled with polymer coils) is shown to demonstrate that deviations from the linear relation between the reduced viscosity η_{red} and the concentration c are caused by intermolecular interactions between the polymer coils. Data from [89]

with polymer coils. Above the critical concentration the polymer coils start to interpenetrate. These temporary network structures cause an additional hindrance in the flow and thus an additional increase of the viscosity. However, the data points in Fig. 5.1 show a non-linear behavior already at concentration above 0.1 c^*, at which only 10% of the solution volume is filled with polymer coils. Interactions between several polymer coils are captured by higher order terms, for example of third order in Eq. (4.1). For an exact description of the flow behavior at high polymer concentrations, these high order terms cannot be neglected. However, for viscosimetric measurements not even third order terms are taken into account since the intrinsic viscosity is determined in dilute solutions. Deviations from linearity are taken into account by the different analysis equations described in Chap. 4.

Other than the concentration c, the molar mass M is a true influence parameter on the intrinsic viscosity. Figure 5.1 shows that the intersection with the y-axis increases with an increasing molar mass. This should not be mistaken as an increase of the polymer segment concentration. Even at the same concentration, a polymer coil expands with an increasing molar mass. An increasing expansion and therefore an increasing intrinsic viscosity leads to a decreasing density ρ_{equ} of the polymer coil in solution with an increasing molar mass M according to Eqs. (4.6) and (4.7). A theoretical relation between the intrinsic viscosity $[\eta]$ and the molar mass M is deduced for polymer-solvent systems with unperturbed dimensions (theta-conditions) in "The Fox-Flory theory" in Chap. 8, Eq. (8.36). In general, the relationship between the intrinsic viscosity $[\eta]$ and the molar mass M is also used for non-theta systems to obtain the $[\eta]$-M-relationships described in Chap. 6. These relationships can then be used to calculate the molar mass from the intrinsic viscosity of a polymer sample.

5.2 Solvent

The solvation of the chain of a polymer has a big impact on the expansion of the polymer coil. Figure 5.2 shows that a big solvating envelope increases the effective volume of a polymer segment and therefore the volume fraction of the polymer coil. This leads to a decrease of the polymer density ρ_{equ} in solution according to Eq. (4.4) and to an increase of the intrinsic viscosity $[\eta]$.

The solvating envelope increases with rising thermodynamic quality of the solvent, whereas thermodynamically poor solvents show a decreasing solvating envelope and increasing intramolecular interactions of the polymer chain segments. This can lead to a partial association of chain segments and therefore to a rising coil density and a decreasing coil volume.

At theta-conditions, the intramolecular interactions of the polymer chain are compensated by the solvation force of the solvent molecules and the polymer coil resumes its unperturbed dimensions ("Dimensions of a real polymer coil" in Chap. 8). These theta-solvents correspond to thermodynamically poor solvents. The temperature at which the theta-conditions occur (theta-temperature) is normally close to the precipitation point of the polymer-solvent system.

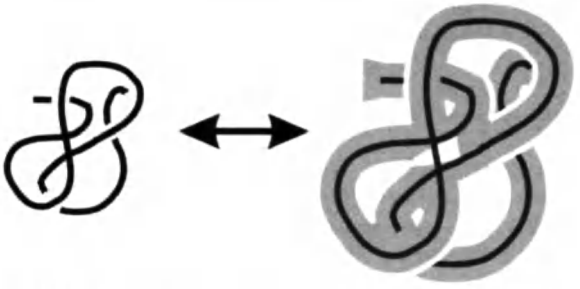

Fig. 5.2. Schematic view of the polymer coil expansion due to the solvation of the polymer chain in a good solvent

Often the retrieval of a suitable solvent for a polymer is not easy. Gnamm and Fuchs showed that the rule of thumb that solvents similar to the polymer show a good solubility cannot be used for all polymer solvent systems [45]. In general, one has to perform practical solution attempts to find a suitable solvent. Especially for complex copolymers with different monomer units no general rule for the solubility can be given.

Figure 5.3 shows plots of dilution series according to the Huggins equation for the same polymer poly(acrylamide) but different solvents. The intrinsic viscosity (intersection with the *y*-axis) increases as expected with the solvent quality (water>formamide>glycol).

At the same time, the slope of the curves in the linear region increases with the solvent quality and the onset of the non-linear behavior is shifted to lower concentrations. The slope of the reduced viscosity is equivalent to the product $K_H \times [\eta]^2$ of the Huggins constant and the intrinsic viscosity squared according to the Huggins Eq. (4.9). The slope is also formal equivalent to a second virial coefficient like A_2 in the equation of the reduced osmotic pressure Π/c:

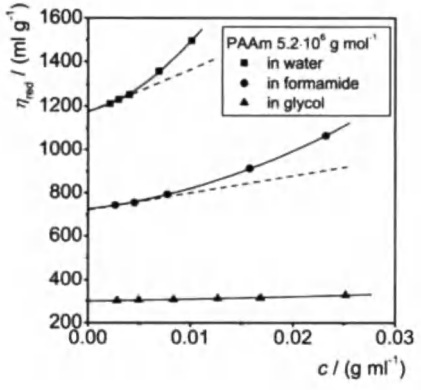

Fig. 5.3. Reduced viscosity η_{red} as a function of the concentration *c* for a poly(acrylamide) (PAAm) in the solvents H_2O, formamide and ethylene glycol at T=25 °C. Data from [89, 90]. The intrinsic viscosity (intersection with the Y-axis) rises with the solvent quality

$$\frac{\Pi}{c} = \frac{R \cdot T}{M} + A_2 \cdot c \tag{5.1}$$

In general, a second virial coefficient is a measure for the thermodynamic interactions of two particles.

In viscosimetric measurements the product $K_H \times [\eta]^2$ is a measure for the solvent quality that describes these additional interactions and the expansion of the coil by the solvent molecules (similar to the exponent *a* of the $[\eta]$-*M*-relationship; see "The influence of the solvent quality on the $[\eta]$-*M*-relationship" in Chap. 6). Solely at theta-conditions the Huggins constant K_H is zero and therefore the product $K_H \times [\eta]^2$. At theta-conditions, the long-range interactions between polymer segments are compensated by the solvent even at higher concentrations (see Chap. 8). In this case, the specific viscosity η_{sp} of a dilute solution increases linearly with the concentration and the reduced viscosity is independent of the concentration and is equivalent to the intrinsic viscosity.

The intrinsic viscosity $[\eta]$ increases with the molar mass (see "Concentration and molar mass" in Chap. 5) even at the same concentration and for the same solvent. The resulting expansion of the polymer coils leads to an increase of the interactions and therefore to an increasing slope $K_H \times [\eta]^2$. Since the Huggins constant K_H is independent of the molar mass for a specific polymer solvent system, the increasing intrinsic viscosity solely causes the increasing slope. This is shown in Fig. 5.4 for sodium poly(styrene sulfonate) of different molar masses at a constant concentration.

$K_H \times [\eta]^2$ is zero in a theta-solvent and therefore independent of the molar mass.

Changes in the viscosity caused by intermolecular interactions between solvent molecules in multi-component solvents are discussed in detail in Chap. 8.

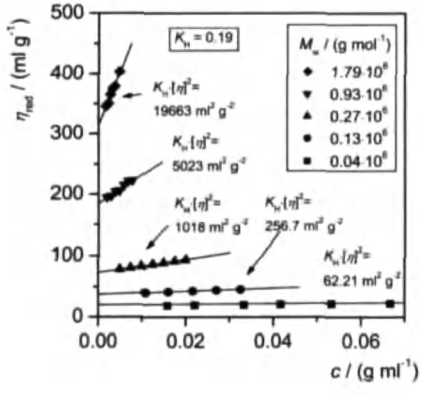

Fig. 5.4. Reduced viscosity η_{red} as a function of the concentration *c* for sodium poly(styrene sulfonate) (PSSNa) of different molar masses in aqueous solution. The second virial coefficient of the viscosimetry, $K_H \cdot [\eta]^2$, is equivalent to the slope of the curves and is given for each molar mass. The Huggins constant K_H is constant and independent of the molar mass. Data from [35, 91]

5.3 Temperature

For exact results while determining the intrinsic viscosity it is crucial to keep the temperature constant. In general, the accuracy of the temperature should be at least better than 0.1. In this context, it is noteworthy that the solvent viscosity as well as the viscosity of the polymer solution is always decreasing with the temperature while the intrinsic viscosity can also increase with the temperature. Figure 5.5 gives an example for aqueous solutions of poly(*N*-isopropyl-acrylamide) (PipAAm) and poly(acrylamide) (PAAm). The viscosity of the pure solvent water is shown as well.

The zero-shear viscosity η_0 of the polymer solutions and the solvent in Fig. 5.5 decreases with an increasing temperature. PipAAm in H_2O is a polymer-solvent system that shows a demixing temperature. At temperatures below this demixing temperature of 33 °C PipAAm is soluble in water while at 33 °C and above the polymer precipitates (phase separation). The viscosity of the polymer solution shows a strong decrease close to the demixing temperature.

The flow activation energy E of the Eyring equation

$$\eta_0 = Ae^{\frac{E}{RT}} \tag{5.2}$$

is positive for polymer solutions and greater than the activation energy of the solvent. Negative flow activation energies are not possible since additional thermal energy leads to an enhanced chain mobility and therefore to a reduction of the flow resistance. The intrinsic viscosity on the other hand reveals a different temperature behavior. The intrinsic viscosity can:

1. Increase with the temperature, $\Delta[\eta]/\Delta T$=positive
2. Be independent of the temperature, $\Delta[\eta]/T$=0
3. Decrease with the temperature $\Delta[\eta]/\Delta T$=negative

This behavior is shown schematically in Fig. 5.6.

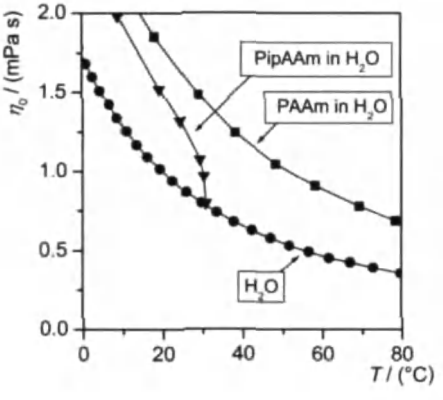

Fig. 5.5. Zero-shear viscosity η_0 as a function of the temperature T for poly (acrylamide) (PAAm) and poly(*N*-isopropyl-acrylamide) (PipAAm) in aqueous solution (c=0.1 wt%). The viscosity for the solvent water as a function of the temperature is plotted as well. Data from [77]

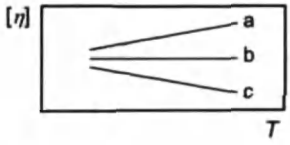

Fig. 5.6. Schematic view of the possible temperature dependence of the intrinsic viscosity [η]

Table 5.1. Temperature behavior of the intrinsic viscosity for different polymer-solvent systems

Polymer	Solvent	$\Delta[\eta]/\Delta T$
PIB	Tetrachloromethane	0
PIB	Benzene	Positive
PVC	Tetrahydrofuran	Negative
PVC	Chlorobenzene	Positive
PipAAm	H_2O	Negative
PAAm	H_2O	Positive

Table 5.1 shows this different temperature behavior of the intrinsic viscosity for some concrete polymer-solvent systems. An increasing intrinsic viscosity can be caused by polymer-polymer interactions as well as polymer-solvent interactions.

The solvating envelope of the polymer chain can increase when the polymer-solvent interaction (solvent quality) increases with the temperature. The rising solvation of the chain leads to an expansion of the polymer coil and therefore to an increasing intrinsic viscosity. Figure 5.7 shows this increase of the intrinsic viscosity with the temperature for poly(acrylamide) in aqueous solution. The zero-shear viscosity of the same sample decreases with the temperature in Fig. 5.5.

The aqueous solution of PipAAm shows a decreasing intrinsic viscosity as well as a decreasing viscosity. In this case, a rising temperature leads to decreasing poly-

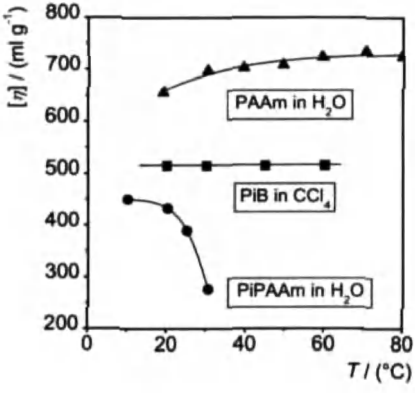

Fig. 5.7. Intrinsic viscosity [η] as a function of the temperature *T* for the poly(acrylamide) (PAAm) and poly(*N*-isopropyl-acrylamide) (PipAAm) in aqueous solution from Fig. 5.5. In addition, the intrinsic viscosity for a poly(isobutene) (PIB) in tetrachloromethane is shown as a function of the temperature. Data from [77]

mer-solvent interactions, increasing intramolecular interactions and therefore to a decreasing coil expansion. This intramolecular aggregation of the coil results in the observed phase separation above 33 °C.

Figure 5.7 also gives an example of a polymer-solvent system, poly(isobutene) (PIB) in cyclohexane, where the intrinsic viscosity is independent of the temperature.

5.4 Shear Rate

The definition of the intrinsic viscosity states that the measurements for the determination of the intrinsic viscosity should be performed at a shear rate $\dot{\gamma} \rightarrow 0$. At higher shear rates, the viscosity might become shear rate dependent (so called non-Newtonian flow behavior). Examples for the occurrence of a shear rate dependent viscosity at low shear rates and for relatively low polymer concentrations are given in Fig. 5.8.

The viscosity is independent of the shear rate $\dot{\gamma}$ at low shear rates as it can be clearly seen in Fig. 5.8. This viscosity is called the zero-shear viscosity η_0. Above a critical shear rate $\dot{\gamma}_{crit}$=80 s^{-1} for the PAAm and $\dot{\gamma}_{crit}$=5 s^{-1} for the xanthan gum solution the viscosity decreases with the shear rate. Table 5.2 shows some examples for aqueous solutions of poly(acrylamide) of different molar masses and concentrations. The critical shear rate is generally shifted to lower values for higher molar masses.

Viscosity measurements are often carried out with capillary viscosimeters because they are relatively cheap and give fast but exact results. Since capillary viscosimeters operate at higher shear rates (see Tables 3.1 and 3.2) it must be checked

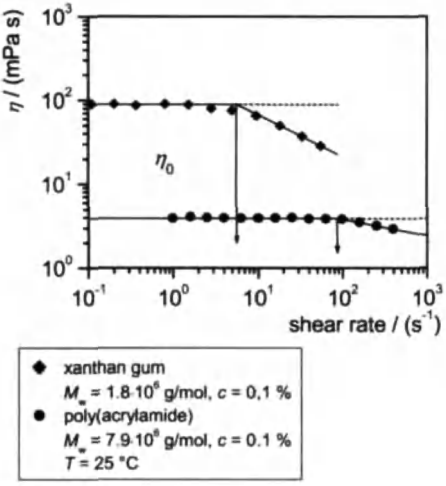

Fig. 5.8. Dynamic viscosity η as a function of the shear rate $\dot{\gamma}$ for an aqueous xanthan gum and an aqueous poly(acrylamide) solution of a comparable degree of polymerization and the same concentration c=0.1 wt% data from [92]. The viscosity depends on the shear rate above a critical shear rate $\dot{\gamma}_{crit}$

Table 5.2. Critical shear rate $\dot{\gamma}_{crit}$ of the onset of non-Newtonian behavior as a function of the molar mass M_w and concentration c for poly(acrylamide) in H_2O, T=25 °C

M_w/(g/mol)	c/(g/cm³)	$\dot{\gamma}_{crit}$/(s⁻¹)
500,000	0.01	>1000
1,000,000	0.01	1000
3,900,000	0.01	2
5,300,000	0.01	0.8
7,900,000	0.001	70

if the acquired viscosity data lies in the zero shear viscosity range. This is for example possible with multi-level viscosimeters (Fig. 3.1d). The different average heights $\bar{h}$ for each reservoir give different pressures according to Eq. (3.2) and therefore different maximum shear rates $\dot{\gamma}_{max}$ in the capillary (Eqs. 3.1 and 3.4). Since the determination of the intrinsic viscosity is conducted on a series of different concentrations, the extrapolation to $\dot{\gamma}\rightarrow 0$ and $c\rightarrow 0$, can be performed in a single diagram [46].

A plot of η_{red} against $c+K\dot{\gamma}$ (where K is an arbitrary constant) allows for a better determination of the intersection with the y-axis for the determination of the intrinsic viscosity (see Fig. 5.9). The rotational viscosimeters introduced in Chap. 3 have the possibility to vary the shear rate over a wider range and are able to allow for measurements at a defined and constant shear rate.

It is possible that the zero-shear viscosity of polymer samples with very high molar mass and strong non-Newtonian flow behavior cannot be measured in a capillary viscosimeter. In case of a maximum shear rate in the capillary above the critical shear rate of the sample the calculated viscosity will be too low as one can see in Fig. 5.10 for different samples of high molar mass xanthan gum.

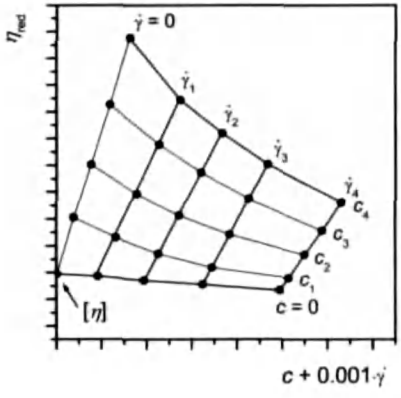

Fig. 5.9. Net diagram for the determination of the intrinsic viscosity $[\eta]$ from measurements of the reduced viscosity at shear rates≠0

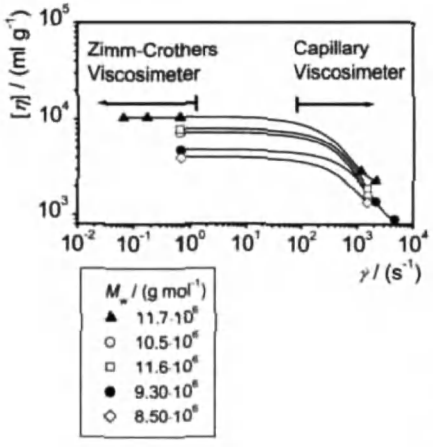

Fig. 5.10. Intrinsic viscosity $[\eta]$ determined at high shear rates $\dot{\gamma}$ with a capillary viscosimeter and at lower shear rates with a Zimm-Crothers viscosimeter for different xanthan gums in 0.1 mol/l sodium chloride (NaCl) solution at 25 °C. Data from [93]. For strongly shear thinning polymer solutions, only low shear viscosimeters reach the shear rate independent viscosity region

In these cases, the viscosity should be measured with a low shear viscosimeter like the Zimm-Crothers viscosimeter introduced in Chap. 3. The Zimm-Crothers viscosimeter measures at shear rate $<1\ s^{-1}$, where nearly all dilute polymer solutions show a shear rate independent viscosity.

5.5 Branching

Branching in a polymer coil leads for polymers of the same molar mass to changes of the intrinsic viscosity. Although the chemical composition is the same, branched polymers have a higher density ρ_{egu} in solution than linear polymers and therefore

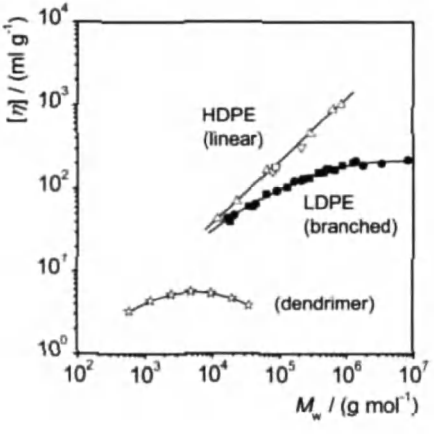

Fig. 5.11. Intrinsic viscosity $[\eta]$ as a function of the molar mass M for linear poly(ethylene) (high density poly(ethylene), HDPE) and longchain branched poly(ethylene) (low density poly(ethylene), LDPE) in tetraline at T=120 °C (data from [47, 94]) as well as for a dendrimer with 3,5-dioxybenzylidene units in tetrahydrofuran at T=30 °C (data from [47, 95])

a smaller intrinsic viscosity. Each sidearm in a branched polymer can be seen as a statistic coil, but these coils are closer to the center of gravity than the segments in a linear polymer. These effects of polymer branching on the intrinsic viscosity become more important with an increasing molar mass as one can see in Fig. 5.11 for linear high-density poly(ethylene) (HDPE) and branched low-density poly(ethylene) (LDPE).

The intrinsic viscosity is nearly the same for linear and branched poly(ethylene) (PE) at low molar masses, whereas at high molar masses the intrinsic viscosity of branched PE levels into a plateau while the intrinsic viscosity of linear PE still increases with the molar mass.

In addition, the type of branching has an impact on the intrinsic viscosity. Short chain branching as shown in Fig. 5.12a influences the properties of solid bodies whereas long chain branching (Fig. 5.12b) also affects the intrinsic viscosity as shown for PE in Fig. 5.11. Star like branched polymers as shown in Fig. 5.12c behave at high molar masses like linear polymers. The intrinsic viscosity of star like polymers increases linearly with the molar mass at high molar masses. In this case each arm acts like a single polymer coil if the molar mass is high enough. However, these "single" polymer coils are closer to each other due to the star connection. Because of this higher density of the polymer segments, the absolute intrinsic viscosity of a star like polymer is lower compared to a linear polymer of equal molar mass. Dendrimers with a regular branching pattern (Fig. 5.12d) exhibit a decreasing intrinsic viscosity above a critical molar mass as demonstrated in Fig. 5.11. Hyperbranched polymers (extremely short chain branched dendrimers) like the poly(α,ε-lysine) in Fig. 6.12 have an intrinsic viscosity that is totally independent from the molar mass.

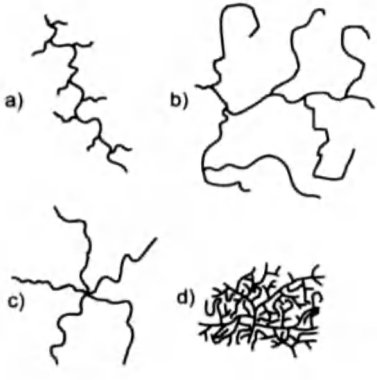

Fig. 5.12a–d. Different types of branching in polymers: **a** short chain branching; **b** long chain branching; **c** star like branching; **d** hyperbranching (dendrimers)

5.6 Chemical Structure

The quantitative determination of the influence of the chemical structure of a polymer on the intrinsic viscosity is not easily determined. The chemical structure of a polymer chain and of the side groups affects the flexibility of the chain. An increasing rigidity affects the ability of the chain to form a random coil and leads to an increased intrinsic viscosity. However, changes in the chemical structure of a polymer also effect the interactions of the polymer segments with the solvent. It is not easy to separate these two effects on the intrinsic viscosity. Figure 5.13 shows a comparison of several different chemical structures of polymers and gives a rough overview of the evolution of the intrinsic viscosity depending on the structures of comparable polymers.

The synthetic polymers poly(ethylene) (PE), poly(isobutene) (PIB) and poly(styrene) (PS) have the same backbone (a polyethylene chain) but different voluminous side groups. PE as the basic polyethylene chain has no side groups. Due to strong van-der-Waals forces, PE is highly coiled in solution and only soluble in organic solvents above 100 °C. Compared to PE, PIB and PS show an expansion of the polymer coil in solution and a higher intrinsic viscosity. The non-polar side groups of PIB and PS obstruct the coiling of the polymer chain and lead to an expanded coil in comparable organic solvents. However, even for similar non-polar side groups it cannot be ruled out that the coil expansion is not only caused by the simple steric hindrance of the side group but also by intermolecular interactions of the side groups with the solvent.

Even polymers with the same chemical composition can show differences in the intrinsic viscosity depending on the chemical structure. Polymers with different tacticities (for example the poly(propylene) in Fig. 5.13) show an expansion of the coil in theta-solvents from atactic to iso- and syndiotactic structures. The different coil expansions are caused by different short-range interactions between the side groups [47] (see "The influence of the tacticity of a polymer" in Chap. 6). In good solvents, the coil expansion is dominated by the solvation of the polymer chain. In this case, there are no observable differences in the intrinsic viscosity of poly(propylenes) with different tacticities. The same observation is made for poly(styrene) in different good solvents in Fig. 6.14.

A comparison of polymers with different polymer backbones is shown in Fig. 5.13 for the non-ionic polymers poly(ethylene oxide) (PEO), poly(acrylamide) (PAAm), and methyl cellulose (ME) in aqueous solution. The heteroatom in the backbone of PEO leads to an expanded coil structure compared to PAAm with the heteroatom in the side chain. Cellulose derivatives have in addition to the heteroatom the ring structure of the anhydroglucose unit in the polymer backbone. The methyl cellulose in this example has a less expanded coil than the synthetic PAAm and PEO. Again, it is hard to distinguish between the influence of the solvation of the polar backbone and the pure steric hindrance of the different backbone structures.

The influence of ionic groups in the side chain of the polymer on the intrinsic viscosity is shown in Fig. 5.13 for the sodium salt of poly(acrylic acid) (PAAcNa)

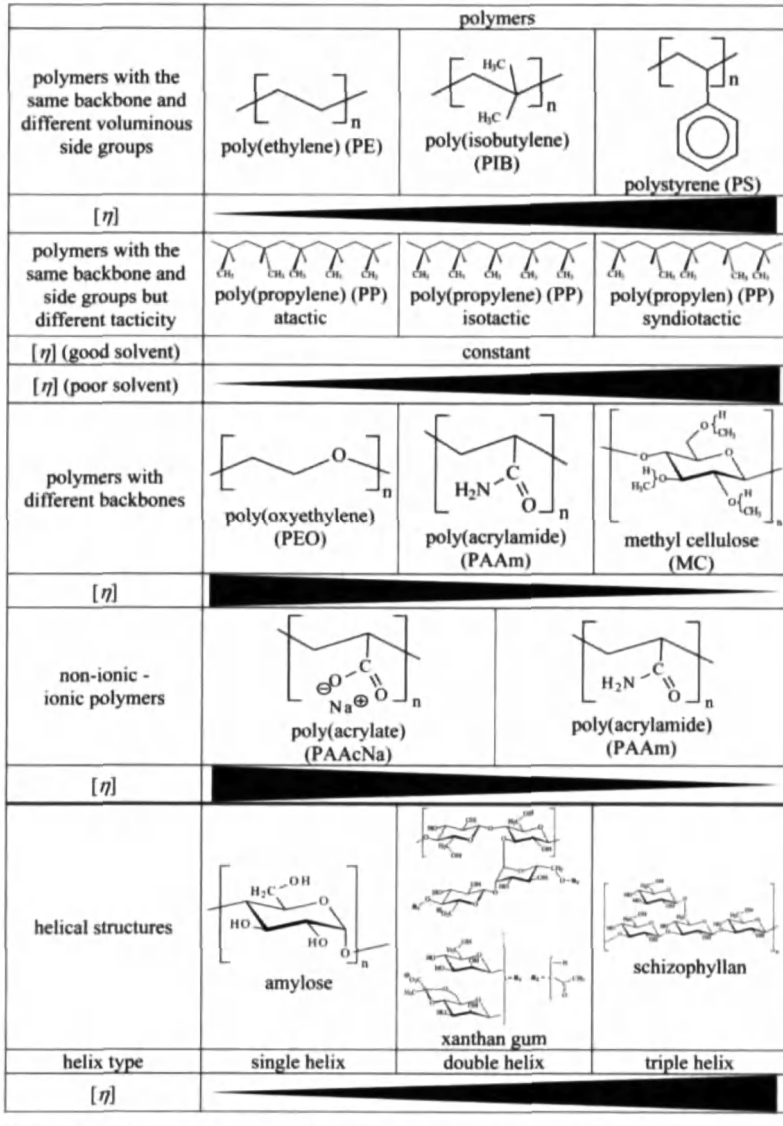

Fig. 5.13. Intrinsic viscosity evolution for different chemical structures of the polymer chain

and the similar poly(acrylamide) (PAAm). The polymer coil of the PAAcNa is expanded due to the coulomb forces between the ionic groups compared to the similar chemical structure of the PAAm. The dissociation of the carboxylic groups of the PAAcNa is strongly dependent on the pH, temperature, concentration and salt content of the solution. "Polyelectrolytes" in Chap. 5 discusses the influence of these parameters on the intrinsic viscosity of polyelectrolytes in detail.

Not only the chemical structure of the polymer backbone, but also the secondary structure of a polymer has a strong influence on the intrinsic viscosity. This is shown for the biopolymers amylose, xanthan gum and schizophyllan in aqueous solution in Fig. 5.13. Amylose is one of the main components of starch. The chemical structure of the linear non-ionic polymer chain causes the amylose to form helical structures in aqueous solution, which result in an expanded structure of the coil. The complex fermentation polymer xanthan gum also has a simple polymer backbone of anhydroglucose units like the amylose, but the chemical structure of the side chains force the xanthan gum to form a double helix in aqueous solution. The rigid double helix results in an even more expanded structure. Schizophyllan, another fermentation polymer, has the most expanded structure in solution and the highest intrinsic viscosity. Its backbone consists of anhydroglucose units like xanthan gum and amylose, but the side groups consisting of β-(1,6)-linked glucose units cause schizophyllan to form a triple helix in solution. The pronounced expansion of polymers with helical structures also causes the onset of the non-Newtonian flow behavior at low shear rates described in Chap. 5. Although the xanthan gum in Fig. 5.8 has a lower molar mass than the PAAm, the 0.1% solution of xanthan gum has a noticeable higher zero-shear viscosity and a lower critical shear rate than the PAAm solution of the same concentration. This is caused by the increased intrinsic viscosity due to the more rigid helical structure of the xanthan gum.

5.7 Polyelectrolytes

Polyelectrolytes are polymers with ionic side groups. The coil expansion of polyelectrolytes is not only determined by the usual parameters molar mass, solvent quality and temperature, but also by the degree of dissociation of the ionic groups. An example for a polyelectrolyte is the poly(acrylic acid) (PAAc) or its sodium salt (PAAcNa). The reduced viscosity η_{red} of this polyelectrolyte is plotted as a function of the concentration c in Fig. 5.14. At high concentrations, the reduced viscosity decreases with a decreasing concentration as expected for a polymer solution. However, at lower concentrations the reduced viscosity levels into a plateau and increases again with a decreasing concentration.

At high polymer concentrations and without additional salts only a few of the ionic groups of polyelectrolytes are dissociated. The concentration of counterions inside the polymer coil is higher than outside and the osmotic pressure forces solvent into the coil leading to an expansion. A decreasing polymer concentration

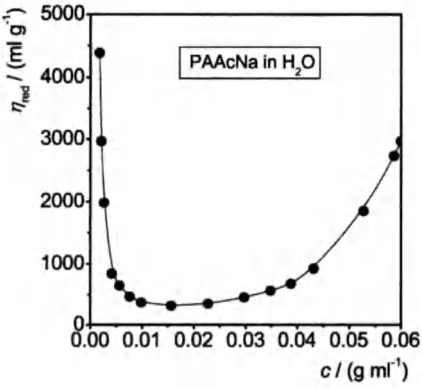

Fig. 5.14. Reduced viscosity η_{red} as a function of the concentration c for the polyelectrolyte sodium salt of poly(acrylic acid) (PAAcNa) in aqueous solution. Data from [96]

results in an increasing dissociation and therefore in a decreasing osmotic pressure and a contraction of the coil. On the other hand, an increasing dissociation is accompanied by increasing coulomb repulsion forces between the ionic groups of the polymer chain. These forces result in an expansion of the coil and lead to the observed strong increase of the reduced viscosity at very low polymer concentrations.

At very low polyelectrolyte concentrations the reduced viscosity decreases again even for very rigid polymer chains and expanded coils, as seen in the plot of the reduced viscosity against the logarithmic concentration (Fig. 5.15) for poly(styrene sulfonate). The data shows a maximum of the reduced viscosity with a decreasing polymer concentration. At concentrations below this maximum, the polymer solution is in a dilute state, even for the nearly fully expanded polyelectrolytes. The intermolecular interactions simply decrease again with the polymer concentration [47].

The addition of low-molecular salts to a polyelectrolyte solution compensates the effects of the osmotic pressure as well as the coulomb forces by shielding the dissociated ionic groups as shown in Fig. 5.16. The addition of these salts allows for an extrapolation of the reduced viscosity to $c \rightarrow 0$ and a determination of an intrinsic viscosity. This is not possible for the salt free polyelectrolyte solution as can clearly be seen in Fig. 5.16. Although the addition of salt enables the determination of intrinsic viscosities, these values do not reflect the coil expansion in the salt free solution.

A concrete example is given in Fig. 5.17. The reduced viscosity η_{red} of two different molar masses of poly(vinylimidazolinium iodide) in aqueous solution is plotted without (a) and with an added salt (b). Figure 5.17a shows a trend similar to the one observed for the sodium salt of PAAc in Fig. 5.14. Again, the reduced viscosity increases with the dilution because of the increasing dissociation of the ionic groups. In the presence of additional salts like the 0.05 mol/l potassium iodide solution in Fig. 5.17b the polyelectrolyte behaves like a neutral polymer and an ex-

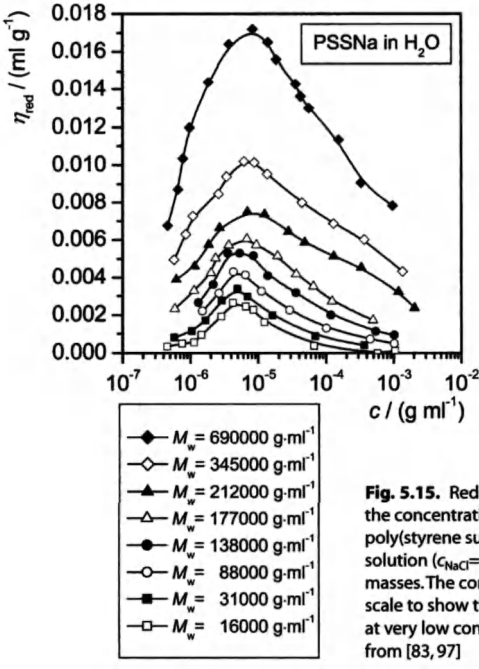

Fig. 5.15. Reduced viscosity η_{red} as a function of the concentration c for the polyelectrolyte sodium poly(styrene sulfonate) in nearly salt free aqueous solution (c_{NaCl}=4×10^{-6} mol l^{-1}) and for different molar masses. The concentration is plotted on a logarithmic scale to show the maximum behavior of the viscosity at very low concentrations of the polyelectrolyte. Data from [83, 97]

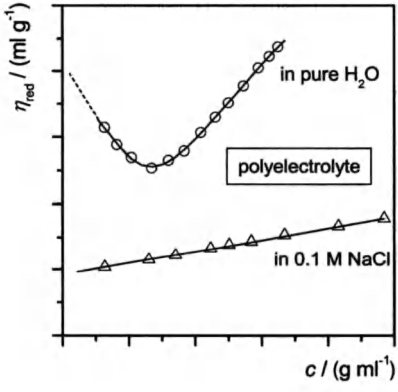

Fig. 5.16. Different behavior of a polyelectrolyte in aqueous solution and a salt solution. At high concentrations of the polyelectrolyte in aqueous solution is the concentration of counter ions inside the polymer coil higher than outside, leading to an expansion of the coil due to osmotic pressure. At low concentrations of the polyelectrolyte in aqueous solution, the polyelectrolyte is highly dissociated, leading to an expansion of the coil due to coulomb repulsion forces. Both expansion effects are compensated in the salt solution

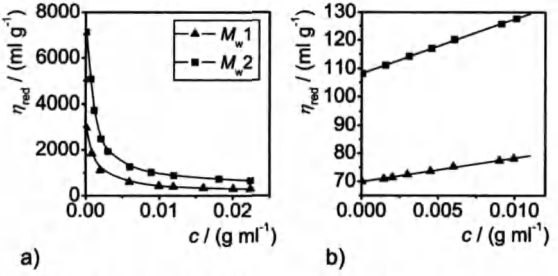

Fig. 5.17a, b. Reduced viscosity η_{red} as a function of the concentration c for the polyelectrolyte poly(vinylimidazolium iodide): **a** in aqueous solution; **b** in 0.05 mol/l potassium iodide solution at 30 °C. Two samples with different molar mass $M_w1<M_w2$ are shown, data from [62, 98]

trapolation of the reduced viscosity to $c\rightarrow 0$ for the determination of an intrinsic viscosity is possible.

Many polyelectrolyte samples have a high content of additional salts from the synthesis. For an exact determination of the intrinsic viscosity at a defined salt concentration, these salt "impurities" have to be removed or the salt content has to be determined and taken into account (see Chap. 3). The impact of different salt concentrations on the reduced viscosity of a polyelectrolyte is shown in Fig. 5.18 for an aqueous solution of sodium pectinate.

For the salt free solution, the typical curve progression of an ionic polymer can be observed as described above. At low salt concentrations (0.4 mmol/l NaCl) the increase of η_{red} is reduced due to the shielding of the coulomb forces by additional counter ions. At low polymer concentration, the reduced viscosity decreases again. This is the same effect as in Fig. 5.15, where the increasing expansion of the polymer coils was not great enough to act against the decreasing concentration of polymer coils. The shielding of the coulomb repulsion forces increases with a higher salt content of the solution. At 1 mmol/l NaCl only a very low increase of the reduced

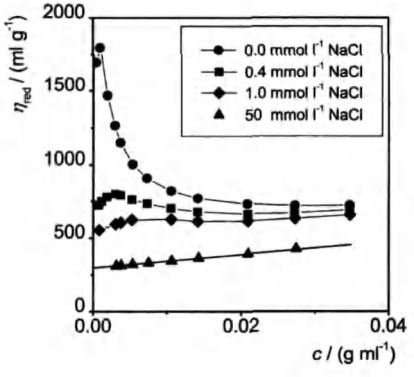

Fig. 5.18. Reduced viscosity η_{red} as a function of the concentration c for sodium pectinate in aqueous solution and different sodium chloride concentrations at T=27 °C, data from [99]

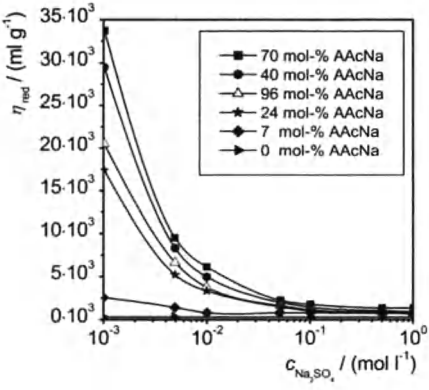

Fig. 5.19. Reduced viscosity η_{red} as a function of the salt concentration c (sodium sulfate, Na_2SO_4) for poly(acrylamide-*co*-acrylate) (PAAm/AAcNa) with different copolymer compositions. The degree of polymerization is kept constant at P_w=32,700, the polymer concentration is c=0.00025 g/ml, data from [100]

viscosity is observed and at 50 mmol/l NaCl the pectinate behaves like a neutral polymer.

Still the coil expansion and the intrinsic viscosity depend on the salt concentration, even for a linear curve progression. For this reason, intrinsic viscosities of polyelectrolytes should be always accompanied by the salt concentration that they were determined at. This is extremely important for the $[\eta]$-M-relationships described in chapter 6. As one can see in Fig. 6.11 theses relationships change for the same polymer, depending on the salt concentration at which the intrinsic viscosity was determined.

Another example for a decreasing coil expansion and a decreasing reduced viscosity caused by an increasing salt concentration is shown in Fig. 5.19.

In this case the reduced viscosity not only depends on the salt concentration, but also on the number of ionic groups in the polymer and therefore on the copolymer composition of the investigated poly(acrylamide-co-acrylate). The copolymers in Fig. 5.19 have a constant degree of polymerization P and chain length distribution. Nevertheless, it is not the copolymer with the highest percentage of ionic groups (with 96% acrylate) that shows the highest reduced viscosity, but the one with 70% acrylate groups. This unexpected behavior is shown in Fig. 5.20. In this figure the relative intrinsic viscosity increment $[\eta]/[\eta]_{PAAm}$ of the poly(acrylamide-*co*-acrylate) (with $[\eta]_{PAAm}$ as the intrinsic viscosity of PAAm with the same degree of polymerization) in concentrated salt solutions is plotted against the copolymer composition. Since these copolymers were not synthesized via a copolymerization but via a polymer analogous reaction of a single poly(acrylamide) sample as shown in Fig. 5.21, the degree of polymerization P is exactly the same for these samples [31]. At the same time, the copolymers show a statistical distribution of the monomer units along the polymer chain.

According to Fig. 5.20, the maximum of the intrinsic viscosity increment is independent of the degree of polymerization and appears at a ratio of acrylamide to

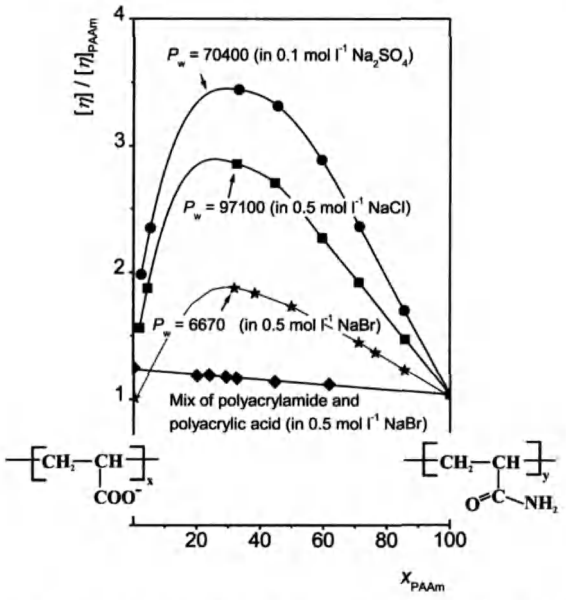

Fig. 5.20. Reduced intrinsic viscosity $[\eta]/[\eta]_{PAAm}$ as a function of the molar fraction x_{PAAm} of acrylamide in the copolymer poly(acrylamide-*co*-acrylate) for samples with different degrees of polymerization *P* and in different salt solutions. The reduced intrinsic viscosity $[\eta]/[\eta]_{PAAm}$ is normalized to the intrinsic viscosity of the pure poly(acrylamide) with the same degree of polymerization *P*. In addition to the copolymers, mixtures of poly(acrylamide) and poly(acrylate) with a value of *P*=~6700 and with comparable mixing ratios in sodium bromide solution are shown. The data is taken from [31, 101]

acrylate monomers of 1:2. Comparable mixtures of pure poly(acrylamide) and poly(acrylate) with the same degree of polymerization do not show this maximum behavior. Hence, the increasing intrinsic viscosity with a rising content of acrylate cannot be attributed only to the repulsing coulomb forces of the ionic groups. The increasing intrinsic viscosity is in fact correlated to an increasing number of regular triose units of the type acrylate-acrylamide-acrylate. Hydrogen bonds in these triose units as shown in Fig. 5.21, and coulomb repulsion forces between the carboxyl groups lead to a more rigid chain structure and therefore to a coil expansion and the observed increasing intrinsic viscosity.

The maximum number of these triose units occurs at 67 mol% of acrylate groups and explains the maximum of the intrinsic viscosity at this point.

The previous example demonstrates that the specification of the copolymer composition is even more important for polyelectrolytes than for non-ionic polymers for an exact determination of the intrinsic viscosity. In particular for biopolymers a characterization of the exact composition is complicated and not often carried out. One of the reasons for the huge number of different $[\eta]$-M-relationships published for the same polymer solvent system is therefore the insufficient char-

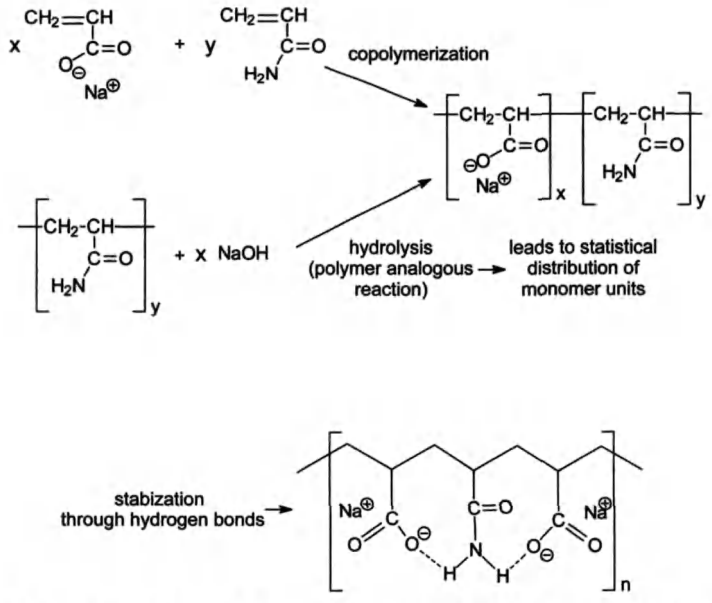

Fig. 5.21. Stabilization of acrylate-acrylamide-acrylate units via hydrogen bonds in the copolymer poly(acrylamide-*co*-acrylate). The copolymer can be synthesized via a copolymerization of acrylic acid and acrylamide or a partial hydrolyses of poly(acrylamide) with sodium hydroxide (NaOH). The hydrolyses as a polymer analogous reaction leads to copolymers with the same degree of polymerization *P*. A hydrolysis to a copolymer with more than 66% of acrylic acid units is only possible at with extreme reaction conditions [31]

acterization of the polymer (see also Chap. 6, especially the xanthan gum example in Table 6.4).

The dissociation of the ionic groups of a polyelectrolyte is not only controlled by the salt concentration but also by the pH of the solution. An example for the resulting dependence of the reduced viscosity from the pH of a solution is shown in Fig. 5.22. In this case, the polyelectrolyte has anionic and cationic groups; the solution has a viscosity minimum at the isoelectric point.

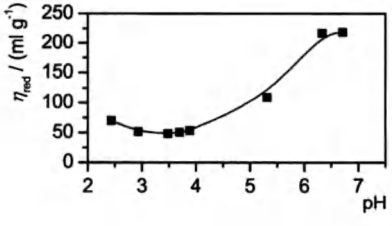

Fig. 5.22. Reduced viscosity η_{red} as a function of the pH of a solution of the ampholytic copolymer poly(maleic acid anhydride-*co*-*N*-methyldiallylamine) in H_2O. Data from [83]. The reduced viscosity has a minimum at the isoelectric point

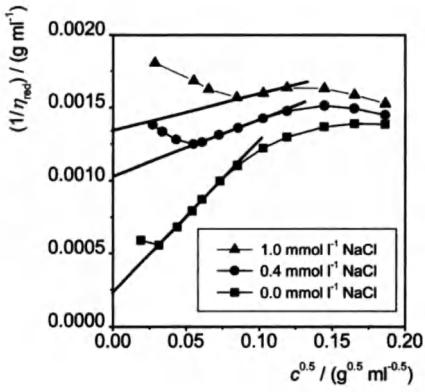

Fig. 5.23. Fuoss plot of the reciprocal reduced viscosity $1/\eta_{red}$ as a function of the square root of the concentration for the sodium pectinate samples from Fig. 5.18 with different concentrations of sodium chloride. The intersection with the Y-axis is not the reciprocal intrinsic viscosity, the Fuoss plot is rather an empirical method to linearize the reduced viscosity data from polyelectrolytes

In the past, a determination of an intrinsic viscosity for polyelectrolyte solutions even at very low salt concentrations was carried out with the empirical Fuoss equation. The increasing reduced viscosity at low polymer concentrations can be described with the following equation:

$$\frac{1}{\eta_{red}} = A_{FS} + K_{FS} \cdot \sqrt{c} \tag{5.3}$$

Figure 5.23 shows a plot of the reciprocal reduced viscosity as a function of the square root of the concentration for the pectinate solutions introduced in Fig. 5.18.

Data points for concentrations above the maximum of the reduced viscosity in Fig. 5.18 can be described by a linear fit according to Eq. (5.3). Elias [47] pointed out that the intersection of the fit with the y-axis is not equivalent to the reciprocal intrinsic viscosity as often assumed in the past:

$$A_{FS} \neq \frac{1}{[\eta]} \tag{5.4}$$

Still the values of $1/A_{FS}$ can be taken as a relative measure of a coil expansion for comparison.

6 Viscosimetric Determination of the Molar Mass

6.1 The $[\eta]$-*M*-Relationship

The intrinsic viscosity $[\eta]$ of a polymer in a certain solvent can be correlated with the molar mass M:

$$[\eta] = K_{[\eta]} \cdot M^a \tag{6.1}$$

In the literature, this dependence is referred to as the $[\eta]$-M-relationship or the Kuhn-Mark-Houwink-Sakurada-relationship (KMHS-relationship). $K_{[\eta]}$ and a are constant for a given solvent and temperature.

The exponent a is a measure for the solvent quality and therefore for the solution structure of the dissolved polymer (see "Influence of the solution structure on the $[\eta]$-M-relationship" below). The knowledge of $K_{[\eta]}$ and a allows for an easy determination of the molar mass of a polymer by measuring the intrinsic viscosity. The determination of the molar mass from Eq. (6.1) yields the viscosity average molar mass M_η. The values of M_η lie between the number average molar mass M_n and the mass average molar mass M_w (Fig. 2.2). An exact definition of the viscosity average molar mass is given in "The viscosity average of the molar mass" in Chap. 8. A general theoretical determination of the constants $K_{[\eta]}$ and a of the $[\eta]$-M-relationship for a polymer solvent system is not possible; they have to be determined experimentally.

6.1.1 The Experimental Determination of the $[\eta]$-*M*-Relationship

The determination of an $[\eta]$-*M*-relationship is conducted with a homologous series of polymer samples with different molar masses. The molar mass distribution of these samples should be as narrow as possible (polydispersity $Q \approx 1$). In this case, the intrinsic viscosity can be assigned to a single molar mass. It is possible to use samples with a broader distribution, but the $[\eta]$-*M*-relationships determined in this way are considered to have a lower heterogeneity class (see "Heterogeneity classes and the influence of the polydispersity on the $[\eta]$-*M*-relationship" in Chap. 8). If only a single polymer sample is available, a homologous series of polymers samples with smaller molar masses can be produced from this sample via ultrasonification as described in the next section.

Table 6.1. Methods for the determination of average molar masses of polymers

Method	Molar mass average	Molar mass limits
Static light scattering	M_w	>100 g/mol
X-Ray and neutron scattering	M_w	>500 g/mol
Sedimentation and diffusion	M_w, M_z	>1000 g/mol
Sedimentation equilibrium	M_w, M_z	>1000 g/mol
Size exclusion chromatography (relative method)	M_n, M_w, M_z	>1000 g/mol
Field-flow fractionation (relative method)	M_n, M_w, M_z	>1000 g/mol
Membrane osmometry	M_n	>5000 g/mol, <1,000,000 g/mol
Ebullioscopy	M_n	<20,000 g/mol
End group assay	M_n	<40,000 g/mol
Vapor-pressure osmometry	M_n	<50,000 g/mol
Mass spectroscopy	M_n, M_w, M_z	<200,000 g/mol
Sedimentation (relative method)	M_w, M_z	<1,000,000 g/mol
Dynamic light scattering (relative method)	M_z	<10,000,000 g/mol

The intrinsic viscosity of each sample has to be measured (as described in Chap. 4). In addition to this, the molar mass M of each sample has to be determined. For commercial samples, the molar mass is often already measured and supplied with the sample (as well as the polydispersity Q). If these parameters are not known for a polymer sample, they have to be determined. Different methods (absolute and relative) of determining the molar mass of a polymer sample are listed in Table 6.1.

The different methods yield different average molar masses (see "Molar mass" in Chap. 2). In general the mass average M_w is used for the determination of a molar mass. In any case, the used average should be indicated for listed $[\eta]$-M-relationships.

Equation (6.1) can be written as

$$\log [\eta] = \log K_{[\eta]} + a \cdot \log M \tag{6.2}$$

A plot of the common logarithm of the intrinsic viscosity as a function of the logarithmic molar mass yields a linear dependence. The intersection with the y-axis of a linear fit of the data gives the constant $\log K_{[\eta]}$, the slope of the curve the constant a. An example is shown in Fig. 6.1 for the intrinsic viscosities determined in Fig. 4.2.

The unit of the constant factor $K_{[\eta]}$ depends on the order of the exponent a according to Eq. (6.1). Therefore, in most cases the unit of $K_{[\eta]}$ is not an integer value. For most $[\eta]$-M-relationships only the number value of $K_{[\eta]}$ determined via

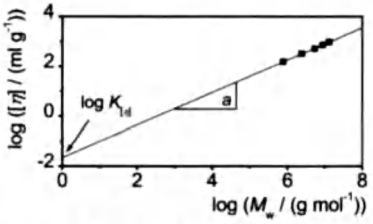

Fig. 6.1. Determination of the exponent *a* from the slope and the constant $K_{[\eta]}$ from the intersection with the y-axis when plotting log [η] as a function of log *M*. Values for the intrinsic viscosity [η] of the polycation poly(acrylamide-*co*-(*N*,*N*,*N*-trimethyl-*N*-[2-methacryloethyl]-ammoniumchloride) (PTMAC) in 0.1 mol/l $NaNO_3$ solution are taken from Fig. 4.2. The copolymer consists of 8 mol% TMAC and 92 mol% AAm. Molar mass values were determined with multi-angle laser light scattering (MALLS), data from [102]

Eq. (6.2) is given. In this case the units of the molar mass and intrinsic viscosity used for the determination of the [η]-*M*-relationship have to be listed with the relationship.

A regular distribution of the molar masses on a logarithmic scale helps to minimize the error of the linear fit according to Eq. (6.2) and enables the usage of the [η]-*M*-relationship over a wide range of molar masses. For this reason, the molar masses in Fig. 6.2 have an even distribution over a wide range of molar masses.

However, a single [η]-*M*-relationship is not valid over the whole range of molar masses. Especially at low molar masses, a systematic deviation is observed as can be seen in Fig. 6.2 (see "The influence of the molar mass" below). The linear fit according to Eq. (6.1) should only be done in actual linear regions for an exact determination of a [η]-*M*-relationship. For the applicability of a listed [η]-*M*-relationship, a valid range of molar masses should always be specified. The [η]-*M*-relationship is only valid in this range! The relationships listed in the Polymer Handbook [48] are always accompanied by the molar mass range.

The quality of an [η]-*M*-relationship also depends on the number of samples used for its determination, thus reliable sources for [η]-*M*-relationships specify the number of samples. Especially for widely used polymers with many published

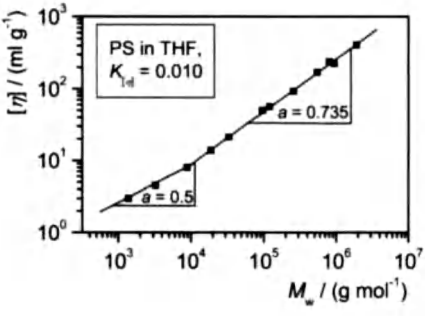

Fig. 6.2. Determination of the parameters *a* and $K_{[\eta]}$ of the [η]-*M*-relationship via plotting the intrinsic viscosity [η] as a function of the molar mass M_w for poly(styrene) (PS) in tetrahydrofuran (THF) at *T*=30 °C. Data points below a critical molar mass of 20,000 g mol^{-1} show a slope of *a*=0.5, above the critical molar mass a slope of 0.735. Data as a courtesy from PSS Polymer Standards Service, Mainz, Germany

Table 6.2. $[\eta]$-M-Relationships for poly(styrene) intoluene ($[\eta]$ in cm³/g). In addition to the molecular mass range the number of samples (fractions) used for the determination of the relationship is shown (taken from [88])

	T/ (°C)	Molar mass range/(g mol^{-1})	No. of fractions	Ref.
$[\eta]=11.2\times10^{-3}M_w^{0.72}$	20	2.9×10^4–2.4×10^5	6	[114]
$[\eta]=10.69\times10^{-3}M_w^{0.724}$	20	2.9×10^4–4.0×10^7	20	[115]
$[\eta]=4.16\times10^{-3}M_w^{0.788}$	20	4.0×10^4–1.37×10^6	10	[116]
$[\eta]=34.5\times10^{-3}M_w^{0.62}$	25	4×10^3–2.3×10^6	21	[117]
$[\eta]=17.0\times10^{-3}M_w^{0.69}$	25	3×10^3–1.6×10^6	9	[118]
$[\eta]=11.6\times10^{-3}M_w^{0.72}$	25	5.0×10^4–1.6×10^6	11	[119]
$[\eta]=10.5\times10^{-3}M_w^{0.73}$	25	1.6×10^5–6.9×10^5	7	[120]
$[\eta]=8.62\times10^{-3}M_w^{0.736}$	25	3.0×10^4–2.4×10^7	11	[88]
$[\eta]=7.85\times10^{-3}M_w^{0.747}$	25	5.0×10^4–1×10^6	10	[121]
$[\eta]=8.48\times10^{-3}M_w^{0.748}$	25	4.0×10^4–5.2×10^5	7	[122]
$[\eta]=7.5\times10^{-3}M_w^{0.75}$	25	1.2×10^5–2.8×10^6	8	[123]
$[\eta]=13.4\times10^{-3}M_w^{0.71}$	25	7.0×10^4–1.5×10^6	5	[124]
$[\eta]=8.52\times10^{-3}M_w^{0.61}$	25	1×10^7–2.2×10^7	4	[125]
$[\eta]=12.0\times10^{-3}M_w^{0.71}$	30	4×10^5–3.7×10^6	8	[126]
$[\eta]=9.23\times10^{-3}M_w^{0.72}$	30	4×10^4–1.5×10^6	9	[127]
$[\eta]=11.0\times10^{-3}M_n^{0.725}$	30	3.3×10^4–8.5×10^5	14	[128]
$[\eta]=9.77\times10^{-3}M_n^{0.73}$	30	7×10^4–1.27×10^6	5	[129]
$[\eta]=10.4\times10^{-3}M_w^{0.733}$	30	2.7×10^4–5×10^5	9	[130]
$[\eta]=8.81\times10^{-3}M_w^{0.75}$	30	2.5×10^5–3×10^6	5	[131]
$[\eta]=9.5\times10^{-3}M_n^{0.77}$	30	–	–	[132]
$[\eta]=12.6\times10^{-3}M_w^{0.71}$	35	3×10^4–6.5×10^6	14	[133]

$[\eta]$-M-relationships for the same molar mass range (for example see poly(styrene) in toluene in Table 6.2), the number of samples used gives a guideline for the selection of a good relationship from a number of similar ones.

Exercises and several practical examples of calculations of the molar mass or the intrinsic viscosity from $[\eta]$-M-relationships and vice versa are given in [49].

6.1.2 Ultrasonic Degradation of Native Samples

Six to nine polymer samples of different molar masses but similar molar mass distributions are required to establish a reliable $[\eta]$-M-relationship. For many polymers it is no problem to get these samples from different synthesis conditions. However, for new synthesis methods, expensive samples or biopolymers from a single native sample it is often not possible nor feasible to get the required number of samples with different molar masses. In these cases, it is possible to produce a homologous series of molar masses from a single sample by degradation methods.

The degradation of a polymer can be achieved by several means. Nevertheless, a controlled reduction of the molar mass is only possible if no statistical degradation occurs. In principal, a reduction of the molar mass of a polymer is possible by thermal, chemical and mechanical methods and also by enzymatic degradation or by an energy input via radiation. Thermal and chemical degradation (acidic, alkaline and oxidative) are statistical processes that lead to unwanted mono- and oligomers. In addition, they can lead to modifications of the chemical microstructure of the side groups. In contrast, mechanical degradation methods in pebble beds, [50], shear flow [51, 52] or ultrasonification [53] yield bigger chain segments and no monomer units [54]. Both degradation in a pebble bed and degradation in a shear flow field are not very effective for a controlled reduction of the molar mass. High intensity ultrasound on the other hand is an established and widely used method for the degradation of polymers in solution [55].

6.1.2.1 Principles of the Ultrasonic Degradation

Sound waves from an ultrasound generator cause pressure variations in solution. Local pressure differences in the fluid lead to an evaporation of the solvent that forms bubbles of the order of magnitude of up to 100 micrometers. These bubbles collapse with high energy in microseconds, this process is called cavitation.

The collapsing bubbles induce a strong elongational flow field in the solution as shown in Fig. 6.3. These flow fields [53, 56–58] and the shock wave of the cavitation [59] tear the polymer molecules apart and form polymer radicals. The chain breaks in its center of gravity due to the even distribution of the hydrodynamic forces in the elongational flow field [55, 60]. Big polymer coils degrade faster due to the larger hydrodynamic interactions with the solvent in the elongational flow field [61]. The molar mass of a polymer decreases exponentially with time and reaches a nearly constant minimum molar mass. Below a certain chain length, the hydrodynamic forces are not high enough to cause a rupture of the polymer chain. Figure 6.4 shows this for two different polymers in aqueous solution. The minimum molar mass depends on the type of polymer and on the energy input of the ultrasound.

Spectroscopical detection methods show that the chemical structure of the polymer side groups is not affected by the degradation process. Even large side groups in biopolymers stay intact as long as their length is below the minimum length of the polymer backbone [53]. The polydispersity decreases slightly with the time

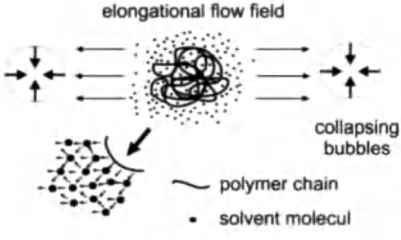

Fig. 6.3. Polymer chain disruption in an elongational flow field between two collapsing bubbles induced by ultra sound. The chain breaks in its center of gravity due to the even distribution of the hydrodynamic forces in the elongational flow field

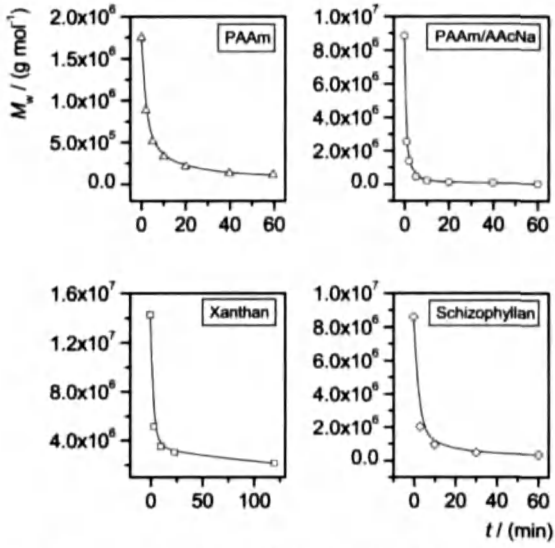

Fig. 6.4. Ultrasonic degradation of poly(acrylamide) (PAAm), c=0.0045 g ml^{-1}, M_w=1.8 to 0.1×10^6 g mol^{-1}, of poly(acrylamide-*co*-acrylate) (PAAm/AAcNa), c=0.0045 g ml^{-1}, M_w=8.8 to 0.06×10^6 g mol^{-1}, of xanthan gum, c=0.0005 g ml^{-1}, M_w=14.3 to 2.1×10^6 g mol^{-1} and schizophyllan, c=0.001 g ml^{-1}, M_w=8.9 to 0.35×10^6 g mol^{-1}. Ultrasonic power output for PAAm and PAAm/AAcNa approx. 25 W cm^{-2}, for xanthan gum and schizophyllan approx. 30 W cm^{-2}. The molar mass reaches a constant value after longer sonification times. Data from [53]

during an ultrasonic degradation, if the original polymer sample had a broad distribution.

6.1.2.2 Conducting an Ultrasonic Degradation

For an ultrasonic degradation of a polymer, a resonator is used as shown in Fig. 6.5. The setup in Fig. 6.5 for example uses a resonator with an output of ~400 W with a working frequency of ~20 kHz and an inert 3/4" titan tip. The solution volume for the setup in Fig. 6.5 should not exceed 200 ml and the concentration of the polymer solution should not exceed the critical concentration c^* (see "The critical concentration from the intrinsic viscosity" in Chap. 7, as a rule of thumb the concentration should be below 0.5 wt%). The resonator tip should immerse approx. 10 mm into the solution. The temperature of the solution during the ultrasonification should be kept below 30 °C to avoid a thermal degradation. A schematic view of the setup for an ultrasonic degradation is shown in Fig. 6.5.

Metal abrasion of the resonator tip has to be removed after the ultrasonification (for example via centrifugation). After the solvent has been removed (freeze-drying), the degraded polymer sample can be used for further investigations.

The molar mass of the degraded sample depends on the sonification time. This is shown for a hydroxyethylsulfoethyl cellulose (HESEC) in aqueous solution in

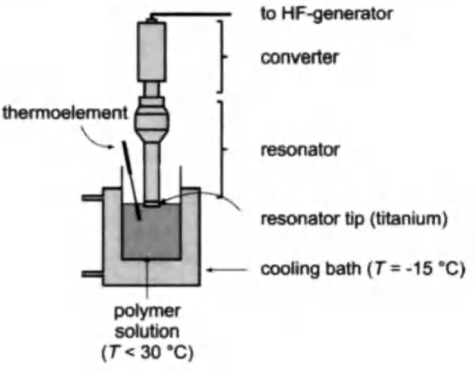

Fig. 6.5. Schematic view of the experimental setup of an ultrasonic degradation for the production of a homologous series of molar masses from a single polymer sample

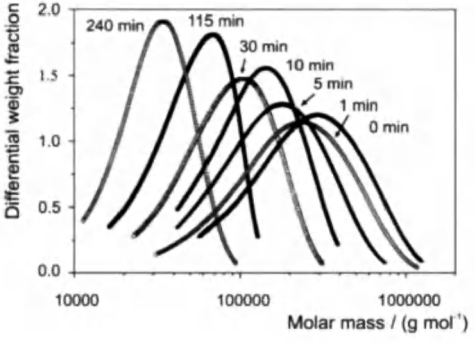

Fig. 6.6. Differential distribution of the molar mass *M* for a homologous series of ultrasonically degraded hydroxyethylsulfoethyl cellulose. The sonification time is given for each data set. Data from [55]

Fig. 6.6. Accordingly, the molar mass shows an exponential decay with the sonification time. After 4 h a minimum molar mass of 40,000 g mol^{-1} is reached. Longer ultrasonification times do not lead to a further decrease of the molar mass.

The intrinsic viscosity as a function of the sonification time in Table 6.3 shows a similar progression as the molar mass. The intrinsic viscosity decreases exponentially with time and reaches the minimum value of 140 ml/g for this polymer and the chosen energy input. The polydispersity M_w/M_n also decreases slightly with the sonification time.

The ultrasonic degradation of polymers is an established and capable method for the production of homologues series of molar masses. Ultrasonic degradation does not lead to a broadening of the molar mass distribution and a separation of monomer units and is therefore an indispensable operation for the determination of [η]-*M*-relationships (see above) from a single polymer sample.

Table 6.3. Molecular parameters as a function of the time for the ultrasonic degradation of hydroxyethylsulfoethyl cellulose (HESEC) in aqueous solution. The radii of gyration and the molar masses were determined via light scattering methods

Degradation time/(min)	M_n/ (g/mol)	M_w/ (g/mol)	M_z/ (g/mol)	M_w/M_n	R_{Gw}/ (nm)	R_{Gz}/ (nm)	$[\eta]$/ (cm^3/g)
0	218,000	337,000	487,000	1.54	51.3	64.2	617
1	197,000	290,000	407,000	1.47	49.7	61.7	495.5
5	144,000	207,000	286,000	1.44	40.6	48.4	328.5
10	110,000	142,000	185,000	1.29	34.7	39.4	322.1
30	84,000	107,000	132,000	1.27	26.7	30.4	223.9
115	46,000	58,000	69,000	1.26	23.5	23.7	140.8
240	28,000	35,000	42,000	1.23	23.1	23.4	140.0

6.2 The Influence of the Solvent Quality on the $[\eta]$-M-Relationship

The intrinsic viscosity $[\eta]$ of a polymer increases with rising solvent quality (see "Solvent" in Chap. 5) due to the increased solvating envelope of the polymer chain. An increased effective volume of the chain leads to an expansion of the polymer coil and therefore to an increased intrinsic viscosity (see Fig. 5.2). The solvent quality can also be seen in the exponent a of the $[\eta]$-M-relationship. In the case that the interactions of the solvent molecules with the chain are so small that the coil is not contracted or expanded, theta-conditions are reached and the coil has its unperturbed dimensions in solution. A theta solvent is referred to as a thermodynamically poor solvent. In this solution state a theoretical value for the exponent a=0.5 can be derived (the required Eqs. 8.22 and 8.33 are discussed in detail in "A deeper insight into" in Chap. 8). This value of a=0.5 is also experimentally observed as shown in Fig. 6.7 for the theta system poly(styrene) in cyclohexane (T=34.5 °C).

The exponent a of the $[\eta]$-M-relationship increases with the solvent quality. In a good solvent, a coil has its so-called perturbed dimensions. In a good solvent the exponent a can reach a theoretical value of 0.76 according to the mean-field theory [47]. Slopes between 0.5 and 0.76 are also experimentally observed, for example for poly(acrylamide) in H_2O at 25 °C in Fig. 6.7. Exponents a greater than 0.76 are experimentally not observed for flexible coils in good solvents [47]. Therefore, exponents a greater than 0.76 are not solely caused by the solvation of the polymer chain. In these cases, the coil expansion is also determined by the chemical structure of the polymer chain as shown in the following.

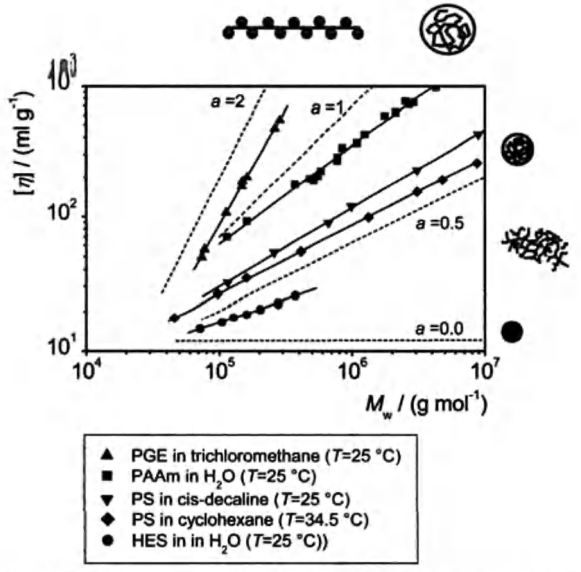

Fig. 6.7. Intrinsic viscosity [η] as a function of the molar mass M_w for different polymer-solvent systems. In addition to the experimental data, theoretical possible slopes of the [η]-*M*-relationships are shown for a better visualization. Data for poly(glutamic acid benzyl ester) (PGE) in trichloromethane at 25 °C, poly(acrylamide) (PAAm) in H_2O at 25 °C and poly(styrene) (PS) in *cis*-decaline at 25 °C are taken from [77], poly(styrene) (PS) in the theta-solvent-cyclohexane at 34.5 °C from [64], and hydroxyethyl starch (HES) in H_2O at 25 °C from [103]

6.3 Influence of the Solution Structure on the [η]-*M*-Relationship

In addition to the solvation of the polymer, the expansion of a polymer coil in solution and the value of the exponent *a* of the [η]-*M*-relationship is caused by the structure of the polymer chain. Certain polymers, for example poly(glutamic acid benzyl ester), form different structures in solution, for example flexible coils or helices, depending on the solvent quality as shown in Fig. 6.8 [62].

At a critical molar mass (M=65,000 g mol^{-1}) the linear [η]-*M*-relationships intersect (see Fig. 6.8). In general the curves of log [η]=f(log *M*) intersect only for different polymers in solution. For the same polymer in different solvents the curves do not intersect if the solution structure stays the same. The curves might merge at low molar masses (see "The influence of the molar mass" below). The intersection shown in Fig. 6.8 is therefore solely caused by changes in the solution structure. Helical structures of the polymer in solution are stiffer than the polymer chain in a flexible coil and lead to semi-flexible coils or rigid rod-like structures. The exponent *a* of the [η]-*M*-relationship shows for these extremely expanded structures values of $1 \leq a \leq 2$ (the poly(glutamic acid benzyl ester)

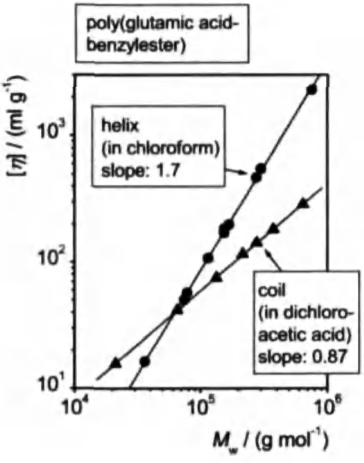

Fig. 6.8. Intrinsic viscosity $[\eta]$ as a function of the molar mass M_w for poly(glutamic acid benzyl ester) (PGE) in two different solvents at 25 °C (data from [62]). The slope of 1.7 for the $[\eta]$-M-relationship for chloroform as a solvent indicates a rod-like (helical) structure, whereas in dichloroacetic acid a slope of 0.87 indicates a flexible coil for the solution structure

shown in Fig. 6.8 for example has a value of a=1.7 for the helical structure in solution).

However, even polymers with rigid helical segments behave like a flexible coil at very high molar masses, although the distance between two flexible joints of the chain is in this case not the bond length but the length of a helical part of the chain. The $[\eta]$-M-relationship for very high molar masses shows again a slope of a≈0.8 like a flexible polymer in a good solvent, as can be seen in Fig. 6.9 for DNA in aqueous solution or poly(hexylisocyanate) (PHIC) in hexane.

The transition from slopes a<0.8 for semi-flexible rods at low molar masses to a=0.8 for flexible coils at high molar masses is often not detected because of the narrow range of molar masses available for the determination of a $[\eta]$-M-relationship. This is another reason that many different $[\eta]$-M-relationships are pub-

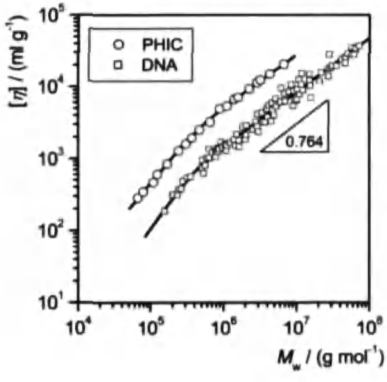

Fig. 6.9. Intrinsic viscosity $[\eta]$ as a function of the molar mass M_w for the rod-like polymers deoxyribonucleic acid (DNA) in aqueous NaCl solution at 20 °C (data from [47, 104]) and poly(hexylisocyanate) (PHIC) in hexane at 25 °C (data from [47, 105]). At very high molar mass even rod-like polymers behave like flexible coils and show the slope of a flexible coil in a good solvent

Table 6.4. [η]-*M*-Relationships for xanthan gum in aqueous solution. In addition to the molecular mass range, the salt content of the solution and temperature the degree of substitution with acetate and pyruvate is shown for some relationships

$K_{[\eta]}$	a	M_w/(g/mol)	Ac/ (mol%)	Py/ (mol%)	T/(°C)	c_{NaCl}	Ref.
3.21×10^{-5}	1.25	2×10^5–4×10^6		0.4	25	0.1 mol/l	[134]
4.64×10^{-6}	1.41	″2.5×10^5			25	0.1 mol/l	[135]
4.41×10^{-4}	1.07	1×10^6–7.5×10^6			25	0.1 mol/l	[135]
2.1×10^{-3}	0.90	1.5×10^6–1×10^7				0.05 mol/l $NaSO_4$	
6.3×10^{-3}	0.93	10^6–5×10^6		1.6	30	5 g/l	[136]
3.5×10^{-5}	1.244	4.2×10^4–3.3×10^6	1	0.6–1	25	0.1 mol/l	[137]
1.52×10^{-5}	1.32	3.3×10^5–3.3×10^6	1	1	25	0.1 mol/l	[137]
9.3×10^{-5}	1.20	6.5×10^5–7×10^6	0.48	0.36	25	0.1 mol/l	[138]
1.72×10^{-4}	1.14	3×10^5–10^7			25	0.1 mol/l	[139]
1.7×10^{-4}	1.14	3×10^5–7×10^6	0.75	0.4	25	0.1 mol/l	[137]
2.4×10^{-4}	1.10	3×10^5–1×10^6			25	0.1 mol/l $NaNO_3$	[140]
9.41×10^{-4}	0.956	1.5×10^6–1×10^7	0.62	0.48	25	0.1 mol/l	[141]
5.66×10^{-4}	1.0	3×10^5–10^7			25	0.3 mol/l	[140]
1.72×10^{-4}	1.14	3×10^5–10^7			25	0.1 mol/l	[140]
4×10^{-5}	1.23	3×10^5–10^7			25	0.03 mol/l	[140]
3.14×10^{-5}	1.26	3×10^5–10^7			25	0.01 mol/l	[140]
2.83×10^{-5}	1.27	″2×10^5			25	0.01 mol/l	[142]
5.71×10^{-5}	1.21	2×10^5–10^6			25	0.01 mol/l	[142]
2.57×10^{-4}	1.09	″2×10^5			80	0.01 mol/l	[142]
1.82×10^{-3}	0.93	2×10^5–10^6			80	0.01 mol/l	[142]
1.64×10^{-5}	1.29	1×10^5–10^6		0.34	25	0.01 mol/l	[143]
	1.35	″10^6			20	0.75 mol/l	[144]
	0.96	$\geq10^6$			20	0.75 mol/l	[144]
8.66×10^{-3}	0.84	2×10^6–9×10^6			25	0.01 mol/l	
1.05×10^{-4}	1.18	2×10^6–7×10^6			25	0.01 mol/l	

lished for the same polymer-solvent system. This is shown in Table 6.4 for the fermentation polymer xanthan gum, which forms a double helical structure in aqueous solution (see also Chap. 5). The published exponents a of the [η]-*M*-relationship show values ranging from a=0.9 for molar mass ranges at 10^7 g mol^{-1} to a=1.4 at 10^5 g mol^{-1}. It is therefore of great importance to use an [η]-*M*-relationship only in the specified molar mass range respectively to specify the molar mass range for a new [η]-*M*-relationship.

In addition to the molar mass range, small changes in the chemical structure can also lead to changes in the solution structure. Table 6.4 also lists the degree of substitution with acetate and pyruvate groups for some xanthan gums. Different degrees of substitution lead to changes in the $[\eta]$-M-relationship, even for the same molar mass range. The influence of changes in the chemical structure on the parameters a and $K_{[\eta]}$ of the $[\eta]$-M-relationship is much more pronounced for the poly(acrylamide-*co*-acrylic acid) copolymers introduced in Fig. 5.20.

Figure 6.10 shows the dependence of a and $K_{[\eta]}$ from the content of acrylic acid groups for a copolymer with a constant degree of polymerization P. Although the molar mass is nearly constant and the solvent is the same, the parameters of the $[\eta]$-M-relationship show a complex maximum or minimum behavior due to the changing intramolecular interactions and the resulting solution structure. Hence, the composition of complex bio- and co-polymers should also be specified for an $[\eta]$-M-relationship in addition to the molar mass range.

However, not only helical structures result in high coil expansions and high values of a. Polyelectrolytes with a high degree of dissociated ionic groups have very rigid polymer chains due to the coulomb repulsion forces of the ionic groups along the backbone. This can lead to highly expanded coils. The polymer chain behaves, depending on the charge density, as a semi-flexible coil or a rigid rod. The exponent a shows values between a=0.8 and a=2. However, the determination of an $[\eta]$-M-relationship for a polyelectrolyte in salt free aqueous solution is quite complicated. As shown in "Polyelectrolytes" in Chap. 5, the determination of an intrinsic viscosity is only possible with the addition of salts, although the intrinsic

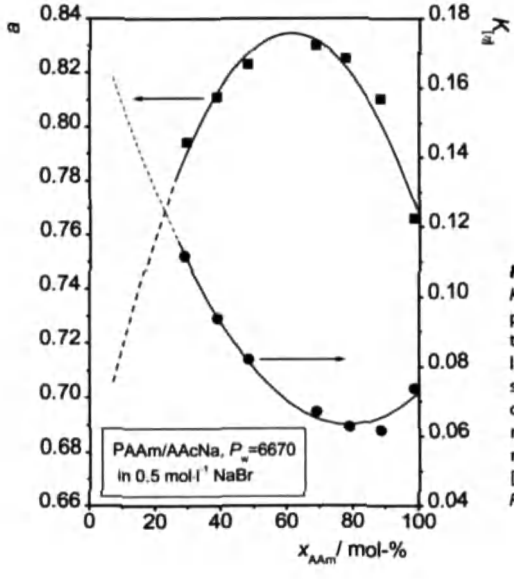

Fig. 6.10. *Exponent a and constant $K_{[\eta]}$* of the $[\eta]$-M-relationship depending on the copolymer composition of a poly(acrylamide-*co*-acrylate) dissolved in 0.5 mol l^{-1} NaBr solution. The composition of the copolymer is determined by the molar fraction of acrylamide (AAm) monomers given in % (data from [106]). The degree of polymerization P is kept constant at P=6670

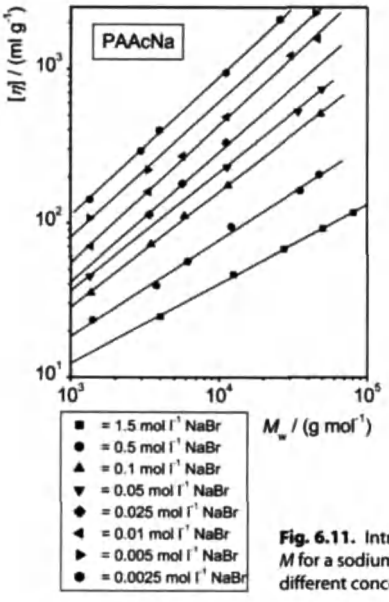

Fig. 6.11. Intrinsic viscosity [η] as a function of the molar mass *M* for a sodium poly(acrylate) (PAAcNa) in aqueous solution with different concentrations of sodium bromide at *T*=25 °C

viscosities determined with added salts do not reflect the coil expansion of the polyelectrolytes in salt free solution. Hence the exponents of a=2 in salt free solutions are more of a theoretical nature.

[η]-*M*-relationships of polyelectrolytes should always be listed with the salt concentration used for the determination of the intrinsic viscosities, since the coil expansion and therefore the intrinsic viscosity decreases with the salt concentration.

Figure 6.11 shows [η]-*M*-relationships for the same polymer-solvent system but for different salt concentrations. The slope a decreases with an increasing salt concentration. This can also be seen in Table 6.5 where [η]-*M*-relationships for several different polyelectrolytes and different salt concentrations are listed.

The chemical structure of a polymer can also cause a contraction of the polymer coil compared to the unperturbed dimensions at theta-conditions. In this case the exponent a of the [η]-*M*-relationship shows values of $a \leq 0.5$. A contraction of the coil occurs if the attractive intramolecular interactions between the polymer segments become larger than the interactions with the solvent molecules. In extreme cases, the solvent is forced out of the polymer coil and the chain segments start to form compact aggregates. The density of the polymer coil is then independent of the molar mass and the intrinsic viscosity is constant. In this case the exponent a is zero. An example is shown in Fig. 6.12 for compact glycogen in aqueous solution.

A dependence of the intrinsic viscosity on the molar mass for branched polymers was already shown in Fig. 5.11. The intrinsic viscosity of branched polymers is lower than the intrinsic viscosity of linear polymers with the same molar mass.

Table 6.5. Selected $[\eta]$-M-Relationships for polyelectrolytes in solutions with different salt concentrations. Data from [83]

Polyelectrolyte	Salt	T/(°C)	c_{salt} (mol l^{-1})	$M\times10^{-4}$/ (g mol^{-1})	$K\times10^{3}$/ (ml g^{-1})	a
Polyanions						
Sodium poly(acrylate)	NaBr	15	0.0025	1.5–50	2.49	0.89
			0.05		2.81	0.77
			1.5		12.4	0.50
			0.01		1.32	0.91
			0.1		3.12	*0.76*
			0.5		5.06	0.66
	NaBr	25	0.9–80			
Sodium poly(styrene sulfonate)	NaCl	25	0.005	39–230	0.23	0.93
			0.05		1.39	0.72
			0.5		1.86	0.64
			4.17		2.04	0.50
Sodium poly(2-acrylamido-2-methylpropane sulfonate)	NaCl	25	0.01	14–87	0.083	1.0
			0.1		0.16	0.88
			1.0		0.36	0.77
			5.0		0.53	0.72
Carboxymethyl cellulose, DS≈1.06	NaCl	*21*	*0.005*	*15–110*	*0.72*	*0.95*
			0.05		1.9	0.82
			0.2		4.3	0.74
Alginate	NaCl	25	0.01	0.11–270	0.05	1.15
			0.1		0.2	1.0
			1.0		0.91	0.87
Polycations						
Poly(2-trimethyl ammonium-methyl methacrylate chloride)	NaCl	25	0.1	0.77–1110	0.63	0.76
			1.0		0.75	0.71
			4.0		0.99	0.69
Poly(4-vinylbenzyl trimethyl ammonium chloride)	NaCl	25	0.002	1.3–21	0.58	0.88
			0.01		0.79	0.85
			0.1		1.9	0.70
			0.5		2.0	0.67
Poly(allylammonium chloride)	NaCl	25	0.05	2.8–18	0.24	0.98
			0.2		0.72	0.82
			0.5		0.72	0.79
			1.0		1.4	0.71

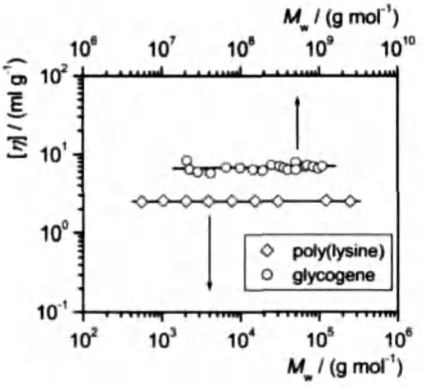

Fig. 6.12. Compact polymer coils in solution: intrinsic viscosity [η] as a function of the molar mass M_w for the sphere like, aggregated glycogen in aqueous solution at T=25 °C [107] and the hyperbranched poly(α,ε-lysine) in *N,N*-dimethylformamide at T=35 °C [108]. Both solution structures show an intrinsic viscosity that is independent of the molar mass, indicating a constant density of the polymer coil in solution regardless of the molar mass according to Eq. (7.1)

This effect increases with an increasing molar mass. Hence, [η]-*M*-relationships for branched polymers are only valid for very narrow molar mass ranges. As can be seen in Fig. 5.11, the intrinsic viscosity of branched polymers becomes nearly independent of the molar mass at high molar masses. The slope *a* of [η]-*M*-relationships for high molar masses of branched polymers is therefore low and can acquire values of $a \leq 0.5$.

Hyperbranched polymers show this independence of the intrinsic viscosity from the molar mass already at low molar masses. Figure 6.12 for example shows a hyperbranched poly(lysine) with an exponent *a* of the [η]-*M*-relationship of a=0 over the whole accessible molar mass range. Hyperbranched polymers with very short distances between the branching points have a high density of polymer segments and a very low content of solvent molecules inside the coil. Even though the attractive intramolecular interactions between the coils may not be very high, these polymers have a structure similar to the aggregated glycogen in Fig. 6.12.

The possible influence parameters on the expansion or contraction of a polymer in solution are summarized in Fig. 6.13.

In addition to Fig. 6.13, Table 6.6 correlates the exponent *a* of the [η]-*M*-relationship with the solution structures introduced in the last two chapters.

Table 6.6. Different solution structures of a polymer coil and the related exponents *a* of the [η]-*M*- and *v* of the R_G-*M*-relationship

a	v	Polymer structure in solution
0	0.333	Aggregated compact sphere, hyperbranched compact structure
0.5	0.5	Theta-condition in a poor solvent, unperturbed dimensions of the coil
0.8	0.6	Expanded (disturbed) coil in a good solvent
1–2	0.67–1	Semiflexible rod, helical structure
2	1	Rigid rod

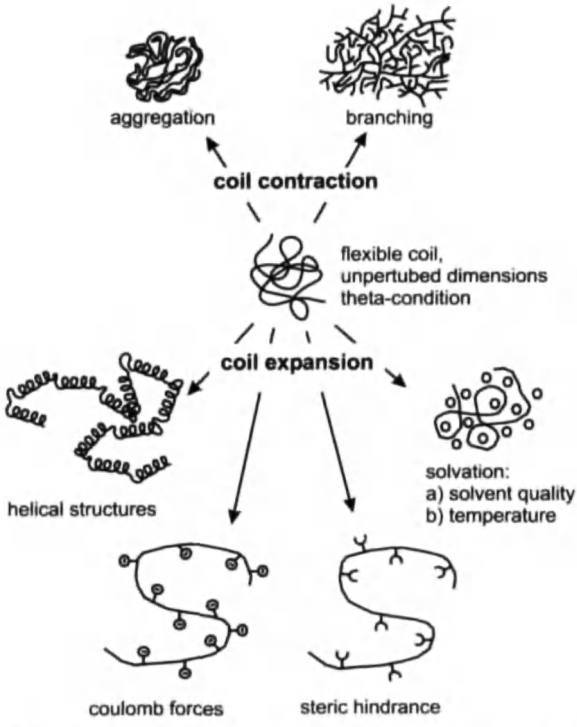

Fig. 6.13. Different solution structure causing an expansion or contraction of the polymer coil in solution compared to the linear, flexible coil in its unperturbed dimensions

6.4 The Influence of the Tacticity of a Polymer

Figure 6.14 shows the dependence of the intrinsic viscosity from the molar mass for linear poly(styrene) (PS) in the good solvents trichlorobenzene (TCB) and toluene. Whereas the chemical composition of the polymers in this example is not changed, the tacticity (the stereo chemical position of the side group) differs between the used samples.

These polymers show great differences in solid phases due to the different tacticity, but nearly the same properties in solution. Figure 6.14 shows that the intrinsic viscosities of atactic and syndiotactic PS in TCB as well as the atactic and isotactic PS in toluene, show the same molar mass dependence. Since there are no direct interactions of the polymer segments as in a solid, only the short-range interactions (restricted rotation of the chain) are effected by different tacticities. In a good solvent, the short-range interactions are negligible compared to the long-range interaction caused by the excluded volume and the solvating envelope (see

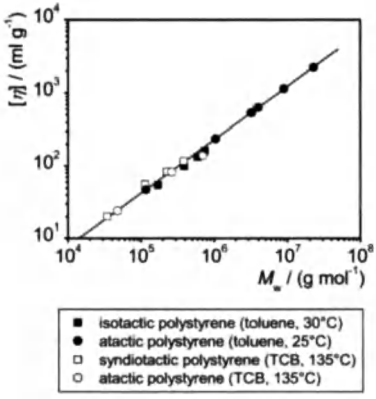

Fig. 6.14. Intrinsic viscosity [η] as function of the molar mass M_w for poly(styrene) of different tacticities. A comparison of the data is possible between atactic and syndiotactic poly(styrene) (PS) in trichlorobenzene (TCB) at 135 °C [109] and atactic PS at 25 °C [88] and isotactic PS at 35 °C [110] in toluene

Chap. 8). The long-range interactions are not effected by the tacticity and no change in the intrinsic viscosity is observed for different tacticities.

In theta-solvents and polymer-solvent systems with an exponent a of the [η]-M-relationship>0.5 the short range interactions dominate the structure of the polymer coil. In these solvents, differences of the radii of the polymer coils of up to 20% can be observed between iso- and syndiotactic polymers of the same molar mass [47]. However, already in solvents with qualities slightly better than theta-solvents, the long-range interactions dominate and the intrinsic viscosity becomes independent of the tacticity.

6.5 The Influence of the Molar Mass on the [η]-*M*-Relationship

It is desirable to establish an [η]-M-relationship over a wide range of molar masses. However, it was pointed out above that [η]-M-relationships are only valid for a limited range of molar masses. This is especially true for low molar masses. As shown in Fig. 6.15, different slopes and values for $K_{[\eta]}$ and a for different solvents are only observed above a critical molar mass [63].

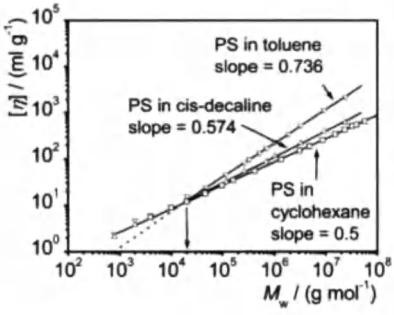

Fig. 6.15. Intrinsic viscosity [η] as function of the molar mass M_w for poly(styrene) in the good solvent toluene at 25 °C [111], in *cis*-decaline at 25 °C [63], and the theta solvent cyclohexane at 34.5 °C [64]

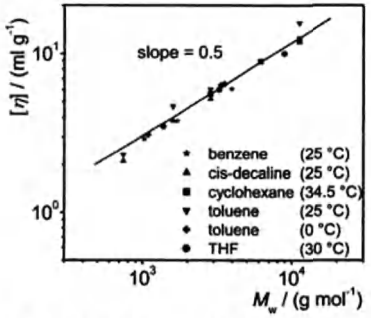

Fig. 6.16. Intrinsic viscosity $[\eta]$ as function of the molar mass M_w for poly(styrene) (PS) of low average molar mass in different solvents. The slope of the $[\eta]$-M-relationship in this molar mass range is independent of the solvent quality. (Data for benzene from [65], for toluene at T=0 °C from [66], for toluene at 25 °C from [111], cyclohexane at 34.5 °C from [64] *cis*-decaline at 25 °C from [63] and THF at 30 °C as a courtesy from PSS Polymer Standards Service, Mainz, Germany

Below this critical molar mass of M_w=20,000 g mol^{-1} all data points fall on a single line with a slope of 0.5 for the example of poly(styrene). This observation was confirmed for other polymer systems [64–66] independent of the solvent or temperature (Fig. 6.16).

This behavior is probably caused by a rising influence of the chain ends. Below a critical molar mass, the number of polymer segments is too low to form a flexible coil. In addition to this, short polymer chains have no excluded volume and the influence of the solvation envelope on the coil expansion disappears. In addition, coil substructures like helical parts have an effect on the overall coil structure above a critical number of polymer segments.

Figure 6.17 shows for an aqueous solution of poly(acrylamide) (PAAm) that below the critical molar mass the $[\eta]$-M-relationship does not necessarily acquire the slope of 0.5 of a theta-system. In the given example, the data points lie on a line with a slope of 0.7, corresponding to a good solvent. So far there is no explanation

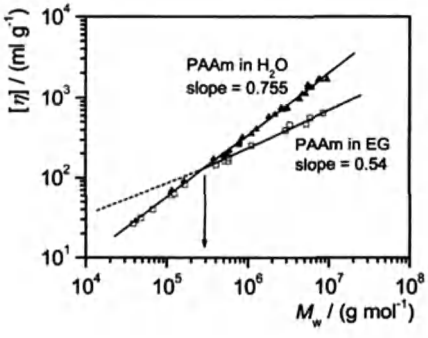

Fig. 6.17. Intrinsic viscosity $[\eta]$ as function of the molar mass M_w for poly(acrylamide) (PAAm) in H_2O and in ethylene glycol (EG). Below a critical molar mass the intrinsic viscosity becomes independent of the solvent and the slope of the $[\eta]$-M-relationship becomes that of a good solvent system (data from [92, 112])

why the slope of the PAAm solution below the critical molar mass is not that of a theta solvent. Compared to poly(styrene) the critical molar mass is also approx. a decade higher for PAAm.

6.6 Tabulated [η]-*M*-Relationships

Here several [η]-*M*-relationships are listed. Table 6.7 shows [η]-*M*-relationships of important polymer-solvent systems. Most of these relationships where determined from sample sets with a very narrow molar mass distribution *Q*, the heterogeneity class is specified for each [η]-*M*-relationship (see "Heterogeneity classes and the influence of the polydispersity on the [η]-*M*-relationship" in Chap. 8). The [η]-*M*-relationships are only valid for the listed range of molar masses. More [η]-*M*-relationships are listed in Tables 6.2, 6.4, 6.5 and 8.5. For rare polymer-solvent systems and copolymers with a defined composition, the reader is referred to the Polymer Handbook [48], Gnamm and Fuchs [45] as well as [67, 68].

Table 6.7. Selected [η]-*M*-relationships for different polymersolvent systems with good and very good heterogeneity classes

Polymer	Solvent	*T*/(°C)	$K \times 10^3$/(ml/g)	*a*	$M \times 10^{-4}$/(g mol^{-1})	Class	Refs.
Poly(acrylamide)	Water	25	10.0	0.755	14–900	B	[92]
	Ethylene glycol	25	136	0.54	50–600	B	[112]
	Formamide	25	12.7	0.74	50–600	B	[112]
Poly(acrylonitrile)	γ-Butyro-lactone	20	34.3	0.730	4–40	A	[145]
	Dimethyl-formamide	25	52.0	0.690	5–52	B	[146]
	Dimethyl-formamide	35	31.7	0.746	9–76	A	[145]
Poly(butadiene) 79%-*trans*, 21%-*cis*	Cyclohexane	20	36	0.70	23–130	B	[147]
Poly(butadiene-*co*-styrene), Buna-S linear fraction	Toluene	30	21.4	0.74	3–20	A	[148]
Poly(butyl methacrylate)	Chloroform	20	2.9	0.78	4–800	B	[149]
	2-Propanol	21.5(θ)	38	0.50	4–800	B	[149]
Poly(butyl isocyanate)	Benzene	20	1.10	1.11	1.8 –21	A	[150]
Poly(chloroprene), Neoprene W	Benzene	25	15.5	0.72	5–80	B	[151]
Poly(4-chlorostyrene)	Toluene	30	13.0	0.64	3–140	B	[152]

Table 6.7 (continued)

Polymer	Solvent	T/(°C)	$K\times10^3$/ (ml/g)	a	$M\times10^{-4}$/ (g mol^{-1})	Class	Refs.
Poly(ethyl acrylate)	Acetone	25	51	0.59	35–450	B	[153]
Poly(ethylene) low pressure	Decalin	135	62	0.70	2–105	B	[154]
	Tetralin	130	51	0.725	0.4–50	B	[155]
	p-Xylene	105	51	0.725	0.4–50	B	[156]
Poly(imino-adipolimino-hexamethylene), Nylon 66	90% Formic acid	25	32.8	0.74	1–5	C	[157]
Poly[imino(1-oxo-dodecamethylene)], Nylon 12	*m*-Cresol	25	81	0.74	0.3–13	B	[158]
	85% Formic acid	25	22.6	0.82	0.7–12	B	[159]
Poly(isobutene)	Benzene	25	83	0.53	0.05–126	B	[160]
	Cyclohexane	30	27.6	0.69	4–71	A	[161]
	Diiso-butylene	20	36	0.64	1–130	A	[162]
	Toluene	30	20	0.67	1–146	B	[160]
Poly(isoprene), natural rubber	Toluene	25	50.2	0.667	7–100	B	[163]
Poly(isoprene), 85–91%-*cis*	Toluene	30	20.0	0.728	14–580	A	[164]
Poly(isoprene), gutta percha	Benzene	25	35.5	0.71	0.2–5	A	[165]
Poly(propylene) atactic	Decalin	135	11.0	0.80	2–62	A	[166]
Poly(isopropyl acrylate)	Benzene	25	12.4	0.701	4–100	B	[167]
Poly(methyl acrylate)	Acetone	25	5.5	0.77	28–160	B	[168]
	Benzene	30	3.56	0.798	25–190	B	[169]
	Butanone	20	3.5	0.81	6–240	A-B	[168]
Poly(methyl meth-acrylate) atactic	Acetone	25	5.3	0.73	2–780	A-B	[170]
	Acetonitrile	45 (θ)	48	0.5	10–260	A-B	[171]
	Benzene	25	5.5	0.76	2–740	A-B	[170]
Poly(methyl meth-acrylate), living type	1,2-Dichloro-ethane	30	5.3	0.77	6–263	A-B	[172]
Poly[oxy(dimethyl-silylene)]	Bromo-cyclohexane	29.0(θ)	74	0.50	3.3–106	A	[173]
Poly(oxyethylene)	Acetone	25	32	0.67	7–100	A	[174]
	Benzene	25	39.7	0.686	8–520	A	[175]
	Water	35	6.4	0.82	3–700	C	[176]

Table 6.7 (continued)

Polymer	Solvent	T/(°C)	$K\times10^3$/(ml/g)	a	$M\times10^{-4}$/(g mol^{-1})	Class	Refs.
Poly(propylene) isotactic	Decalin	135	10.0	0.80	10–100	A	[177]
	Tetralin	135	9.17	0.80	4–54	A	[178]
Poly(styrene) atactic	Benzene	20	12.3	0.72	0.6–520	A	[65]
	n-Butyl-benzene	25	16.4	0.684		A	[179]
	Butanone	25	39	0.58	1–180	A	[118]
	Cyclohexane	34.5 (θ)	84.6	0.50	14–200	A	[180]
	Toluene	25	8.62	0.736	3–2400	A	[88]
Poly(vinyl alcohol)	Water	30	45.3	0.64	1–80	A	[181]
Poly(vinyl acetate)	Acetone	30	10.1	0.73	6–150	A	[182]
Poly(vinyl chloride)	Cyclo-hexanone	25	13.8	0.75	1–12	A-B	[183]
	Tetrahydro-furan	25	16.3	0.766	2–30	A.B	[184]
Poly(vinyl-pyrrolidone)	Water	30	39.3	0.59	8–110	A	[185]

7 Determination of the Polymer Coil Dimensions from the Intrinsic Viscosity

7.1 Introduction

The concentration of a polymer in solution yields no information on how much of the solution volume is filled with polymer coils. Depending on the influence parameters described in the previous chapters, the expansion of a polymer coil in solution can increase or decrease. Even at polymer concentrations that are seemingly relatively low, for example $c<0.1\%$, polymer coils with large intrinsic viscosities (in this case $[\eta]>2500$ ml g^{-1}) completely fill the solution volume. Although the intrinsic viscosity contains this information, some experience is needed to estimate the percentage of solution volume filled with polymers given the intrinsic viscosity. Thus in the following the calculation of the volume V_{coil} and diameter d of a single polymer coil from the intrinsic viscosity is shown. These dimensions allow for the calculation of the volume demand of the polymer in solution, especially the concentration where 100% of the solution volume is filled. This concentration is denoted in the next section as the critical concentration c^*. Since nearly all technical applications of polymer solutions require concentrations above c^*, viscosimetry permits an easy determination of the required minimum concentration of the polymer via the intrinsic viscosity.

7.2 The Dimension of a Single Polymer Coil

The knowledge of the intrinsic viscosity allows for the determination of the size of a single polymer coil in a dilute solution. The coil expansion and the density of the polymer coil in solution are directly given by Eqs. (4.6) and (4.7):

$$\rho_{equ} = \frac{2.5}{[\eta]} \tag{7.1}$$

The diameter d of a single polymer coil can be obtained from the density ρ_{equ}, the molar mass M (Eq. 2.12) and the volume V_{coil} of the coil:

$$\rho_{equ} = \frac{m_{coil}}{V_{coil}} = \frac{M}{V_{coil} \cdot N_A} \tag{7.2}$$

$$V_{coil} = \frac{m_{coil}}{\rho_{equ}} = \frac{M \cdot [\eta]}{N_A \cdot 2.5} = \frac{1}{6} \pi \cdot d^3 \tag{7.3}$$

$$d = \left(\frac{6 \cdot M \cdot [\eta]}{2.5 \cdot \pi \cdot N_A} \right)^{\frac{1}{3}} \tag{7.4}$$

These calculations still assume that the polymer coil in solution is a hard sphere with an even density throughout the sphere and with a fixed boundary to the solvent. For a more realistic discussion of the dimensions of a real polymer coil in solution, the reader is referred to Chap. 8. In particular, the correlation of diameter d, molar mass M and intrinsic viscosity $[\eta]$ in Eq. (7.4) is discussed in detail in Chap. 8 in the form of the Fox-Flory equation that correlates the intrinsic viscosity with the radius of gyration R_G of a polymer coil and with the molar mass:

$$[\eta] = \Phi \cdot \frac{R_G^3}{M} \tag{7.5}$$

7.3 The Critical Concentration from the Intrinsic Viscosity

The knowledge of the dimensions of a single polymer coil allows for the calculation of the solution volume filled with polymer. A matter of particular interest is the polymer concentration where the solution is completely filled with polymer coils and the coils start to interpenetrate as shown in Fig. 7.1.

This concentration is denoted as the critical concentration c^*. The critical concentration marks the transition from a dilute to a semi-concentrated solution. This transition is accompanied by great changes in the flow properties of a polymer solution. At concentrations above c^* the flow behavior is dominated by the intermolecular interactions of the polymer coils whereas below c^* mainly the polymer-solvent interactions determine the flow properties. Nearly all technical applications of polymer solutions require concentrations equal to or above c^*. For example, the

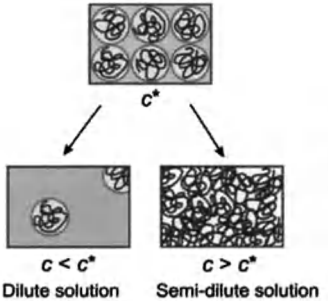

Fig. 7.1. Schematic drawing of the critical concentration c^* in a polymer solution. At the critical concentration, the solution volume is totally filled with polymer coils. Above the critical concentration in the semi-dilute solution regime, the polymer coils interpenetrate and the solution behavior is dominated by intermolecular interactions. Below c^* in the dilute solution regime the solution behavior is controlled by polymer-solvent interactions

blood plasma volume expander hydroxyethyl starch (HES) is used at the critical concentration to obtain a maximum polymer concentration without a superproportional increase of the viscosity.

The critical concentration is reached for a volume fraction ϕ of the polymer of one. In this case, Eq. (4.3) yields

$$V_{\text{solution}} = V_{\text{polymer}} = \frac{m_{\text{polymer}}}{\rho_{\text{equ}}} \tag{7.6}$$

With Eq. (7.1) the critical concentration of the viscosimetry $c^*_{[\eta]}$ is obtained:

$$c^*_{[\eta]} = \frac{m_{\text{polymer}}}{V_{\text{solution}}} = \rho_{\text{equ}} = \frac{2.5}{[\eta]} \tag{7.7}$$

Therefore the critical concentration $c^*_{[\eta]}$ is proportional to the reciprocal intrinsic viscosity. The factor of 2.5 assumes that the polymer coils behave like hard spheres in solution. Viscosimetric measurements for the determination of the intrinsic viscosity have to be performed in dilute solutions at concentrations clearly below c^* for an exact linear extrapolation according to the Huggins equation (Eq. 4.9). This condition is fulfilled for example in Fig. 4.2, where it is shown that the data points for the viscosimetric determination are below the critical concentration calculated from Eq. (7.7).

7.4 The Critical Concentration from Absolute Polymer Coil Radii

If the absolute diameter or radius of a polymer coil is known, a direct calculation of a critical concentration is possible without viscosimetric data. Common methods for the determination of absolute coil dimensions are the different light scattering methods. The critical concentration calculated from these dimensions is therefore often denoted as the critical concentration of light scattering, c^*_{LS}, since the radius R (see Chap. 8) can be determined directly from static light scattering.

The critical concentration is then directly calculated from the molar mass and the radius of the polymer coil:

$$c^*_{\text{LS}} = \frac{M}{\frac{4}{3} \cdot N_{\text{A}} \cdot \pi \cdot R^3} \tag{7.8}$$

For polymers in good solvents the critical concentration c^*_{LS} is approx. a factor of ~10 lower than the critical concentration $c^*_{[\eta]}$, obtained from the intrinsic viscosity according to Eq. (7.7), as shown in Fig. 7.2 for poly(acrylamide) and poly(styrene) in good solvents. However, for other systems with a less good solvent quality smaller ratios of the critical concentrations have been observed, for example for

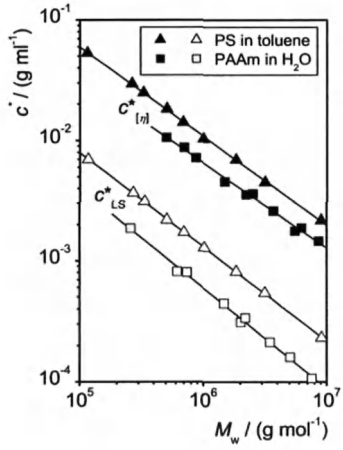

Fig. 7.2. Critical concentration c^* as function of the mass average molar mass M_w for poly(styrene) (PS) in toluene at T=25 °C and poly(acrylamide) (PAAm) in H_2O. The *closed symbols* show the critical concentration of the viscosimetry $c^*_{[\eta]}$ (Eq. 7.7), the *open symbols* the critical concentration from the radius of gyration (from light scattering measurements) c^*_{LS} (Eq. 8.30). Data from [92]

acetyl starch in aqueous solution a ratio of $c^*_{[\eta]}/c^*_{LS}$=8.7 or for barley glucan in aqueous solution of $c^*_{[\eta]}/c^*_{LS}$=3 [69].

Nevertheless, even the critical concentration c^*_{LS}, obtained from absolute polymer coil dimensions, is only a relative value since the radii measured with scattering experiments are not equal to the hydrodynamic radii of the same polymer coils in solution. A detailed discussion on how to calculate a hydrodynamic radius is given in "The critical concentration of a real coil" in Chap. 8.

8 A Deeper Insight into Viscosimetry

8.1 The Viscosity of Mixtures of Solvents

The viscosity of a mixture of solvents cannot be derived from a simple summation of the proportionate viscosities of the single solvent components. Intermolecular interactions between the different components can lead to an increasing, but also to a decreasing viscosity of the mixture compared to the viscosities of the single components. Listed relationships for a calculation of the viscosity of the mixture from the viscosities of the components are partially semi-theoretical, but most of the time of an empirical nature. A critical compilation of 54 mixing rules for solvents is given in [70, 71]. The mixing rules introduced in this chapter are only valid for binary mixtures of homogeneous, completely miscible and salt free fluids. The composition of the mixtures can be indicated by different fractions, w_i=mass fraction, x_i=molar fraction, and ϕ_i=volume fraction, with i=1,2.

These fractions describe the proportion of the mass, mol or volume of a component to the total mass, mol or volume of the mixture. The volume fraction is referenced to the sum of the volumina of the single components, a volume expansion or contraction of the mixture is therefore not taken into account and it is not necessary to determine the total volume of the mixture. This definition of the different fractions results in the following equation:

$$w_1 + w_2 = x_1 + x_2 = \phi_1 + \phi_2 = 1 \tag{8.1}$$

With the molar masses M_1 and M_2 of the components and the corresponding densities ρ_1 and ρ_2, the following fractions can be calculated:

$$w_2 = \frac{M_2 \cdot x_2}{M_1 \cdot (1 - x_2) + M_2 \cdot x_2} \tag{8.2}$$

$$x_2 = \frac{M_1 \cdot w_2}{M_2 \cdot (1 - w_2) + M_1 \cdot w_2} \tag{8.3}$$

$$\phi_2 = \frac{\rho_1 \cdot w_2}{\rho_2 \cdot (1 - w_2) + \rho_1 \cdot w_2} \tag{8.4}$$

The efficiency of a mixing rule can depend on the used type of fraction. In most cases, the mass fraction is used for the mixing rules.

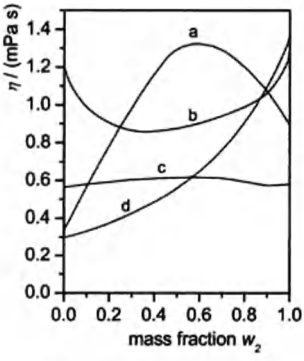

Fig. 8.1. Viscosity η of mixtures of two solvents as a function of the mass fraction w_2 of the second component

Even binary solvent mixtures can show a very complex behavior of the viscosity depending on the mixing ratio, with minima, maxima and inflection points. The viscosity can also show values of more than double the viscosity of single components. A few examples are shown in Fig. 8.1.

Most mixing rules are only valid for the calculation of a dynamic viscosity; so far there are only a few relationships for kinematic viscosities published. However, for solvents with great differences of the density the progression of the kinematic viscosity can be very different from the dynamic viscosity, depending on the composition of the mixture.

For practical applications, only those mixing rules are of interest that are valid over a wide range of mixture compositions and that depend only on the viscosity of the components. The number of free parameters should be no greater than two. The simplest mixing rules have the form

$$f(\eta) = y_1 \cdot f(\eta_1) + y_2 \cdot f(\eta_2) \tag{8.5}$$

and do not have any other constants than the viscosities of the components. The function of the viscosity $f(\eta)$ is often η, $\ln\eta$ or $1/\eta$, y_1 and y_2 donate the fraction of the components (w_i, x_i or θ_i). An example for this type of mixing rule is the equation from Arrhenius shown in Table 8.1.

Other mixing rules in Table 8.1 include one or more free parameters. These parameters have to be determined experimentally for a mixture, before these equations can be used. The applicability of a mixing rule depends on the type of solvents used. There are four basic classes of binary fluid mixtures: two non-polar components (low dipole moment), two polar components, a polar and a non-polar solvent and finally mixtures of solvents with the very polar H_2O. Mixing rules without free parameters are in general only valid for mixtures of apolar solvents that show no

Table 8.1. Mixing equations for binary mixtures of homogeneous, miscible solvents from [25]

Equations with no free parameter	
$\ln \eta = \rho_1 \cdot \ln \eta_1 + \rho_2 \cdot \ln \eta_2$	Arrhenius
$\frac{1}{\eta} = w_1 \cdot \frac{1}{\eta_1} + w_2 \cdot \frac{1}{\eta_2}$	Bingham
$\left(\frac{1}{\eta}\right)^{\frac{1}{3}} = x_1 \cdot \left(\frac{1}{\eta_1}\right)^{\frac{1}{3}} + x_2 \cdot \left(\frac{1}{\eta_2}\right)^{\frac{1}{3}}$	Lautié
$\eta = x^2{}_1 \cdot \eta_1 + x^2{}_2 \cdot \eta_2 + x_1 \cdot x_2 \cdot (\eta_1 + \eta_2)$	Hind, McLaughlin, Ubbelohde
Equations with one free parameter	
$\left(\frac{1}{\eta}\right)^m = \rho_1 \cdot \left(\frac{1}{\eta_1}\right)^m + \rho_2 \cdot \left(\frac{1}{\eta_2}\right)^m$	Lees
$\ln \eta = x^2{}_1 \cdot \ln \eta_1 + x^2{}_2 \cdot \ln \eta_2 + 2x_1x_2 \cdot V$	Van der Wyk
$\ln \eta = x_1 \cdot \ln \eta_1 + x_2 \cdot \ln \eta_2 + 2x_1x_2 \cdot G$	Grundberg, Nissan
$\ln \eta = \frac{x_1}{x_1 + x_2 \cdot s} \cdot \ln \eta_1 + \frac{x_2 \cdot s}{x_1 + x_2 \cdot s} \cdot \ln \eta_2$	Lederer
Equations with two free parameters	
$\ln \eta = \eta_1 - \frac{x_2}{a \cdot x_2 - b}$	Cokelet, Hollander, Smith
$\ln \eta = \ln \eta_1 + D \cdot w_2 + E$	Ganguly, Chakrabertty

minimum or maximum, as can be seen in Fig. 8.1d. Still, even for mixtures of apolar solvents, mixing rules with only one free parameter give a much better fit. Mixtures of polar components as shown in Fig. 8.1a, b that have minima or maxima can only be described with one or more free parameters in the mixing rule. There is no general rule for the selection of a mixing rule for the mixtures of polar and apolar solvent or for aqueous mixtures. In these cases, a suitable mixing rule can only be determined by comparing experiments. However, for many standard binary solvent mixtures the mixing rules are already established (see for example [70]).

8.2 The Influence of the Molar Mass Distribution

8.2.1 The Viscosity Average of the Molar Mass

The molar mass determined with an $[\eta]$-M-relationship is the so-called viscosity average molar masses M_η, rather than mass (M_w) or number average (M_n) molar mass (see Chap. 2). This seems to be peculiar on first glance, since the molar masses used for the determination of the $[\eta]$-M-relationships were either number or mass average molar masses (depending on the determination method). However, the samples used for the determination of the $[\eta]$-M-relationship should have had a very narrow molar mass distribution. The unknown sample on the other hand has an unknown distribution function of the molar mass. Only in the case that the distribution function of the unknown sample and the sample used for the determination are the same, M_w or M_n are determined directly from the viscosimetric measurement.

In any other case it has to be assumed that the unknown sample has a different distribution function of the molar mass and therefore a different distribution function of the intrinsic viscosities of each fraction of the sample. According to Philippoff [72], it could be shown that the measured intrinsic viscosity is a mass average (see Chap. 2) of the intrinsic viscosity distribution:

$$[\eta] = \frac{\sum m_i \cdot [\eta]_i}{\sum m_i} \tag{8.6}$$

Replacing the intrinsic viscosities according to Eq. (6.1), yields the following equation for the average molar mass:

$$M = \left(\frac{\sum m_i \cdot M_i^a}{\sum m_i} \right)^{\frac{1}{a}} \equiv M_\eta \tag{8.7}$$

The molar mass average determined with viscosimetric measurements M_η is called the viscosimetric average and lies, depending on the exponent a of the $[\eta]$-M-relationship, between the number average molar mass M_n and the mass average molar mass M_w (see Fig. 2.2).

8.2.2 Heterogeneity Classes and the Influence of the Polydispersity on the $[\eta]$-M-Relationship

The viscosity average molar mass M_η is only obtained from $[\eta]$-M-relationships that have been determined with polymer samples of a polydispersity of Q=1. For those cases, where the $[\eta]$-M-relationship was determined from polymer samples with polydispersities $Q>1$ and the average molar mass M_w or M_n was used, the $[\eta]$-M-relationship can be corrected with a factor q, if the distribution function of the molar mass is known:

$$[\eta] = K_w \cdot q_w \cdot M_w^a = K_\eta \cdot M_\eta^a \tag{8.8}$$

$$[\eta] = K_n \cdot q_n \cdot M_n^a = K_\eta \cdot M_\eta^a \tag{8.9}$$

The factors for the common Schulz-Zimm distribution function are listed in Table 8.2. For other distribution functions the reader is referred to [47, 48].

Table 8.2 shows, that the error without the correction factor q for mass average molar masses increases with the polydispersity Q. It is therefore extremely important that $[\eta]$-M-relationships are always quoted with the average molar mass and the polydispersity of the used sample, if the relationship is not already corrected. For $[\eta]$-M-relationships listed in the "Polymer Handbook" [48] the polydispersity range is shown in form of heterogeneity classes (see Table 8.3).

In general a correction of the $[\eta]$-M-relationship is not necessary for a heterogeneity class of A, since the error in this case is smaller than the general error of a viscosimetric measurement (for number average molar masses even $[\eta]$-M-relationships of a heterogeneity class B do not need to be corrected). For all lower heterogeneity classes the correction must be done.

For the (rare) cases that the distribution function of an unknown polymer sample is known (for example from the type of synthesis), the molar mass M_w or

Table 8.2. Correction factors q for $[\eta]$-M-relationships that have been determined from polymer samples with a known mass average molar mass M_w and a known polydispersity Q (taken from [47])

$Q=M_w/M_n$	q_w				
	a=0.000	a=0.500	a=0.764	a=1.000	a=2.000
1.1	1.000	0.989	0.992	1.000	1.091
1.3	1.000	0.971	0.980	1.000	1.231
1.5	1.000	0.959	0.971	1.000	1.333
2.0	1.000	0.940	0.958	1.000	1.250
3.0	1.000	0.921	0.946	1.000	1.667
5.0	1.000	0.907	0.912	1.000	1.800
$Q=M_w/M_n$	q_n				
	a=0.000	a=0.500	a=0.764	a=1.000	a=2.000
1.1	1.000	1.037	1.157	1.100	1.320
1.3	1.000	1.108	1.196	1.300	2.080
1.5	1.000	1.175	1.324	1.500	3.000
2.0	1.000	1.329	1.627	2.000	6.000
3.0	1.000	1.596	2.071	3.000	15.000
5.0	1.000	2.028	3.201	5.000	45.000

Table 8.3. Heterogeneity classes for $[\eta]$-M-relationships according to [48]

Heterogeneity class	Polydispersity range
A	$Q=M_w/M_n \leq 1.25$
B	$1.30 \leq Q \leq 1.75$
C	$1.80 \leq Q \leq 2.4$
D	$Q \geq 1.75$

M_n can be calculated directly from the intrinsic viscosity $[\eta]$, the $[\eta]$-$M_{[\eta]}$-relationship and the appropriate correction factor q:

$$[\eta] = \frac{K_{[\eta]}}{q_w} \cdot M_\eta^a = K_w \cdot M_w^a \tag{8.10}$$

$$[\eta] = \frac{K_{[\eta]}}{q_n} \cdot M_\eta^a = K_n \cdot M_n^a \tag{8.11}$$

8.3 Dimensions of a Real Polymer Coil

The assumption in "Determination of the polymer coil dimensions from the intrinsic viscosity" in Chap. 7 that the polymer coils in solution behave like hard spheres with a constant density inside the coil and a fixed boundary to the solvent is only a simple approximation. In reality, a polymer chain shows a dynamic behavior with fast and statistically changing conformations.

However, it is possible to describe the dimensions even of dynamic polymer coils in solution with the radius of gyration R_G and the average end-to-end distance $\langle r^2 \rangle^{1/2}$ of the chain. They can be calculated for a polymer coil in its unperturbed dimensions from the bond angles and lengths and the steric factors of the monomer units as shown in the following chapters.

8.3.1 The End-to-End Distance

The end-to-end distance r_o of a freely jointed chain r_o directly describes the absolute distance of the chain ends as shown in Fig. 8.2.

For a close-up of a polymer chain with two bond lengths b, the distance r_{oo} of the ends can simply be calculated from the bond angle τ between the two bonds:

$$r_{oo}^2 = 2b^2 - 2b^2 \cos \tau \tag{8.12}$$

For N bonds in the polymer coil and a random angle τ, the second term equals zero. The average end-to-end distance (denoted by the brackets $\langle\ \rangle$) for all possible conformation, $\langle r^2 \rangle_{oo}$, is therefore

$$\langle r^2 \rangle_{oo} = Nb^2 \tag{8.13}$$

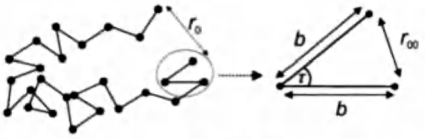

Fig. 8.2. Segment model of a freely jointed polymer chain with the end-to-end distance r_0. The end-to-end distance is referred to as r_{00} if the bond angle τ is not fixed and b equals a real bond length in the polymer chain

In a real polymer coil, not all angles τ are possible. As one can see in Fig. 8.3, in a real polymer chain, the bond angle τ is fixed and the rotation of the chain is restricted and reduced to the most probable torsion angle θ. Additional short-range interactions of the polymer chain segments can be captured with an additional factor ζ. In consideration of all these short-range interactions, the end-to-end distance of a polymer coil in its unperturbed dimensions, $\langle r^2 \rangle_0$, can be described with the following expression:

$$\langle r^2 \rangle_0 = Nb^2 \left(\frac{1 - \cos \tau}{1 + \cos \tau} \right) \left(\frac{1 - \cos \theta}{1 + \cos \theta} \right) \zeta \tag{8.14}$$

8.3.2 The Characteristic Ratio and the Steric Hindrance Parameter

Fortunately, most of the variables in Eq. (8.14) are fixed for a polymer-solvent system and can be combined into the constant so-called characteristic ratio C_∞:

$$\langle r^2 \rangle_0 = C_\infty \cdot Nb^2 \tag{8.15}$$

The characteristic ratio C_∞ contains all steric hindrance factors that reduce a freely jointed chain to a polymer chain in its unperturbed dimensions. The characteristic ratio is listed for a lot of polymers in the "Polymer Handbook" [48]. The num-

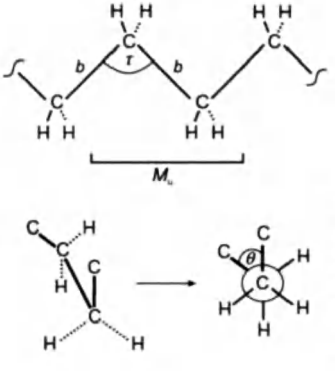

Fig. 8.3. Schematic drawing of a polyethylene chain backbone in all-trans conformation, showing the bond length b, the bond angle τ and the structural composition of a monomer unit with the molar mass M_u. The torsion angle θ between the first bond of a monomer unit to the first bond of the next monomer unit is shown along the connecting bond of the monomers

ber of bond lengths N can be calculated from the degree of polymerization P or the molar mass M (and the molar mass of a monomer unit in the chain M_u):

$$N = 2P \tag{8.16}$$

$$N = \frac{2M}{M_u} \tag{8.17}$$

With the bond length b (0.154 nm for a simple polyethylene backbone) the average end-to-end distance $\langle r^2 \rangle_0$ of a polymer coils in its unperturbed dimensions (so-called theta-conditions) can be calculated directly from Eq. (8.15).

For polymers with a more complicated backbone structure and different bond lengths along the backbone (for example polysaccharides), it is not possible to assume a simple bond length b. In this case, the average end-to-end distance is not described via the characteristic ratio, but the steric hindrance parameter σ:

$$\langle r^2 \rangle_0 = \sigma^2 \cdot \left(\frac{K}{\sqrt{M_u}} \right)^2 \cdot M \tag{8.18}$$

Again values of σ are listed, for example in the "Polymer Handbook" [48] as well as values for K (in many cases as $K/M_u^{0.5}$ with M_u as the molar mass of the monomer unit in the chain) that are constant for a certain chain type. Some values for $K/M_u^{0.5}$ are listed in Table 8.4. $K/M_u^{0.5}$ is comparable to the bond length in Eq. (8.15), whereas the information about the number of bond lengths is contained in the molar mass M.

8.3.3 The Persistence Length

The characteristic ratio as well as the hindrance parameter is a measure for the rigidity of the polymer chain. However, both values are not suitable to compare the rigidity of different chain types, since Eqs. (8.15) and (8.18) both need an additional

Table 8.4. Dimension factors $K/M_u^{0.5}$ for different polymer chain types

Chain type	$\frac{K}{M_u^{0.5}}$ /(nm mol$^{0.5}$/g$^{0.5}$)
Polyethylene chain	$0.308/M_u^{0.5}$
Amylosic chain	$0.426/M_u^{0.5}$
Cellulosic chain	$0.790/M_u^{0.5}$
Gutta-percha (*trans* polydiene)	$0.580/M_u^{0.5}$
Natural rubber (*cis* polydiene)	$0.402/M_u^{0.5}$
Polypeptide	$0.383/M_u^{0.5}$

measure of the bond length that differs for different chain types. Therefore, the bond length b and the characteristic ratio C_∞ are combined to obtain a general measure for the rigidity of the chain. The so-called persistence length L_p is defined as

$$L_p = \frac{C_\infty \cdot b}{2} \tag{8.19}$$

The persistence length can be seen as half of the shortest chain length that is needed to form a circle without obstruction from the chain rigidity. The smaller the persistence length (or C_∞), the more flexible a chain is and the more coiled it is in its unperturbed dimensions. The persistence length is independent of the chain type and can be used to compare the rigidity and coil expansion of different polymers without knowledge of the bond length.

8.3.4 The Radius of Gyration

The average end-to-end distance is not experimentally observable. Directly measurable (for example via light scattering) is the radius of gyration R_G. The radius of gyration R_G is correlated to the end-to-end distance [73]:

$$\langle r^2 \rangle_0 = 6R_G^2 \tag{8.20}$$

In the following sections the dimensions of a polymer coil are expressed in form of the radius rather than the end-to-end distance. The radius of gyration is the average distance of all mass points in a polymer coil from the center of gravity. Other than in a homogeneous hard sphere, the polymer segment density in a real coil is highest in the center of gravity and decreases with the distance from the midpoint as shown in Fig. 8.4.

According to Fig. 8.4 only 92% of the polymer segments are inside a sphere with the radius R_G, 8% of the segments are outside of this sphere.

The size of a polymer coil is influenced by the interactions of the polymer chain with the surrounding solvent molecules. The solvation of the chain increases the effective volume of the chain. However, the solvent molecules shield a polymer segment and reduce its attractive or repulsive interaction with other segments. Therefore, the effective volume of the coil can increase or decrease compared to the unperturbed dimensions under the ideal theta conditions. These long-range interactions, as well as the fact that a polymer chain segment cannot take the exact place of another segment are denoted as the so-called "excluded volume" of a polymer coil in solution (as opposed to the short-range interactions discussed above). The real radius of gyration R_G of a polymer coil in solution can be calculated from the radius of gyration with unperturbed dimensions with an expansion factor α specific for each polymer-solvent system:

$$R_G = \alpha_{RG} \cdot R_{G,\theta} \tag{8.21}$$

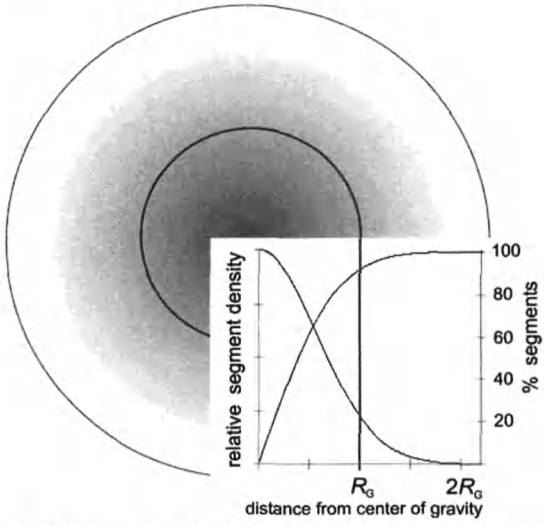

Fig. 8.4. Schematic view of the relative segment density of a polymer coil in solution as a function of the distance from the center of gravity; 92% of the segments lie within the radius of gyration

Solvents where α_{RG} has the value one are so-called "theta"-solvents with the coil in its unperturbed dimensions. In general, all solvents for a certain polymer can behave as a theta-solvent at "theta"-temperature, since the solvent polymer interactions depend on the temperature. Theta-temperatures are listed for several polymer-solvent systems [13, 45]. The values for C_∞ listed in the polymer handbook are determined for theta-systems. Only for these systems, a calculation of the radius of gyration according to Eq. (8.15) is acceptable. The parameter α is experimentally not accessible and therefore not tabulated. Since α also depends on the molar mass M, the radius of gyration for non-theta systems is generally determined directly from the molar mass via an R_G-M-relationship.

8.3.5 R_G-M-Relationship

For theta systems, the radius of gyration R_G can be correlated directly with the molar mass M. Combining Eq. (8.15) with Eq. (8.17) yields a correlation of the end-to-end distance of a coil in its unperturbed dimensions with the molar mass:

$$\langle r^2 \rangle_0 = \frac{2 \cdot b^2 \cdot C_\infty}{M_u} \cdot \mathrm{M} \tag{8.22}$$

Since the only variable on the right side of the equation is the molar mass, a substitution of the end-to-end distance $\langle r^2 \rangle_0$ with the radius of gyration R_G according

to Eq. (8.20) gives a direct dependence of the radius from the square root of the molar mass:

$$R_G = \sqrt{\frac{1}{6}\langle r^2\rangle_o} = \sqrt{\frac{b^2 \cdot C_\infty}{3 \cdot M_u}} \cdot \sqrt{M} \tag{8.23}$$

or with Eq. (8.18):

$$R_G = \sqrt{\frac{\sigma^2 \cdot K^2}{6 \cdot M_u}} \cdot \sqrt{M} \tag{8.24}$$

For polymer coils in non-theta systems, this simple square root relation is not valid. In this case, a dependence of the radius from the molar mass similar to the $[\eta]$-M-relation is observed:

$$R_G = K_{RG} \cdot M^{\nu} \tag{8.25}$$

The exponent ν is a measure for the solvent quality or the solution structure and is correlated to the exponent a of the $[\eta]$-M-relationship (see Table 6.6 and "The Fox-Flory theory" below):

$$a = 3 \cdot \nu - 1 \tag{8.26}$$

R_G-M-relationships can be derived from homologous series of molar masses the same way as $[\eta]$-M-relationships, R_G and M values can be derived for example from static laser light scattering experiments. Table 8.5 for example shows in addition to the experimentally determined $[\eta]$-M-relationships for cellulose derivatives in aqueous solution also the parameters of experimentally determined R_G-M-relationships.

By this means the relation of a and ν as shown in Eq. (8.26) can be verified experimentally.

A theoretical approach for the determination of a R_G-M-relationships is possible from the viscosimetry, if ν is calculated from the exponent a of the $[\eta]$-M-relationship according to Eq. (8.26) and the constant K_{RG} according to the Fox-Flory theory via Eq. (8.42) from the constant $K_{[\eta]}$.

8.4 The Critical Concentration of a Real Coil

The critical concentration c^* of a polymer-solvent system was calculated in "The critical concentration from absolute polymer coil radii" in Chap. 7 for polymer coils with an absolute radius. For a real polymer coil the question arises, at which concentration the polymer coils touch each other and which absolute radius should be used to calculate the critical concentration.

In the simplest case, the radius of the polymer coil is assumed to equal the radius of gyration R_G, even though 8% of the polymer segments of a coil are outside this radius (see above).

The radius of gyration is often corrected with a factor ξ that converts the radius of gyration R_G of a real coil with a density that decreases with the radius, into the

Table 8.5. $[\eta]$-M-Relationships for several cellulosederivatives in aqueous solution

Cellulose derivative	ν	K_{RG}	a	$K_{[\eta]}$	Ref.
Methyl cellulose	0.55	4.4×10^{-2}	0.82	8.0×10^{-2}	[186]
Methyl cellulose			0.55	3.16×10^{-1}	[187]
Sulfoethyl cellulose (0.1 mol/l $NaNO_3$)	0.65	1.2×10^{-2}	1.19	1.74×10^{-4}	[186]
Carboxymethyl cellulose (0.1 mol/l NaCl)	0.53	5.6×10^{-3}	0.87	1.11×10^{-2}	[55]
Carboxymethyl cellulose (0.1 mol/l NaCl)	0.70	6.6×10^{-3}			[186]
Carboxymethyl cellulose (0.1 mol/l NaCl)			0.91	1.23×10^{-2}	[188]
Carboxymethylsulfoethyl cellulose (0.1 mol/l $NaNO_3$)			0.91	6.58×10^{-3}	[186]
Hydroxyethylsulfoethyl cellulose (0.1 mol/l $NaNO_3$)	0.58	3.8×10^{-2}	0.80	2.3×10^{-2}	[186]
Hydroxyethyl cellulose	0.59	2.6×10^{-2}	0.73	4.1×10^{-2}	[186]
Hydroxyethyl cellulose	0.55	3.3×10^{-2}	0.65	1.0×10^{-2}	[55]
Hydroxyethyl cellulose			0.87	9.5×10^{-3}	[189]
Hydroxypropyl cellulose	0.56	2.5×10^{-2}	0.68	4.2×10^{-2}	[186]
Hydroxyethylmethyl cellulose	0.53	3.8×10^{-2}	0.60	1.7×10^{-1}	[186]
Hydroxyethylmethyl cellulose	0.59	2.6×10^{-2}	0.83	2.1×10^{-2}	[55]
Hydroxyethylethyl cellulose	0.63	1.4×10^{-2}	0.88	2.1×10^{-2}	[186]
Hydroxyethylethyl cellulose			0.80	3.7×10^{-2}	[190]
Hydroxypropylmethyl cellulose	0.51	4.7×10^{-2}	0.53	3.6×10^{-1}	[186]
Celluloseacetate			0.60	2.1×10^{-2}	[191]
Cellulosesulfate	0.55	5.8×10^{-2}			[186]

radius of gyration R_{sph} of an equivalent hard sphere with the same molar mass and the same average density:

$$R_{sph} = \xi \cdot R_G = \sqrt{\frac{5}{3}} \cdot R_G \tag{8.27}$$

The volume V_{coil} of a single coil with this corrected radius of gyration then calculates to

$$V_{coil} = \frac{4}{3} \pi R_{sph}^3 \tag{8.28}$$

The critical concentration is reached when the solution volume is completely filled with polymer coils:

$$\frac{V_{\text{polymer}}}{V_{\text{solution}}} = 1 = \frac{V_{\text{coil}} \cdot \dfrac{m_{\text{polymer}} \cdot N_A}{M}}{V_{\text{solution}}} = V_{\text{coil}} \cdot \frac{c \cdot N_A}{M} \tag{8.29}$$

The critical concentration can now be calculated directly from the molar mass M and the radius of gyration R_G (if the R_G-M-relationship introduced above is known, only one of these variables has to be determined):

$$c^*_{LS} = \frac{M}{\frac{4}{3} \cdot N_A \cdot \pi \cdot \xi \cdot R_G^3} \tag{8.30}$$

A critical concentration determined in this way is also denoted as the critical concentration of light scattering, c^*_{LS}, since the radius of gyration can be determined directly via light scattering experiments [74]. As shown in Fig. 7.2 for two different polymer-solvent systems, the critical concentration c^*_{LS} is roughly a factor of ~10 smaller than the critical concentration of the viscosimetry $c^*_{[\eta]}$ (Eq. 7.7).

Still, the radius of gyration does not equal the effective radius of a polymer coil in solution in terms of the flow behavior. For the calculation of a so-called hydrodynamic radius R_H that reflects this effective radius of the polymer coil in a flow field, several theoretical approaches have been made. For theta conditions for example, the modified Kirkwood-Riseman theory [47] predicts a ratio of radius of gyration to hydrodynamic radius of

$$\frac{R_{G,\theta}}{R_{H,\theta}} = 1.20 \tag{8.31}$$

A correction of Eq. (8.30) with this factor yields a hydrodynamical, critical concentration for a theta-system that lies between $c^*_{[\eta]}$ and c^*_{LS}.

However, for practical applications even an exact hydrodynamical, critical concentration is just a guideline, since superproportional changes of the flow behavior do not occur abruptly at the critical concentration. Due to the diffuse character of a real polymer coil in solution, a change in the flow behavior above c^* occurs gradually over a range of concentrations around c^*. For practical applications a determination of $c^*_{[\eta]}$ or c^*_{LS} is sufficient. The discussion about an exact determination of the hydrodynamic radius is therefore more of an academic nature. However, for a classification of the critical concentration of the viscosimetry $c^*_{[\eta]}$ or c^*_{LS}, it is important to know about the possible range of critical concentrations.

8.5 The Fox-Flory Theory

P.J. Fox and T.G. Flory developed a theoretical correlation of the intrinsic viscosity $[\eta]$, the radius of gyration R_G and the molar mass M [75]. For the case of hard spheres, the intrinsic viscosity is related to R_G and M if the volume of a polymer coil in Eq. (7.3) is replaced with the volume of an equivalent sphere with a radius of gyration according to Eq. (8.28):

$$[\eta] = \frac{4}{3} \cdot \pi \cdot \xi^3 \cdot R_G^3 \cdot \frac{2.5 \cdot N_A}{M} \tag{8.32}$$

Combining the constants yields the so-called Fox-Flory equation:

$$[\eta] = \Phi \cdot \frac{R_G^3}{M} \tag{8.33}$$

with a Flory constant Φ for the case of hard spheres of

$$\Phi = 1.357 \cdot 10^{25}\ \text{mol}^{-1} \tag{8.34}$$

For real polymer coils in solution the Flory constant Φ is lower, depending on the conversion factor ξ. Several attempts for a theoretical calculation of a Flory constant have been published (Flory and Fox calculated a value of Φ=4.17×10^{24} mol^{-1}); according to Yamakawa [76] a practical Flory constant for different polymer-solvent systems at theta conditions Φ_θ is

$$\Phi_\theta = 3.69 \cdot 10^{24}\ \text{mol}^{-1} \tag{8.35}$$

The Fox-Flory equation (Eq. 8.33) in combination with the square root relation of the molar mass (Eq. 8.22) and the calculation of the radius of gyration from the end-to-end distance (Eq. 8.14) allows for a derivation of the $[\eta]$-M-relationship for theta conditions:

$$[\eta] = \Phi_\theta \cdot \left(\frac{b^2 \cdot C_\infty}{3 \cdot M_u}\right)^{\frac{3}{2}} \cdot M^{0.5} = K_{[\eta],\theta} \cdot M^{0.5} \tag{8.36}$$

The exponent a of the $[\eta]$-M-relationship shows therefore also from a theoretical approach a value of 0.5.

For non-theta systems, the Fox-Flory equation can be corrected. The intrinsic viscosity $[\eta]$ can be corrected with an expansion parameter $\alpha_{[\eta]}$ that has to be determined experimentally:

$$\alpha_{[\eta]}^3 = \frac{[\eta]}{[\eta]_\theta} \tag{8.37}$$

The radius of gyration can be corrected in a similar way according to Eq. (8.21) with a factor α_{RG}. Since this factor cannot as easily be determined experimentally,

for good solvents an empirical correction factor ε for the Flory constant can be used [77]:

$$\Phi = \Phi_\theta \cdot (1 - 2.63 \cdot \varepsilon - 2.86 \cdot \varepsilon^2) \tag{8.38}$$

The factor ε is correlated with the exponent ν of the R_G-M-relationship:

$$\varepsilon = 2\nu - 1 \tag{8.39}$$

or the exponent a of the $[\eta]$-M-relationship:

$$\varepsilon = \frac{2a - 1}{3} \tag{8.40}$$

These relations yield for the intrinsic viscosity of a non-theta system a corrected Fox-Flory equation:

$$[\eta] = \Phi_\theta \cdot (1 - 2.63 \cdot \varepsilon - 2.86 \cdot \varepsilon^2) \cdot \alpha_{[\eta]}^3 \cdot \frac{R_G^3}{M} \tag{8.41}$$

An experimental verification of the Flory constant Φ is possible with known R_G-M- and $[\eta]$-M-relationships for a polymer solvent system. A substitution of Eqs. (6.1), (8.25), and (8.26) in Eq. (8.33) yields the following expression for the Flory constant:

$$\Phi = \frac{K_{[\eta]}}{K_{RG}^3} \tag{8.42}$$

9 List of References

1. Flory PJ (1977) Angew Chem 22:787
2. Kulicke WM, Lenk S, Detzner HD, Weiss T (1993) Chem Ing Technik 65:541
3. von Homeyer A, Krentz DO, Kulicke WM, Lerche D (1999) Colloid Polym Sci 277:637
4. Parker S, Kulicke WM, Böhm N, Kotz J, Jaeger W (1997) Angew Makromol Chem 250:15
5. Grigorescu G, Kulicke WM (2000) Adv Polym Sci 152:1
6. Kulicke WM, Kotter M, Grager H (1989) Adv Polym Sci 89:1
7. Kulicke WM, Böse N, Bouldin M (1988) In: Schulz DN, Stahl GA (eds) Water-soluble polymers for petroleum recovery. Plenum Press, New York, p 1
8. Zeidler H, Altmann S, John B, Gaffga R, Kulicke WM (1979) Rheol Acta 18:151
9. Altmann S, Zeidler H, Gaffga R, Kulicke WM (1980) Rheol Acta 19:642
10. Ver Strate G, Struglinski MJ (1991) In: Schulz DN, Glass JE (eds) ACS Symposium Series 462 – Polymers as rheology modifiers. American Chemical Society, Washington, DC, p 256
11. Kulicke WM, Roessner D, Kull W (1993) Starch-Starke 45:445
12. Heins D, Kulicke WM, Kauper P, Thielking H (1998) Starch-Starke 50:431
13. Lide DR (2002) CRC Handbook of chemistry and physics. CRC Press, New York
14. Stephan K, Lucas K (1979) Viscosity of dense fluids. Plenum Press, London
15. Macosko C (1994) Rheology: principles, measurements, and applications. VCH Publishers, New York
16. Pahl M, Gleißle W, Laun HM (1995) Praktische Rheologie der Kunststoffe und Elastomere. VDI, Düsseldorf
17. Ferry JD (1980) Viscoelastic properties of polymers. Wiley, New York
18. Larson RG (1999) The structure and rheology of complex fluids. Oxford University Press, New York
19. Mezger T (2001) Das Rheologie-Handbuch. Curt R. Vincent Verlag, Hannover
20. Zimm BH, Crothers DM (1962) Proc Nat Acad Sci 48:905
21. Elias HG (1999) Makromoleküle: Chemische Struktur und Synthesen. Wiley-VCH, Weinheim
22. Schurz J (1972) Viskositätsmessungen an Hochpolymeren. Verlag Berliner Union GmbH, Stuttgart
23. Gruber E, Sezen MC, Schurz J (1973) Angew Makromol Chem 28:57
24. Kulicke WM (1987) In: Houben J, Weyl T (eds) Methods of organic chemistry, vol E20. Georg Thieme Verlag, Stuttgart, p 1176
25. Bauer H (1985) In: Kulicke WM (ed) Fließverhalten von Stoffen und Stoffgemischen. Hüthig & Wepf Verlag, Heidelberg, p 100
26. Schurz J, Kashmoula T, Falcke FJ (1972) Angew Makromol Chem 25:51
27. Braun D, Walter E (1980) Colloid Polym Sci 258:376
28. Lechner MD, Mattern R (1984) Angew Makromol Chem 123:45
29. Kulicke WM, Kniewske R, Klein J (1980) Abstr Pap Am Chem Soc 180:30
30. Kulicke WM (1986) Makromol Chem Macromol Symp 2:137
31. Kulicke WM, Horl HH (1985) Colloid Polym Sci 263:530
32. Kulicke WM, Kniewske R (1980) Makromol Chem Macromol Chem Phys 181:823
33. Kulicke WM, Kniewske R (1981) Makromol Chem Macromol Chem Phys 182:2277
34. Cho CS, Nakagami A, Komoto T, Kawai T (1978) Makromol Chem Macromol Chem Phys 179:1345
35. Kulicke WM, Horl HH (1983) Angew Makromol Chem 116:149
36. Meister JJ (1952), Dissertation, Universität Freiburg

37. McCormick CL, Chen GS, Park LS, Neidlinger HH (1981) Abstr Pap Am Chem Soc 181:122
38. Wilk J, Kryk H, Hartmann J, Wagner D (2001) Theorie und Praxis der Kapillarviskosimeter. Schott Glas Business GmbH, Mainz
39. Jentsch C (1978) Chem Unserer Zeit 12:56
40. Klein J, Muller HG (1982) Erdol Kohle Erdgas Petrochem 35:187
41. Stepina V, Vesely V, Trebicky V (1987) Tribologie Schmierungstechnik 34:113
42. Greif P (1979) Monatsschrift Brauerei 32:356
43. Elias HG (2003) Makromoleküle: Anwendungen von Polymeren. Wiley-VCH, Weinheim
44. Elias HG (1971) Makromoleküle, Struktur – Eigenschaften – Synthesen – Stoffe. Hüthig & Wepf Verlag, Basel
45. Gnamm H, Fuchs O (1998) Lösungs- und Weichmachungsmittel. Wissenschaftliche Verlagsgesellschaft mbH, Stuttgart
46. Schurz J (1974) Struktur-Rheologie. Berliner Union, Stuttgart
47. Elias HG (2001) Makromoleküle: Physikalische Strukturen und Eigenschaften. Wiley-VCH, Weinheim
48. Brandrup J, Immergut EH (1999) Polymer handbook. Wiley, New York
49. Bledzki AK, Spychaj T (1991) Molekulargewichtsbestimmung von hochmolekularen Stoffen. Hüthig & Wepf, Basel
50. Kulicke WM (1986) Chem Ing Technik 58:325
51. Kulicke WM, Kniewske R, Muller RJ, Prescher M, Kehler H (1986) Angew Makromol Chem 142:29
52. Bouldin M, Kulicke WM, Kehler H (1988) Colloid Polym Sci 266:793
53. Kulicke WM, Otto M, Baar A (1993) Makromol Chem Macromol Chem Phys 194:751
54. Casale A, Porter RS (1978) Polymer stress reactions. Academic Press, New York
55. Schittenhelm N, Kulicke WM (2000) Macromol Chem Phys 201:1976
56. Peacocke AR, Pritchard NJ (1968) Biopolymers 6:605
57. Pritchard NJ, Hughes DE, Peacocke AR (1966) Biopolymers 4:259
58. Okuyama M, Hirose T (1968) Kolloid Z Z Polym 226:70
59. Gooberman G, Lamb J (1960) J Polym Sci 42:35
60. Basedow AM, Ebert KH (1977) Adv Polym Sci 22:83
61. Marx-Figini M (1997) Angew Makromol Chem 250:85
62. Vollmert B (1980) Grundriss der Makromolekularen Chemie. E. Vollmert Verlag, Karlsruhe
63. Kulicke WM, Prescher M (1984) Makromol Chem Macromol Chem Phys 185:2619
64. Einaga Y, Miyaki Y, Fujita H (1979) J Polym Sci Polym Phys Ed 17:2103
65. Meyerhoff G (1955) Z Phys Chem Int J Res Phys Chem Chem Phys 4:335
66. Marzolph H, Schulz GV (1954) Makromol Chem Macromol Chem Phys 13:120
67. Kurata M, Stockmayer WH (1963) Fortschritte Hochpolymeren-Forschung 3:196
68. Meyerhoff G (1961) Fortschritte Hochpolymeren-Forschung 3:59
69. Bohm N, Kulicke WM (1999) Carbohydr Res 315:293
70. Irving JB (1977) National Engineering Laboratory, East Kilbride, Glasgow
71. Irving JB (1977). National Engineering Laboratory, East Kilbride, Glasgow
72. Philippoff W (1937) Ber Dtsch Chem Ges 70B:827
73. Lechner MD, Gehrke K, Nordmeier EH (1993) Makromolekulare Chemie: Ein Lehrbuch für Chemiker, Materialwissenschaftler und Verfahrenstechniker. Birkhäuser Verlag, Basel
74. Roessner D, Kulicke WM (1994) J Chromatogr A 687:249
75. Flory PJ, Fox TG Jr (1951) J Am Chem Soc 73:1904
76. Yamakawa H (1971) Modern theory of polymer solutions. Harper and Row, New York
77. Kulicke WM (1985) In: Kulicke WM (ed) Fließverhalten von Stoffen und Stoffgemischen. Hüthig & Wepf Verlag, Heidelberg, p 23
78. Wandrey C, Hernandez-Barajas J, Hunkeler D (1999) Radical polymerisation polyeletrolytes (Adv Polym Sci, vol 145). Springer, Berlin Heidelberg New York, p 123
79. Stahl GA, Schulz DN (1988) Water-soluble polymers for petroleum recovery. Plenum Press, New York
80. Harris P (1990). Elsevier Science Science Publishers Ltd, New York p 476
81. Walter R (1998). Marcel Dekker, New York
82. Bauer KH, Fromming KH, Fuhrer C (1986) Pharmazeutische Technologie. Georg Thime Verlag, Stuttgart

83. Dautzenberg H, Jaeger W, Kotz J, Philipp B, Seidel C, Stscherbina D (1994) Polyelectrolytes: formation, characterization, and application. Carl Hanser Verlag, München
84. Kulicke WM, Lettau AI, Thielking H (1997) Carbohydr Res 297:135
85. Bieleman J (1998) Lackadditive. Wiley-VCH Verlag, Weinheim
86. Glass JE (1989) In: Comstock MJ (ed) Advances in chemistry series. American Chemical Society, Washington, DC, p 575
87. Jacobs A (1995), Dissertation, Universität Hamburg
88. Kniewske R, Kulicke WM (1983) Makromol Chem Macromol Chem Phys 184:2173
89. Kulicke WM, Klein J (1978) Angew Makromol Chem 69:169
90. Kulicke WM, Klein J (1978) Angew Makromol Chem 69:189
91. Horl HH (1982) Dissertation, Technische Universität Carolo-Wilhelmina zu Braunschweig
92. Kulicke WM, Kniewske R, Klein J (1982) Prog Polym Sci 8:373
93. Kulicke WM, Oertel R, Otto M, Kleinitz W, Littmann W (1990) Erdol Kohle Erdgas Petrochem 43:471
94. Kuhn R, Kroemer H, Rossmanith G (1974) Angew Makromol Chem 40/41:361
95. Mourey TH, Turner SR, Rubinstein M, Frechet JMJ, Hawker CJ, Wooley KL (1992) Macromolecules 25:2401
96. Staudinger H (1950) Organische Kolloid Chemie. Vieweg & Sohn, Braunschweig
97. Cohen J, Priel Z, Rabin Y (1988) J Chem Phys 88:7111
98. Blau A (1977) Dissertation, Universität Karlsruhe
99. Pals DTF, Hermans JJ (1952) Recl Trav Chim 71:433
100. Kulicke WM, Klein J (1985) In: Gambert B (ed) The influence of polymer additives on velocity and temperature fields. Springer, Berlin Heidelberg New York, p 43
101. Klein J, Heitzmann R (1978) Makromol Chem Macromol Chem Phys 179:1895
102. von Homeyer A (1999) Dissertation, Univerität Hamburg
103. Granat H (1969) Starch-Starke 21:251
104. Eigner J, Doty P (1965) J Mol Biol 12:549
105. Murakami H, Norisuye T, Fujita H (1980) Macromolecules 13:345
106. Klein J, Kulicke WM (1980) SPE Fifth International Symposium on Oilfield and Geothermal Chemistry. American Institute of Mining Metallurgical and Petroleum Engineers, Inc., Stanford, CA, p 51
107. Geddes R, Harvey JD, Wills PR (1977) Biochem J 163:201
108. Aharoni SM, Murthy NS (1983) Polym Commun 24:132
109. Kix M, Lenk S, Kaminsky W, Kulicke WM (1998) Polym Bull 41:349
110. Trossarelli L, Campi E, Saini G (1959) J Polym Sci 35:205
111. Kulicke WM, Kniewske R (1984) Rheol Acta 23:75
112. Klein J, Hannemann G, Kulicke WM (1980) Colloid Polym Sci 258:719
113. Barnes HA, Hutton JF, Walters K (1989) An Introduction to rheology. Elsevier, Amsterdam
114. Meyerhoff G (1960) Z Phys Chem Int J Res Phys Chem Chem Phys 23:100
115. Meyerhoff G, Appelt B (1979) Macromolecules 12:968
116. Utiyama H (1960), PhD Thesis, Kyoto University
117. Mukherjea RN, Rempp P (1959) J Chim Phys 56:95
118. Outer P, Carr CI, Zimm BH (1950) J Chem Phys 18:830
119. Petrus V, Porsch B, Nystrom B, Sundelof LO (1982) Makromol Chem Macromol Chem Phys 183:1279
120. Breitenbach JW, Gabler H, Olaj OF (1964) Makromol Chem Macromol Chem Phys 81:32
121. McCormick HW (1959) J Polym Sci 36:341
122. Papazian LA (1969) Polymer 10:399
123. Oth J, Desreux V (1954) Bull Soc Chim Belg 63:285
124. Bawn C, Freeman R, Kamaliddin A (1954) Trans Faraday Soc 46:1107
125. Chrastova V, Mikulasova D, Lacok J, Citovicky P (1981) Polymer 22:1054
126. Oyama T, Kawahara K, Ueda M (1959) Nippon Kagaku Zasshi 79:727
127. Chinai SN, Scherer PC, Bondurat CW, Levi DW (1956) J Polym Sci 22:527
128. Danusso F, Moraglio G (1957) J Polym Sci 24:161
129. Fox TG Jr, Flory PJ (1951) J Am Chem Soc 73:1915

130. Cowie JMG, Worsfeld DJ, Bywater S (1961) Trans Faraday Soc 57:705
131. Yamamoto A, Fujii M, Tanaka G, Yamakawa H (1971) Polym J 2:799
132. Ang F (1957) J Polym Sci 25:126
133. Nakata M (1971) Makromol Chem Macromol Chem Phys 149:99
134. Sho T, Sato T, Norisuye T (1986) Biophys Chem 25:307
135. Sato T, Kojima S, Norisuye T, Fujita H (1984) Polym J 16:423
136. Muller G, Lecourtier J, Chauveteau G, Allain C (1984) Makromol Chem Rapid Commun 5:203
137. Milas M, Rinaudo M, Tinland B (1985) Polym Bull 14:157
138. Callet F, Milas M, Rinaudo M (1987) Int J Biol Macromol 9:291
139. Tinland B, Mazet J, Rinaudo M (1988) Makromol Chem Rapid Commun 9:69
140. Tinland B, Rinaudo M (1989) Macromolecules 22:1863
141. Ach A (1987), Dissertation, Technische Universität Carolo-Wilhelmina zu Braunschweig
142. Liu W, Sato T, Norisuye T, Fujita H (1987) Carbohydr Res 160:267
143. Zhang L, Liu W, Norisuye T, Fujita H (1987) Biopolymers 26:333
144. Holzwarth G (1978) Carbohydr Res 66:173
145. Fujisaki Y, Kobayashi H (1962) Kobunshi Kagaku 19:81
146. Kamide K, Miyazaki Y, Kobayashi H (1985) Polym J 17:607
147. Ribeyrolles PL, Guyot A, Benoit H (1959) J Chim Phys 56:377
148. Abe M, Iwama M, Homma T (1969) Kogyo Kaguka Zasshi 72:2313
149. Tsvetkov VN, Klenin SI (1959) Zh Tekhn Fiz 29:1393
150. Burchard WR (1963) Makromol Chem Macromol Chem Phys 67:182
151. Hanafusa K, Teramoto A, Fujita H (1966) J Chem Phys 70:4004
152. Kotera A, Saito T, Matsuda H, Kamata R (1960) Rept Progr Polym Phys Japan 3:51
153. Giurgea M, Ghita C, Baltog I, Lupu A (1966) J Polym Sci A-2 4:529
154. Chiang R (1965) J Chem Phys 69:1645
155. Kaufmann HS, Walsh EK (1957) J Polym Sci 26:124
156. Mendelson RA, Drott EE (1968) J Polym Sci Part B 11:795
157. Howard GJ (1959) J Polym Sci 37:310
158. Lanska B, Bohdanecky M, Sebenda J, Tuzar Z (1978) Eur Polym J 14:807
159. Mattiussi A, Gechele GB, Francesconi R (1969) J Polym Sci A-2 7:411
160. Fox TG Jr, Flory PJ (1949) J Phys Colloid Chem 53:197
161. Krigbaum WR, Flory PJ (1953) J Am Chem Soc 75:1775
162. Flory PJ (1943) J Am Chem Soc 65:372
163. Carter WC, Scott RL, Magat M (1946) J Am Chem Soc 68:1480
164. Beattie WH (1963) J Appl Polym Sci 7:507
165. Poddubnyi IA, Erenberg YG, Yeremina MA (1968) Vysokomole kulyarnye Soedineiya. Series A 10:1381
166. Kinsinger JB, Hughes RE (1959) J Phys Chem 63:2002
167. Wessling RA, Mark JE, Hughes RE (1966) J Phys Chem 70:1903
168. Krause S (1961) Dilute solution properties of acrylic and methacrylic polymers. Rohm & Haas, Philadelphia
169. Matsuda H, Yamano K, Inagaki H (1969) J Polym Sci Part A 7:609
170. Cantov H-J, Schulz GV (1954) Z Phys Chem Int J Res Phys Chem Chem Phys 2:117
171. Fox TG Jr (1962) Polymer 3:111
172. Cohn-Ginsberg E, Fox TG Jr, Mason HF (1962) Polymer 3:97
173. Schulz GV, Haug A (1962) Z Phys Chem Int J Res Phys Chem Chem Phys 34:328
174. Beech DR, Booth C (1969) J Polym Sci A-2 7:575
175. Allen G, Booth C, Hurst SJ, Jones MN, Price C (1967) Polymer 8:391
176. Bailey FE, Callard RW Jr (1959) J Appl Polym Sci 1:56
177. Chiang R (1958) J Polym Sci 38:235
178. Parrini P, Sebastiano F, Messina G (1960) Makromol Chem Macromol Chem Phys 38:27
179. Kehler H (1987), Dissertation, Universität Hamburg
180. Inagaki H, Suzuki H, Fujii M, Matsuo T (1966) J Phys Chem 70:1781
181. Matsumoto M, Ohyanagi Y (1960) Kobunshi Kagaku 6:460
182. Ueda M, Kajitani K (1967) Makromol Chem Macromol Chem Phys 108:138

183. Bohdanecky M, Solc K, Kratochvil P, Kolinsky M, Psyka M, Lim D (1967) J Polym Sci A-2 5:343
184. Freeman M, Manning PP (1964) J Polym Sci Part A 2:2017
185. Cerney LC, Helminial TE, Meier JF (1960) J Polym Sci 44:539
186. Clasen C, Kulicke WM (2001) Prog Polym Sci 26:1839
187. Kamide K, Saito M, Abe T (1981) Polym J 13:421
188. Manley RSJ (1979) Arkiv Kemi 9:519
189. Brown W, Henley D, Oehman J (1963) Makromol Chem Macromol Chem Phys 62:164
190. Vink H (1966) Makromol Chem Macromol Chem Phys 94:15
191. Neely WB (1963) J Polym Sci Part A 1:311

10 Subject Index

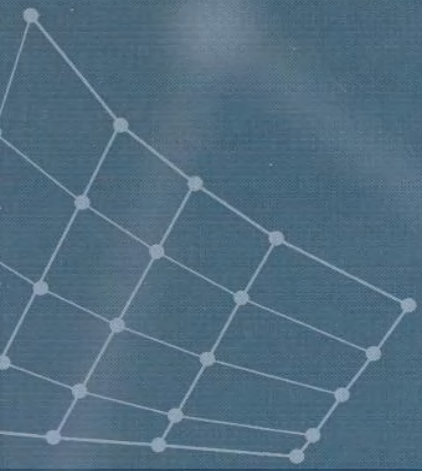

SPRINGER LABORATORY

W.-M. Kulicke · C. Clasen

Viscosimetry of Polymers and Polyelectrolytes

Viscometry is an easy, accessible, but at the same time significant, analytical method for the characterization of polymers in solution. Widely used in pharmaceutical, medical and polymer processing industries as well as in research, viscometry allows for a quick and inexpensive determination of relevant parameters such as solution structure, viscosity and molar mass. This laboratory handbook offers clear guidelines and tips for the practical everyday application of viscosimetry, as well as supplying a comprehensive companion for the interpretation of viscosimetric data from simple to complex polymer solutions. It is written with the premise that general knowledge of the broad behavioral spectrum of polymer solutions is of utmost importance for the correct handling of viscometric equipment and the interpretation of data. Originating from the authors' experience supervising analytical polymer chemistry lab courses, it shows readers how to tackle key practical problems through detailed examples.

ISBN 3-540-40760-X

springeronline.com